CORA Cork Open Research Archive
Cartlann Taighde Oscailte Chorcaí

Title	On mathematical aspects of exact nonlinear rotational water waves
Authors	Rodríguez Sanjurjo, Adrián
Publication date	2019
Original Citation	Rodríguez Sanjurjo, A. 2019. On mathematical aspects of exact nonlinear rotational water waves. PhD Thesis, University College Cork.
Type of publication	Doctoral thesis
Rights	© 2019, Adrián Rodríguez Sanjurjo. - http://creativecommons.org/licenses/by-nc-nd/3.0/
Download date	2026-09-08 03:02:09
Item downloaded from	https://hdl.handle.net/10468/8603

UCC
University College Cork, Ireland
Coláiste na hOllscoile Corcaigh

On Mathematical Aspects of Exact Nonlinear Rotational Water Waves

Adrián Rodríguez Sanjurjo

NATIONAL UNIVERSITY OF IRELAND, CORK

SCHOOL OF MATHEMATICAL SCIENCES

DEPARTMENT OF APPLIED MATHEMATICS

A thesis submitted for the degree of Doctor of Philosophy

April 2019

Head of Department: Prof. Sebastian Wieczorek

Supervisor: Dr. David Henry

Research supported by Science Foundation Ireland

Contents

Abstract ix
Acknowledgements xi
List of publications xiii

1 Preliminaries **1**
1.1 Governing equations 1
1.1.1 Mass conservation equation 2
1.1.2 Momentum equation : Euler equations 2
1.1.3 Boundary conditions 3
1.2 Lagrangian framework 4
1.2.1 Gerstner's wave 7
1.2.2 Lagrangian governing equations 8
1.3 Geophysical flows 14
1.3.1 Rotating framework of reference 14

2 Dynamical analysis of internal waves **19**
2.1 Equatorially-trapped waves 19
2.2 Geophysical model and β-plane equations 20
2.3 Exact solution 23
2.3.1 Solution above the thermocline 24
2.4 Main result: flow dynamically possible 26

3 Internal waves in the f-plane **35**
3.1 f-plane approximation at the Equator 36
3.2 Solution for the five-layer model 37

3.2.1 Deepest layer 39
3.2.2 Transitional layer 39
3.2.3 Uniform-flow layer 40
3.2.4 Layer above the thermocline 41

4 Mean flow properties **47**
4.1 Mean-flow velocities and Stokes drift 48
4.2 Internal wave in the β-plane 49
4.2.1 Mean Lagrangian flow velocity 53
4.2.2 Mean Eulerian flow velocity 53
4.2.3 Eulerian velocity in terms of the current 55
4.2.4 Stokes drift 58
4.2.5 Mass flux for the constant current solution 58
4.3 Internal wave in the f-plane 60
4.3.1 Mean Lagrangian flow velocity 61
4.3.2 Mean Eulerian flow velocity 62
4.3.3 Stokes drift 63
4.3.4 Mass flux for the transverse current 64

5 Hydrodynamic stability **67**
5.1 Introduction 67
5.2 Instability of geophysical flows 68
5.3 Short-wavelength method 69
5.4 Modified β-plane approximation 74
5.4.1 Solution for the modified β-plane equations 76
5.5 Short-wavelength instability for the modified β-plane approximation . 78
5.5.1 Instability in terms of the wave steepness 81
5.6 Instability of the internal wave 82
5.6.1 Instability in terms of the steepness of the internal wave . . . 84

6 Dynamical analysis of Pollard's solution **87**
6.1 The generalised Pollard's solution 88
6.1.1 The governing equations 88
6.1.2 Exact and explicit solution 89

6.2 Dynamically-possible flow 90
Local regularity 92
Sufficient condition for injectivity 93
Necessary condition for injectivity 95
Global diffeomorphism flow map 98

7 Steady periodic gravity water waves **99**
7.1 Fixed-depth formulation for steady periodic waves 101
7.1.1 Hodograph transformation 104
7.2 Two-layer vorticity model 106
7.2.1 The Sturm-Liouville Problem 106
7.2.2 The algebraic equation 109
7.3 Analysis of the dispersion relation 113
7.4 Stability of the laminar solutions 120

Conclusions **127**

Appendix A Complementary results **131**
A.1 Mean-value inequality 131
A.2 Invariance of domain theorem 133
A.3 Viète's formulae 136

I, Adrián Rodríguez Sanjurjo, certify that the work I am submitting is my own and has not been submitted for another degree, either at University College Cork or elsewhere. All external references and sources are clearly acknowledged and identified within the contents. I have read and understood the regulations of University College Cork concerning plagiarism.

Adrián Rodríguez Sanjurjo

A meus pais

"As cousas ben feitas son de quen as fai."

– María do Molín

Abstract

This thesis addresses various theoretical questions regarding exact nonlinear solutions to the geophysical governing equations which are explicit in the Lagrangian framework. Such solutions are scarce, being Gerstner's wave the only-known explicit and exact solution of the nonlinear two-dimensional periodic gravity wave problem with a non-flat free surface under constant density. This remarkable solution was extended by Pollard to an incompressible vertically-stratified fluid in a rotating system. More recently, exact and explicit solutions of the nonlinear governing equations for geophysical water waves, describing several physical scenarios, have been derived. A thorough analysis of these solutions is conducted in this thesis. From a mathematical point of view, the Lagrangian flow map defining a flow motion needs to satisfy certain conditions. It is proven in Chapters 2 and 6 that this is the case for the equatorially-trapped, non-hydrostatic internal water waves [14] and for the generalisation of Pollard's solution [26], respectively. An advantage of some of these explicit solutions is that they are able to accommodate currents, leading to more complicated and interesting flows. This is shown in Chapter 3 where a new solution of the f-plane approximation of the geophysical equations is constructed. This solution incorporates both a constant current in the zonal direction and a transverse current in the meridional direction. The study of this solution and of other internal water waves is further developed in Chapter 4. Relevant mean flow properties are provided, establishing a relation between Eulerian and Lagrangian quantities. Furthermore, the effects of the vorticity present in these flows are compared with those of the better-known irrotational case. In addition, Chapter 5 examines the robustness of these solutions in terms of the hydrodynamic stability. This is done for the internal wave discussed in Chapter 2 and the solution of the modified β-plane approximation equations [61] by applying the short-wavelength instability method. An important aspect of the flows studied throughout this work is that they exhibit vorticity. This is further analysed in the Eulerian framework in Chapter 7 within the context of small-amplitude two-dimensional steady periodic gravity water waves propagating over a flat bed. A dispersion relation for waves with two layers of different vorticity is derived and the existence of such waves is discussed.

Acknowledgements

First and foremost, I would like to express my gratitude to my supervisor Dr. David Henry. He did not only trust me with the task of conceiving this thesis but he has also provided inestimable advice and insight into my researching career. After every meeting, I have always left either with a precise idea of how to solve my problems or with the confidence that I could solve them. In the same way, he was always prompt to help with any other issue, exceeding his obligations as a supervisor. He also acted as a mentor who guided me through the publication process of my papers, as well as through my first teaching experience and the public presentations regarding my research.

I would also like to thank Dr. Gareth Thomas for introducing me to the area of fluid mechanics and for all the wise advice concerning not only that area but also the academic world and many other topics that enriched my experience during these years.

I would like to dedicate a few words in Galician to my family and friends: *Tendo en conta que todo que o diga vai quedarse corto e que non é posible nomear a todas aquelas persoas que me teñen axudado, se o teu nome non está aquí tómao coma un fallo pola miña parte. Quero comezar agradecendo a meus pais, María José e Toño por apoiarme en todas as miñas decisións ao longo dos anos, incluíndo a de deixar o meu país. Sempre demostrando máis confianza en min da que eu teño. Non podería ter soñado en conseguir algo así sen eles.*

Con respecto ao resto da familia, quero agradecer a miña prima Bego por estar sempre aí e por axudarme coas primeiras leccións de física. A Luisa e Victor porque foi en Breogán con aquel exame de inglés onde comecei este camiño e por Iria e Iago. A Amparo que tan ben me deu de comer sempre e a Pepe porque, aínda despois desta

tese, tería muito que ensinarme acerca do río e das truitas. A Pau, Marisa, Pau, Mar, Laia e Joan que se arriscaron a unhas vacacións sen sol. A Maite, Pitus, María e Joan por tódalas interesantes sobremesas e a Bruno, Iago, Max e Boris que me alegraron os veráns. A Isabel polos seus consellos e a Pau por retarme a explicarlle matemáticas. A Diego, Iria, Mane e Tere por unha infancia chea de recordos e a Lara e Mar polo futuro que está por vir. A meus avós María, Manuel, Susa, Tino e a Bis polo seu cariño incondicional.

Quero agradecer a tódolos meus amigos por aturarme todos estes anos e por axudarme a manter a cabeza afastada das matemáticas: Vito, Silveira, Ricardo, Pes, Moirón, Marta, Logares, Joaco, Gonzalo, Enrique e Andrea. Porque en cada viaxe de volta a Santiago sempre houbo alguén esperándome no aeroporto e por moito máis, grazas aos xinetes: Pablo, Loli, Lois, Hadrián, Dani e Andrés. Tamén teño que recordar aqueles que, dunha maneira ou outra, me axudaron a ser un mellor matemático: Rodrigo, Bruno e Andrés Vales. Por último non me quero esquecer das xentes de Couxela: amigos da infancia, Pura, Puri, Tamara e o resto da familia da Cantina, Pilarina e Mariola que, entre outras moitas cousas, non se cansou nunca de "carretarme".

The PhD would have been much more arduous without all my colleagues at UCC, including amongst others Tony, Paula, Paul, Mateusz, Jake, Eduardo, Chun, Chris, Andrew, Andy and especially to Justin, who reviewed this thesis in detail and provided priceless advice. Similarly, I have to thank Oisín and Denise for creating a home away from home for me.

I extend my gratitude to UCC and to the UCC staff, specially the School of Mathematical Sciences, for the warm welcome I received when I first arrived and the help provided during my years here.

Last but not least, I must acknowledge the financial support of the Science Foundation Ireland (SFI) which made this project possible by allowing me to devote all my efforts to this thesis and to attend relevant seminars in several important institutions across Europe.

List of publications related to this thesis

Some of the content of the present thesis has been included in the following articles:

1. Rodríguez-Sanjurjo, A., Global diffeomorphism of the lagrangian flow-map for equatorially-trapped internal water waves, *Nonlinear Analysis: Theory, Methods & Applications* **149**, 156–164, 2017.

2. Rodríguez-Sanjurjo, A. & Kluczek M., Mean flow properties for equatorially trapped internal water wave–current interactions, *Applicable Analysis* **96**, no. 13, 2333–2345, 2017.

3. Rodríguez-Sanjurjo, A., Global diffeomorphism of the lagrangian flow-map for pollard-like solutions, *Annali di Matematica Pura ed Applicata (1923-)* **197**, 1787–1797, 2018.

4. Rodríguez-Sanjurjo, A., Internal equatorial water waves and wave–current interactions in the f-plane, *Monatshefte für Mathematik* **186**, no. 4, 685–701, 2018.

5. Rodríguez-Sanjurjo, A., Instability of equatorially-trapped nonhydrostatic internal geophysical water waves, *Wave Motion* **88**, 144–152, 2019.

6. Rodríguez-Sanjurjo, A., Instability of nonlinear wave-current interactions in a modified equatorial beta-plane approximation, *Journal of Mathematical Fluid Dynamics* **21**, no. 2, 12pp, 2019.

7. Martin, C.I. & Rodríguez-Sanjurjo, A. Dispersion relations for steady periodic water waves of fixed mean-depth with two rotational layers. *Discrete and Continuous Dynamical Systems* **39**, 5149-5169, 2019.

Chapter 1

Preliminaries

1.1 Governing equations

Before starting with the study of the different flows, it is convenient to introduce the relevant governing equations and boundary conditions. Several approximations and modifications of the governing equations accounting for different physical scenarios will be developed throughout this work. The Eulerian version of the governing equations, namely the mass conservation equation and the momentum equation, is presented. This establishes the base for further approximations. The assumption of a piecewise constant density (which constitutes the easiest case of an equation of state) greatly simplifies the discussion and it results in a complete set of equations that together with the appropriate boundary conditions, describe the fluid motions of interest. A brief derivation of the governing equations in the Lagrangian framework is then given. Regarding mathematical considerations, it is noted here that all the fluid quantities are represented by continuously differentiable and bounded functions unless stated otherwise. Our choice of notation follows the standard vector and tensor approach when dealing with the discussion of the equations and other fluid considerations, whereas it turns to a mathematical convention when dealing with purely mathematical statements and their proofs. For instance, the gradient of a vector field is used in some cases while the Jacobian matrix of a function is chosen in others. Taking into account that when a matrix representation of a tensor is possible, the gradient is the transpose of the Jacobian matrix. We hope that with the pertinent clarifications this will reinforce the relation between the fluid dynamic literature and the more abstract mathematical studies.

1.1.1 Mass conservation equation

The following equation expresses the physical principle that mass is neither created nor destroyed within the fluid. Let $\rho(\mathbf{x}, t)$ be a scalar function denoting the density, defined as mass per unit volume, of the fluid at a point $\mathbf{x} = (x, y, z)$ at time t. Let $\mathbf{u}(\mathbf{x}, t) = (u(\mathbf{x}, t), v(\mathbf{x}, t), w(\mathbf{x}, t))$ be the velocity of the fluid at a point $\mathbf{x}$ at time t. Then, the mass conservation equation is given by

$$\frac{\partial \rho}{\partial t} + (\mathbf{u} \cdot \nabla)\rho + \rho(\nabla \cdot \mathbf{u}) = 0\,. \tag{1.1}$$

In general, for any given fluid quantity $\varphi(\mathbf{x}, t)$, the so-called material or convective derivative is defined as

$$\frac{D\varphi}{Dt} = \frac{\partial \varphi}{\partial t} + (\mathbf{u} \cdot \nabla)\varphi \tag{1.2}$$

and it provides the rate of change of the fluid quantity $\varphi(\mathbf{x}, t)$ along the path of a given particle. By means of definition (1.2), the mass conservation equation (1.1) is written as

$$\frac{D\rho}{Dt} + \rho(\nabla \cdot \mathbf{u}) = 0\,. \tag{1.3}$$

A common assumption is that changes in pressure do not produce a variation in density. It is said then that the fluid is incompressible. If that is the case, then the density of each fluid particle remains constant and therefore

$$\frac{D\rho}{Dt} = 0\,. \tag{1.4}$$

It follows that for an incompressible fluid, the mass conservation equation (1.3) reduces to

$$\nabla \cdot \mathbf{u} = 0\,. \tag{1.5}$$

1.1.2 Momentum equation : Euler equations

The momentum equation considered here is the result of applying Newton's Second Law to an inviscid fluid (see [85] for a complete derivation under this assumption). This set of equations is known as Euler equations and they can also be derived as a particular case of the Navier-Stokes equations (see [2] for a detailed derivation). In the absence of viscous forces, the only relevant surface force is the pressure, which is

denoted by the scalar field $P(\mathbf{x}, t)$ and which is defined as force per unit area. The other type of forces to be considered in the dynamics of a fluid are the body forces. This force is defined per unit mass and it will be denoted by the vector field $\mathbf{F}(\mathbf{x}, t)$, which usually accounts for the gravitational force only. Following this notation, the vector form of the Euler equation is

$$\frac{D\mathbf{u}}{Dt} = \mathbf{F} - \frac{1}{\rho}\boldsymbol{\nabla} P \,. \tag{1.6}$$

1.1.3 Boundary conditions

One of the most complex and important aspects of water wave problems is the fact that the boundaries representing the waves are not known beforehand and they have to be derived as part of the solution. Hence, the boundary conditions for the Partial Differential Equations (PDEs) have to be imposed on unknown boundaries, commonly referred to as free surfaces. Boundary conditions in fluid mechanics are divided into kinematic and dynamic boundary conditions. Only conditions relevant to the problems addressed in this these are described here. In that regard, it is assumed that the fluid is inviscid and extends to infinity in all horizontal directions.

Kinematic boundary condition

The kinematic boundary condition expresses the idea that a particle on the boundary remains there at all times. If the free surface is a $\mathscr{C}^1$-surface given by an implicit expression and $\gamma(t) = (x(t), y(t), z(t))$ is a curve defining the path of an arbitrary particle, then the kinematic condition on the free surface is

$$z(t) = \eta(x(t), y(t), t) \,.$$

Differentiating with respect to time and using the relation between the particle position and velocity, it follows that the kinematic boundary condition for the free surface takes the form

$$w = \frac{\partial \eta}{\partial t} + u\frac{\partial \eta}{\partial x} + v\frac{\partial \eta}{\partial y} \quad \text{on } z = \eta(x, y, t) \,. \tag{1.7}$$

When the consideration of a bottom boundary is needed, it will be taken as stationary. Thus, if the bottom is situated at a hight $z = -d$ and assuming that the fluid

is inviscid, it is required that

$$w = 0 \quad \text{on } z = -d\,. \tag{1.8}$$

Otherwise, when dealing with deep water waves, the water is considered as to have infinite depth and the assumption is that the velocity vanishes descending towards this bottom placed (theoretically) at an infinite depth.

Dynamic boundary condition

For gravity waves, the surface tension can be neglected, as long as the mechanisms originating the flow motion are not taken into consideration. Under the inviscid-fluid hypothesis, the stress tensor only involves the pressure. Furthermore, the pressure is required to be continuous within the fluid and it has to be prescribed on the free surface, where it takes a constant value corresponding to the atmospheric pressure (P_{atm}). It follows then that the dynamic boundary condition is given by

$$P(\mathbf{x}, t) = P_{atm} \quad \text{on } z = \eta(x, y, t)\,. \tag{1.9}$$

It is important to note that the pressure is evaluated at the free surface (which is unknown *a priori*) and therefore nontrivial. Also, it is worth noting that this condition means that the motion of the air is decoupled from that of the water.

1.2 Lagrangian framework

The previous equations have been derived in the most common framework in the fluid dynamics literature, namely the Eulerian formulation, which describes the flow at a given time t by its velocity at each given position $\mathbf{x}$. This approach is the most fruitful in the history of fluid dynamics and its use resides in the way the measurements can be obtained. However, the appearance of new technologies might allow the use of the other main framework, the Lagrangian description. This description is solid from a mathematical viewpoint and it provides interesting results that are not available through the Eulerian specification. As most of the solutions herein are presented in the Lagrangian framework and do not have an explicit expression in Eulerian coordinates, an introduction to this description is required. The Lagrangian

approach specifies the position at time t of a particle in terms of a label. The definition of these labels and the suitable mathematical formulation of fluid quantities in terms of them are far from trivial. This is rigorously described in its most general form in [4]. Initially, the notation of [4] will be used and subsequently simplified in order to fit the main purposes of this thesis.

The following discussion assumes a three-dimensional flow, however it can be easily generalised to any dimension. Let $\mathbf{a} = (a_1, a_2, a_3)$ be the label of a given particle at some time τ. The position of that particle provided by a Lagrangian observer (an observer moving with the particle) at a later time t is denoted by the vector

$$\mathscr{X}_i(\mathbf{a}, \tau|t) \quad i = 1, 2, 3.$$

The label may be the particle's position at some time, but it could be any other quantity not related with its position. The importance of the label is that it identifies the particle uniquely. Hence, the relation with the Eulerian formulation can be expressed as follows; an Eulerian observer located at $\mathbf{x} = (x_1, x_2, x_3)$ at time t will detect that particle if and only if

$$x_i = \mathscr{X}_i(\mathbf{a}, \tau|t) \quad i = 1, 2, 3. \tag{1.10}$$

As shown in [4], the essence of Lagrangian fluid dynamics is the consideration of labels as independent variables. The Lagrangian velocity of a particle labelled by $\mathbf{a}$ at time τ is given by

$$u_i(\mathbf{a}, \tau|t) = \frac{\partial}{\partial t}\mathscr{X}_i(\mathbf{a}, \tau|t) \quad i = 1, 2, 3\,, \tag{1.11}$$

where the derivative with respect time is taken as a partial derivative due to the dependence of $\mathscr{X}_i$ on the label $\mathbf{a}$ as well. In the expression (1.11), the parenthesis indicate the evaluation of $\mathscr{X}_i$ at $\mathbf{a}$ and t. The labelling theorem proven in the first chapter of [4] extends to the case of labels other than the particle position at labelling time. Thus, the value of any particle property is independent of the time τ at which it is labelled. From now on the notation is simplified by avoiding the use of the labelling time τ. The transformation from the labelling domain to the spatial domain

$$\mathbf{a} = (a_1, a_2, a_3) \longrightarrow \mathbf{x} = (x_1, x_2, x_3) \tag{1.12}$$

is expressed by the matrix

$$\left(\frac{\partial}{\partial a_j}\mathscr{X}_i(\mathbf{a},t)\right) \quad i,j=1,2,3. \tag{1.13}$$

In order to have a useful relation between labelling and fluid variables, the Jacobian of that matrix must not vanish and the map (1.12) must be a global diffeomorphism. This Jacobian will be of great importance in the analysis of the flows described in this work. It is also important to note that even if the map (1.12) does have an inverse, it might not be possible to provide an explicit expression for it. Therefore, working within one framework is not sufficient in general, as there will be flows with an explicit expression in the Lagrangian framework which cannot be found in the Eulerian. The following definition is provided in order to establish a rigorous mathematical framework for the study of the Lagrangian solutions considered throughout this thesis.

Definition 1.2.1. *The Lagrangian description given by* (1.10) *defines a valid fluid motion and it is said to be* ***dynamically possible*** *if for each time t, the map* (1.10) *is a global diffeomorphism from the labelling domain to the fluid domain that satisfies the fluid mechanics equations and appropriate boundary conditions.*

A few remarks with respect to this definition are necessary. First, when dealing with boundaries, the regularity of the Lagrangian map must be understood as a diffeomorphism in the interior that extends continuously to the boundaries. Second, this definition assures that the solution in the form of (1.10) defines a motion of the whole fluid body, where the fluid particles do not superimpose and any particle in the fluid domain is identified by a unique label.

The governing equations derived in Eulerian coordinates have a Lagrangian counterpart. Gerstner's wave solution is presented along with the derivation of the Lagrangian governing equations in order to illustrate in a better manner the analysis of the geophysical nonlinear water waves presented in this thesis. Thus, the Lagrangian description given by Gerstner is now introduced.

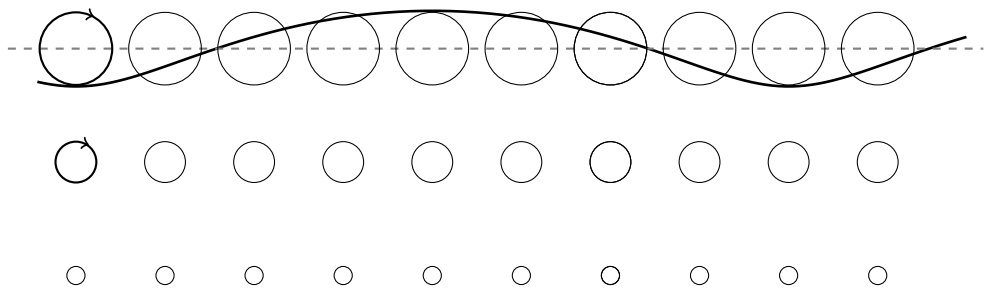

Figure 1.1: Circular paths of the particles in Gerstner's wave together with one of the possible profiles of the free surface

1.2.1 Gerstner's wave

Gerstner's wave constitutes the only-known explicit and exact solution of the nonlinear two-dimensional periodic gravity wave problem with a non-flat free surface. The solution was first found in an homogeneous fluid by Gerstner in [47], and rediscovered by Froude [45], Rankine [108] and Reech [109]. The solution is two dimensional and is only explicitly derivable in Lagrangian coordinates. Taking the labels or identifiers of any particle in the domain $\{(a,b) : a \in \mathbb{R}, b \leq b_0\}$ where $b_0 \leq 0$ is a given fixed value, the position at time t of a particle for Gerstner's wave is given by

$$\begin{cases} \mathscr{X}((a,b),t) = a - \dfrac{e^{kb}}{k}\sin(ka - \sqrt{gk}\,t) \\ \\ \mathscr{Y}((a,b),t) = b + \dfrac{e^{kb}}{k}\cos(ka - \sqrt{gk}\,t)\,, \end{cases} \tag{1.14}$$

where g is the gravity on Earth and k is the wavenumber. The labels are not the position of the particles at any time, but the centre of a circle that constitutes the path of each particle. A particle labelled by $(\tilde{a},\tilde{b})$ moves in a circle centred at $(\tilde{a},\tilde{b})$ with radius $\frac{e^{k\tilde{b}}}{k}$, the motion being clockwise with constant angular speed $\sqrt{gk}$. As b decreases from $b_0 \leq 0$, the radius of the circles diminishes and so Gerstner's wave is formed by particles moving in circles with diminishing radius as going down from the free surface. This is depicted in Figure 1.1. Furthermore, it will be shown that at a given time t, fixing $b = b_0$ corresponds to the free surface and its shape is given by a reversed trochoid.

A trochoid is the curve describing the motion of a fixed point at a given distance

from the centre of a circle which is rolling along a straight line. The parametric equations of a general trochoid, parametrised by σ, are

$$\begin{cases} x(\sigma) = \Upsilon\sigma - \Theta\sin(\sigma) \\ \\ y(\sigma) = \Upsilon - \Theta\cos(\sigma)\,, \end{cases} \tag{1.15}$$

where Υ is the radius of the circle that spins without slipping and Θ is the distance from the centre of that circle to the fixed point which describes the curve. In terms of those two values, there are three main types of trochoids which are depicted in Figure 1.2. From (1.15) it follows that

$$\begin{cases} x(\sigma) = \Upsilon\sigma - \Theta\sin(\sigma) \\ \\ y(\sigma) = \Upsilon + \Theta\cos(\sigma) \end{cases} \tag{1.16}$$

represents a symmetry with respect to the line $y = \Upsilon$, so that the trochoid has now upward cusps. Therefore, choosing

$$\Upsilon = \frac{1}{k}\,, \quad \Theta = \frac{e^{kb}}{k}\,, \quad \text{and} \quad \sigma = ka\,,$$

for a fixed b, we obtain

$$\begin{cases} x(\sigma(a)) = a - \dfrac{e^{kb}}{k}\sin(ka) \\ \\ y(\sigma(a)) = \dfrac{1}{k} + \dfrac{e^{kb}}{k}\cos(ka)\,, \end{cases}$$

where $a \in \mathbb{R} \mapsto \sigma(a) = ka \in \mathbb{R}$ is a change of variables or reparametrisation of a which does not change the domain of the labelling variable. Finally, by displacing the initial position of the sinusoid by $\sqrt{gk}\,t$ for each given time t and shifting the y-coordinate by $b - 1/k$, we recover the solution (1.14) for fixed b and t.

1.2.2 Lagrangian governing equations

It is shown that (1.14) generates a flow that satisfies the fluid mechanics governing equations for an inviscid fluid. This can be done by working with the equations

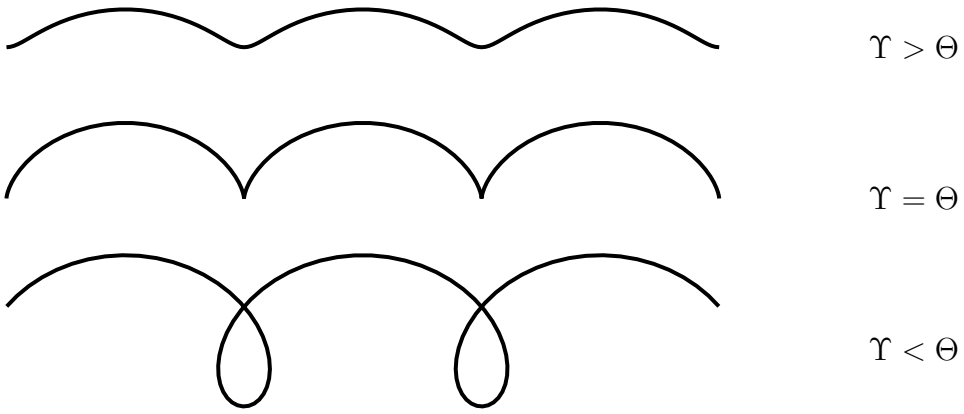

Figure 1.2: Types of trochoids: For the first case, the fixed point is inside the circle and the curve is smooth. In the second case $\Upsilon = \Theta$, the curve is known as a cycloid and presents peaks where the curve is not differentiable. The third curve results from situating the fixed point outside the circle and it intersects itself.

derived in the Eulerian framework and the implicit expression of the velocity obtained from the time derivative of (1.14). However, proceeding in this manner might obscure the fact that the description of this solution is purely Lagrangian and that it does not posses an explicit expression in Eulerian variables. Therefore, it is worth deriving the Lagrangian version of the governing equations from a Lagrangian viewpoint. This will also show that the mathematical difficulty of both approaches is equivalent and one has been chosen over the other primarily due to how measurements of fluid quantities can be taken in real life.

The Lagrangian version of the mass conservation equation can be derived as follows. At time t, let $V(t)$ be a fluid parcel of particles with fixed labels and let A be the set of labels of those particles at the labelling time s. In other words, the fluid parcel $V(t)$ is the image of A through the transformation (1.12). Thus, there are not particles entering or leaving the parcel $V(t)$. It follows that the volume of the fluid comprised by $V(t)$ might change with time but the mass is conserved, i.e. in Eulerian coordinates,

$$\frac{d}{dt}\iiint_{V(t)} \rho(\mathbf{x},t)\, dx_1\, dx_2\, dx_3 = 0\,,$$

while in terms of Lagrangian variables

$$\frac{d}{dt}\iiint_A \rho(\mathbf{a},t)J^t\, da_1\, da_2\, da_3 = 0\,,$$

where J^t is the determinant of (1.13). Hence, the time derivative commutes with the integral and from the regularity of the fluid functions it follows

$$\frac{\partial}{\partial t}\Big[\rho(\mathbf{a},t)J^t\Big] = 0\,, \tag{1.17}$$

which is the Lagrangian expression for the mass conservation. The material derivative for a quantity expressed in Lagrangian variables is just the derivative with respect to time, thus the condition for incompressibility (1.4) reduces to

$$\frac{\partial}{\partial t}\rho(\mathbf{a},t) = 0\,.$$

An application of the chain rule yields the mass conservation for an incompressible fluid in the Lagrangian framework

$$\frac{\partial}{\partial t}J^t = 0\,. \tag{1.18}$$

Particularising this to Gerstner's wave (1.14), we observe that the Jacobian matrix of the Lagrangian flow map, given by

$$\frac{\partial(\mathscr{X},\mathscr{Y})}{\partial(a,b)} = \begin{vmatrix} 1-e^{kb}\cos(ka-\sqrt{gk}\,t) & -e^{kb}\sin(ka-\sqrt{gk}\,t) \\ -e^{kb}\sin(ka-\sqrt{gk}\,t) & 1+e^{kb}\cos(ka-\sqrt{gk}\,t) \end{vmatrix} = 1-e^{2kb}\,,$$

does not depend upon time showing that the mass conservation equation (1.18) is satisfied. Furthermore, the Jacobian is positive for all $b<0$. The case $b=b_0=0$ is considered as a limit case where the wave presents peaks and the differentiability breaks down, although the profile is continuous.

Regarding the Lagrangian momentum equation for an inviscid fluid, first it is assumed that the pressure is the only stress taken into account and the body force $\mathbf{F}$ is only accounting for the gravity force. Thus, if $S(t)$ is the surface of the fluid parcel $V(t)$ at time t, the balance between momentum and forces is expressed in Eulerian coordinates as

$$\frac{d}{dt}\iiint_{V(t)} \rho\,\mathbf{u}(\mathbf{x},t)\, dx_1\, dx_2\, dx_3 = \iiint_{V(t)} \rho\,\mathbf{F}(\mathbf{x},t)\, dx_1\, dx_2\, dx_3 - \\ - \iint_{S(t)} P(\mathbf{x},t)\,\mathbf{n}^t\, dS$$

where $\mathbf{n}^t$ is the outward unit normal on $S(t)$. The next natural step will be to apply the Divergence theorem to the second integral on the right-hand side of the former equation. In order to be perfectly rigorous, the whole derivation should be done in Lagrangian coordinates. However, the algebra is quite tedious and the reader is referred to [4] for the complete derivation. Applying the divergence theorem in Eulerian coordinates gives

$$\frac{d}{dt}\iiint_{V(t)} \rho\,\mathbf{u}(\mathbf{x},t)\,dx_1\,dx_2\,dx_3 = -\iiint_{V(t)} \Big[\boldsymbol{\nabla} P(\mathbf{x},t) + \rho\,\mathbf{F}(\mathbf{x},t)\Big]\,dx_1\,dx_2\,dx_3\,,$$

which after the change of variables to the labelling domain yields

$$\frac{d}{dt}\iiint_{A} \rho\,\mathbf{u}(\mathbf{a},t)J^t\,da_1\,da_2\,da_3 = -\iiint_{A} \Big[\boldsymbol{\nabla} P(\mathbf{a},t) + \rho\,\mathbf{F}(\mathbf{a},t)\Big]J^t\,da_1\,da_2\,da_3\,.$$

The time derivative commutes with the integral and from (1.17) it follows that

$$\iiint_{A} \rho\,\frac{\partial \mathbf{u}}{\partial t}(\mathbf{a},t)J^t\,da_1\,da_2\,da_3 = -\int_{A} \Big[\boldsymbol{\nabla} P(\mathbf{a},t) + \rho\,\mathbf{F}(\mathbf{a},t)\Big]J^t\,da_1\,da_2\,da_3\,.$$

The domain A was arbitrarily chosen and the integrand is continuous, therefore

$$\rho\,\frac{\partial \mathbf{u}}{\partial t} = -\boldsymbol{\nabla} P + \rho\,\mathbf{F}\,. \tag{1.19}$$

Now, by means of the inverse of the transformation (1.12)

$$a_k = a_k(x_i,t) \qquad i,k = 1,2,3$$

which labels the particle that is at the position given by x_i at time t, equation (1.19) is expressed in terms of Lagrangian variables as

$$\rho\,\frac{\partial^2 \mathscr{X}_i}{\partial t^2} = -\sum_{j=1}^{3} \frac{\partial a_j}{\partial x_i}\frac{\partial P}{\partial a_j} + \rho\,F_i \qquad i = 1,2,3.$$

However, as long as (1.12) defines a valid change of variables,

$$\Big(\frac{\partial a_j}{\partial x_i}\Big)_{ji} \qquad i,j = 1,2,3$$

is the inverse matrix of the Jacobian matrix (1.13) and so the Lagrangian version of the momentum equation becomes

$$\rho \sum_{i=1}^{3} \frac{\partial \mathscr{X}_i}{\partial a_j} \left(\frac{\partial^2 \mathscr{X}_i}{\partial t^2} - F_i \right) = -\frac{\partial P}{\partial a_j} \qquad j = 1, 2, 3 \,. \tag{1.20}$$

In order to verify that Gerstner's wave satisfies the two-dimensional version of the equation (1.20), the following notation is used

$$\begin{aligned} a_1 &= a, \quad a_2 = b \,, \\ F_1 &= 0, \quad F_1 = -g \,, \\ \mathscr{X}_1 &= \mathscr{X}, \; \mathscr{X}_2 = \mathscr{Y} \,, \end{aligned}$$

together with the convention that subindeces refer now to partial differentiation. Hence, (1.20) takes the form

$$\begin{cases} P_a = -\rho \mathscr{X}_a \mathscr{X}_{tt} - \rho \mathscr{Y}_a (\mathscr{Y}_{tt} + g) \,, \\ \\ P_b = -\rho \mathscr{X}_b \mathscr{X}_{tt} - \rho \mathscr{Y}_b (\mathscr{Y}_{tt} + g) \,. \end{cases} \tag{1.21}$$

From the regularity of the fluid functions, it follows that $P_{ab} = P_{ba}$, so differentiating both equations yields

$$\mathscr{X}_a \mathscr{X}_{btt} + \mathscr{Y}_a \mathscr{Y}_{btt} = \mathscr{X}_b \mathscr{X}_{att} + \mathscr{Y}_b \mathscr{Y}_{att} \,. \tag{1.22}$$

Returning to Gertsner's wave, it is easy to check from (1.14) that both sides of the previous equation are equal to $gke^{kb} \sin(ka - \sqrt{gk}\, t)$, proving that Gerstner's solution satisfies the momentum equation.

Regarding the boundary conditions for Gerstner's wave, it can be seen from (1.21) that $P_a = 0$, so integrating P_b results in

$$P((a,b),t) \equiv P(b,t) = P(b_0,t) + \frac{\rho g}{2k}(e^{2kb} - e^{2kb_0}) - \rho g (b - b_0) \,. \tag{1.23}$$

The dynamic boundary condition (1.9) expressed in Lagrangian coordinates

$$P((a,b),t) = P_{atm} \quad \text{on the free surface} \,,$$

together with (1.23), implies that the only way of obtaining a pressure agreeing with both equations is by fixing b. Then, let $b = b_0$ be that fixed value defining the free surface. The pressure

$$P((a,b),t) = P_{atm} + \frac{\rho g}{2k}(e^{2kb} - e^{2kb_0}) - \rho g(b - b_0)$$

satisfies the momentum equation and it is equal to the atmospheric pressure P_{atm} along $b = b_0$. On the other hand, it has been shown in the previous subsection that for b_0 at any given time, (1.14) defines a trochoid. The easiest way of checking the kinematic boundary condition is by showing that a particle on the free surface remains there for all time. In general, any label set $\{(a,b) : a \in \mathbb{R},\, b = b^*\}$ maps bijectively into a trochoid; this can be seen in [7, 50] and for more complicated flows in the following chapters. Therefore, as $b = b_0$ represents the free surface, the kinematic boundary condition is satisfied. A particle with label (a, b_0) at a certain time lies on the trochoid representing the free surface. At any future time, this particle will be on the same trochoid although shifted by $\sqrt{gk}\,t$. The proof that the motion is indeed dynamically possible was rigorously shown in [7, 50]; similar techniques will be used in the next chapters to prove that three-dimensional flows describing nonlinear geophysical water waves are dynamically possible.

As a final observation on Gerstner's wave, it is pointed out that the motion described by this solution is rotational. Working in the Eulerian framework and considering the two-dimensional motion embedded in $\mathbb{R}^3$, where $\mathbf{u} = (u, 0, v)$, the vorticity is given by

$$\boldsymbol{\omega} = (0, \omega, 0) = \nabla \times \mathbf{u} = (0, u_y - v_x, 0)\,.$$

The vorticity is often treated as the scalar ω identified with the only nonzero component of the curl of the velocity. For any function $\varphi((a,b),t)$ representing a fluid quantity in terms of the labelling variables, it is possible to obtain an expression for φ in terms of the Eulerian variables by means the inverse of (1.14), i.e.

$$\varphi(x,y,t) = \varphi(\mathscr{X}^{-1}(x,y), \mathscr{Y}^{-1}(x,y), t)\,.$$

However, there is not an explicit expression available for Gerstner's solution. Nevertheless, taking into account that

$$\begin{pmatrix} \varphi_x \\ \varphi_y \end{pmatrix} = \begin{pmatrix} \mathscr{X}_a & \mathscr{Y}_a \\ \mathscr{X}_b & \mathscr{Y}_b \end{pmatrix}^{-1} \begin{pmatrix} \varphi_a \\ \varphi_b \end{pmatrix}$$

it is possible to obtain implicit expressions of the partial derivatives with respect to Eulerian variables and compute

$$\omega = u_y - v_x = \frac{1}{\mathscr{X}_a\mathscr{Y}_b - \mathscr{X}_b\mathscr{Y}_a}\Big[\mathscr{X}_a\mathscr{X}_{bt} - \mathscr{X}_b\mathscr{X}_{at} - \mathscr{Y}_b\mathscr{Y}_{at} + \mathscr{Y}_a\mathscr{Y}_{bt}\Big] = \frac{-2\sqrt{gk}e^{2kb}}{1-e^{2kb}}\,, \tag{1.24}$$

which is well-defined for any $b \leq b_0 < 0$. The vorticity decays as descending towards the bed and it is infinitely large on the free surface, approaching the limit case $b_0 = 0$. Due to the presence of vorticity, these waves cannot be generated from rest by conservatives forces. However, as discussed in [107, 122], once the rotation of the Earth is considered the vorticity is introduced into the problem and swell waves can be well described by Gerstner-like waves.

1.3 Geophysical flows

As defined in [33], geophysical fluid dynamics is the study of flows occurring naturally on Earth. The main factor distinguishing this discipline from traditional fluid mechanics is the consideration of rotational effects and, in some cases, the incorporation of stratification into the modelling of the flows. The presence of ambient rotation, such as the one due to the Earth's spin about its axis, introduces two acceleration terms in the equations of motion. In the rotating framework, these terms can be interpreted as forces: the Coriolis and the centripetal force. On the other hand, stratification arises when dealing with flows where fluids with different densities coexist. Under gravitational forces, the heaviest fluid tends to be the lowest. However, fluid motions might disturb this equilibrium and small perturbations can generate internal waves, such as the ones analysed in subsequent chapters. Large perturbations, especially those maintained over time, may also cause mixing and convection.

1.3.1 Rotating framework of reference

Taking into account the importance of rotation in geophysical flows, it is wise to work with a rotating framework instead of an inertial framework of reference. Here, an inertial framework refers to a coordinate system at rest or moving at a constant

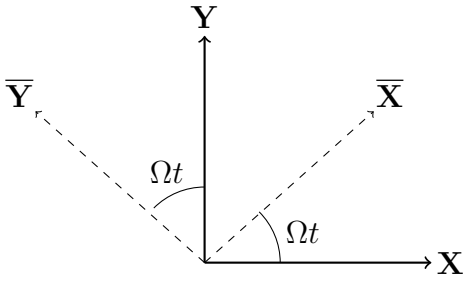

Figure 1.3: Axes rotation

velocity without rotation. In the case of the Earth this could be, for instance, a set of rigid axes with the origin on a distant "fixed" star. The consideration of a rotating framework adds extra terms to the equations of motion but eliminates moving boundaries and having to subtract the ambient rotation. Let us consider a two-dimensional coordinate system as depicted in Figure 1.3, with a set of axes $\{\mathbf{X}, \mathbf{Y}\}$ and its rotation by an angle Ωt at a given time t with axes $\{\overline{\mathbf{X}}, \overline{\mathbf{Y}}\}$. Any vector has an expression in both coordinate systems related by

$$\begin{pmatrix} \overline{x} \\ \overline{y} \end{pmatrix} = \begin{pmatrix} \cos(\Omega t) & \sin(\Omega t) \\ -\sin(\Omega t) & \cos(\Omega t) \end{pmatrix} \begin{pmatrix} x \\ y \end{pmatrix}. \tag{1.25}$$

In particular, if $\mathbf{r}(t) = (x(t), y(t))$ is a position vector describing an arbitrary motion in terms of t and $(\overline{x}(t), \overline{y}(t))$ are the coordinates of the same vector in the rotation framework, it follows that

$$\begin{pmatrix} \overline{x}(t) \\ \overline{y}(t) \end{pmatrix} = \begin{pmatrix} \cos(\Omega t) & \sin(\Omega t) \\ -\sin(\Omega t) & \cos(\Omega t) \end{pmatrix} \begin{pmatrix} x(t) \\ y(t) \end{pmatrix} = \begin{pmatrix} \cos(\Omega t)x(t) + \sin(\Omega t)y(t) \\ -\sin(\Omega t)x(t) + \cos(\Omega t)y(t) \end{pmatrix}.$$

Now, let

$$(\overline{u}, \overline{v}) = \left(\frac{d\overline{x}}{dt}, \frac{d\overline{y}}{dt}\right)$$

be the velocity in the rotating framework and let

$$(U, V) = \left(\frac{dx}{dt}, \frac{dy}{dt}\right)$$

be the velocity in the inertial (fixed) frame. The previous velocity (U, V) can be expressed in the rotating frame by means of (1.25),

$$\begin{pmatrix} \overline{U} \\ \overline{V} \end{pmatrix} = \begin{pmatrix} \cos(\Omega t) & \sin(\Omega t) \\ -\sin(\Omega t) & \cos(\Omega t) \end{pmatrix} \begin{pmatrix} U \\ V \end{pmatrix}.$$

Then, it follows that the relation between the velocities in the rotating framework is

$$\begin{pmatrix} \overline{U} \\ \overline{V} \end{pmatrix} = \begin{pmatrix} \overline{u} \\ \overline{v} \end{pmatrix} - \Omega \begin{pmatrix} \overline{y} \\ -\overline{x} \end{pmatrix}.$$

Differentiating again with respect to time, we establish the relationship between $(\overline{a}, \overline{b})$ which refers to the acceleration in the rotating frame and $(\overline{A}, \overline{B})$ which is the acceleration in the inertial frame expressed in terms of the rotating coordinate system

$$\begin{pmatrix} \overline{A} \\ \overline{B} \end{pmatrix} = \begin{pmatrix} \overline{a} \\ \overline{b} \end{pmatrix} + 2\Omega \begin{pmatrix} -\overline{v} \\ \overline{u} \end{pmatrix} - \Omega^2 \begin{pmatrix} \overline{x} \\ \overline{y} \end{pmatrix}. \tag{1.26}$$

On the other hand, if $\mathbf{K}$ is the unit vector in the direction of the North-South pole axis and Ω is the angular velocity of Earth's rotation, the rotation in three dimensions is given by

$$\boldsymbol{\Omega} = \Omega \mathbf{K}\,.$$

Therefore, for a flow described in the Eulerian framework, the absolute acceleration (1.26) takes the form

$$\mathbf{A} = \frac{D\mathbf{u}}{Dt} + 2(\boldsymbol{\Omega} \times \mathbf{u}) + \boldsymbol{\Omega} \times (\boldsymbol{\Omega} \times \mathbf{r})\,, \tag{1.27}$$

where the lines over the letters have been dropped but they still express quantities in the rotating frame. The first term on the right hand side of (1.27) represents the convective derivative of the velocity of a flow expressed in the Eulerian framework. The second term on the right hand side of (1.27) represents the Coriolis force and the final term is the centripetal force.

In order to describe the wave motion in the rotating Earth, a framework with the origin at a point on Earth's surface is considered. The zonal coordinate x is taken pointing horizontally due East, the meridional coordinate y is pointing horizontally due North and the coordinate z is in the direction of the local vertical oriented "upwards" (in the direction of the line joining the centre of the Earth with the point of the surface taken as origin, see Figure (1.4a)). For the purposes of the present study, the Earth is taken to be a perfect sphere of radius $R = 6378\,\text{km}$, rotating with constant rotational speed of $\Omega = 7.29 \times 10^{-5}\,\text{rad}\,\text{s}^{-1}$ around the polar axis towards East. Then, for any given latitude ϕ, the rotation axis in terms of the unit vectors

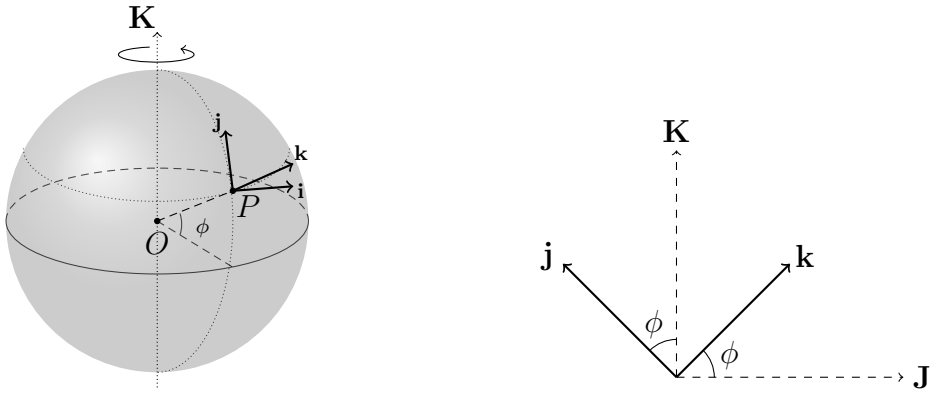

(a) Rectangular coordinate system at a point P on the Earth's surface at latitude ϕ

(b) Latitude angle ϕ in terms of the polar axis for x fixed.

Figure 1.4: Rotational framework of reference.

given in Figure 1.4 is

$$\mathbf{K} = \cos\phi\,\mathbf{j} + \sin\phi\,\mathbf{k}\,.$$

Therefore, the momentum equation (1.6) incorporating the rotational acceleration (1.27) takes the form

$$\frac{D\mathbf{u}}{Dt} + 2(\mathbf{\Omega}\times\mathbf{u}) + \mathbf{\Omega}\times(\mathbf{\Omega}\times\mathbf{r}) = -\frac{1}{\rho}\nabla P + \mathbf{F}\,, \tag{1.28}$$

where $\mathbf{\Omega} = \Omega\cos\phi\,\mathbf{j} + \Omega\sin\phi\,\mathbf{k}$. Ignoring the term involving the centripetal force, the so-called geophysical equations are obtained, cf. [33],

$$\begin{cases} u_t + uu_x + vu_y + wu_z + 2\Omega w\cos\phi - 2\Omega v\sin\phi = -\dfrac{1}{\rho}P_x\,, \\[2ex] v_t + uv_x + vv_y + wv_z + 2\Omega u\sin\phi = -\dfrac{1}{\rho}P_y\,, \\[2ex] w_t + uw_x + vw_y + ww_z - 2\Omega u\cos\phi = -\dfrac{1}{\rho}P_z - g\,, \end{cases} \tag{1.29}$$

where ϕ represents the latitude, $g = 9.8\,\mathrm{m\,s^{-2}}$ is the gravitational constant, ρ represents the water density and P is the pressure. Here the Coriolis parameters $f = 2\Omega\sin\phi$ and $\hat{f} = 2\Omega\cos\phi$ have been made explicit and it is noted that (1.29)

constitutes the base momentum equation used throughout this work. Different approximations will apply depending on the physical situations described in each case.

Chapter 2

Dynamical analysis of equatorially-trapped internal water waves

In this chapter, a recently-derived flow describing equatorially-trapped water waves is proven to be dynamically possible. The flow is given in the Lagrangian framework outlined in Chapter 1. The main result of this chapter, published in [110], establishes that three-dimensional Lagrangian flow map, which describes a nonlinear exact solution to the geophysical governing equations, is a global diffeomorphism.

2.1 Equatorially-trapped waves

The solution analysed in this chapter was derived in [14] by Constantin and it describes equatorially-trapped nonhydrostatic internal water waves propagating eastward in a layer above a thermocline and beneath a near-surface layer with predominance of wind waves. A thermocline is a thin interface within which an abrupt change in temperature occurs. Consequently, the thermocline divides two ocean layers of different temperature which results in two layers of different density. More generally, a pycnocline is an interface where density changes rapidly. This can be due to a change in temperature but not only, for instance salinity differences can account for that change in density as well. Therefore, as only changes in density are considered throughout this work, the interface described here should be referred to as a pycnocline. However, to be in accordance with [14] and the rest of the literature referenced, the term thermocline is used. Remarkably, a kinematic boundary condition on the thermocline is accommodated by considering a layer with a uniform current that decays towards the motionless deep water layer, producing a more realistic scenario than the previous hydrostatic models considered in [13, 64]. The

consideration of a thermocline has been justified by observations near the equator that reveal the existence of an approximately 120 m-deep layer of warm and less dense water overlaying a deeper layer of colder water. In that scenario, the generation of an internal wave, which constitutes the three-dimensional analogue of a surface wave, is possible; more details are given in [14].

The aim of this chapter is to complete the mathematical analysis of the solution [14], showing for the first time that the Lagrangian map describing the flow motion defines a global diffeomorphism, thereby proving that the fluid motion is dynamically possible. This provides the first rigorous justification of such explicit internal wave solutions.

The solution presented here belongs to the so-called Gerstner-like solutions. Several solutions describing a variety of physical and geophysical models have been derived and analysed in [6, 11, 13, 14, 20, 58–60, 63, 64, 76, 78, 100, 120]. A general overview of these Gerstner-like solutions is available in [62] and the importance of further investigations combining these theoretical analyses with laboratory experiments is discussed in [5].

2.2 Geophysical model and β-plane equations

In order to provide an complete explanation of the main result of this chapter, the five-layer model considered in [14] describing equatorially-trapped internal waves is briefly outlined. The waves studied here are assumed to be affected by Coriolis forces. Hence, following the derivation of the geophysical governing equations in Section 1.3.1, where (1.29) was obtained, the following approximation is adopted. Generally, for oceanographic studies which rely on a local flat Cartesian coordinate system, it is reasonable to approximate a given latitude in the spherical setting by $\phi = y/R$, where y is the meridional coordinate and R is the Earth's radius. If the motion is restricted to a small latitudinal strip around a given reference latitude ϕ_0, a first-order Taylor expansion about ϕ_0 of the Coriolis terms

$$f(\phi) = 2\Omega \sin\phi \approx 2\Omega \sin\phi_0 + 2\Omega \cos(\phi_0)\Big(\frac{y}{R} - \phi_0\Big)\,, \tag{2.1}$$

$$\hat{f}(\phi) = 2\Omega \cos\phi \approx 2\Omega \cos\phi_0 - 2\Omega \sin(\phi_0)\Big(\frac{y}{R} - \phi_0\Big) \tag{2.2}$$

normally offers a reasonably good approximation. In this particular case, the flow is located around the equator and therefore ϕ_0 is taken to be zero. Furthermore, the equator acts like a natural boundary and the waves are confined to a equatorial strip spreading roughly from 2.5°S to 2.5°N, justifying the previous Taylor approximation. Then, if $\beta := 2\Omega/R$, it follows that

$$f \approx \beta y \quad \text{and} \quad \hat{f} \approx 2\Omega\,.$$

Now, if $\mathbf{u} = (u, v, w)$ denotes the velocity field of the flow, the equations (1.29) are approximated by

$$\begin{cases} u_t + uu_x + vu_y + wu_z + 2\Omega w - \beta yv = -\dfrac{1}{\rho}P_x\,, \\[2ex] v_t + uv_x + vv_y + wv_z + \beta yu = -\dfrac{1}{\rho}P_y\,, \\[2ex] w_t + uw_x + vw_y + ww_z - 2\Omega u = -\dfrac{1}{\rho}P_z - g\,, \end{cases} \tag{2.3}$$

which are known as the β-plane approximation of the governing equations for geophysical ocean waves (cf. [33]). In addition, the velocity still has to satisfy the mass conservation equation (1.5).

Let us now briefly describe the physical model, depicted in Figure 2.1, which accommodates the oscillations of the thermocline by means of a kinematic boundary condition. The two densities above and below the thermocline are given by $\rho_0 < \rho_+$. Then, the model describes internal geophysical water waves propagating at constant speed c towards east. These waves have vanishing meridional velocity (i.e. $v = 0$) and their motion is confined to a region beneath the near-surface layer denoted by $\mathcal{L}(t)$ whose lower boundary is given by $z = \eta_+(x, y, t)$.

From the assumption on the periodicity of the waves and the eastward propagation at constant speed c, the space-time dependence can be made explicit. In particular, the velocity field, the internal free surface and the boundaries between the different regions can be expressed as functions of $(x - ct, y)$. In this way, the previous interface takes the form $z = \eta_+(x, y, t) = \eta_+(x - ct, y)$ and the thermocline is the surface given by $z = \eta_0(x - ct, y)$. These two interfaces determine the region

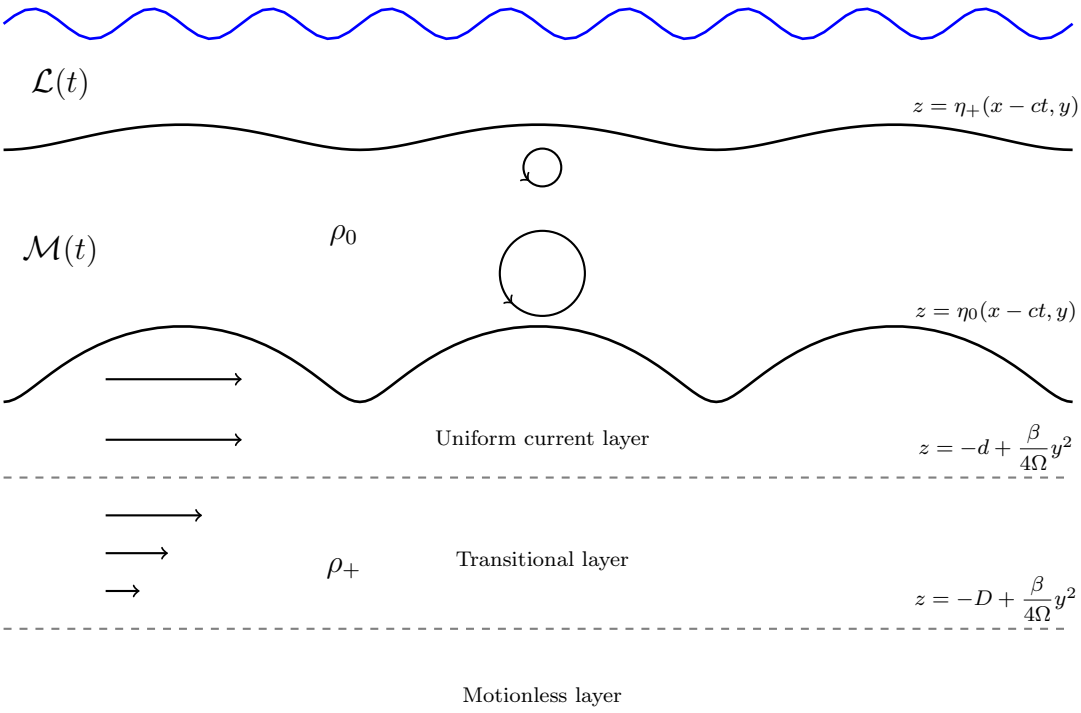

Figure 2.1: Depiction of the different flow regions for a fixed latitude y. $\mathcal{L}(t)$ denotes the region where the wind waves take place and for which the motion is not addressed. The thermocline $z = \eta_0(x - ct, y)$ is specified by an inverted trochoid propagating eastward at constant speed c. Above it, we have the region $\mathcal{M}(t)$ where the oscillations of the thermocline are important and which flow motion constitutes the analysis of this chapter. The two regions below $\mathcal{M}(t)$ accommodate the nonhydrostatic condition by means of a current decaying towards the motionless bed.

$\mathcal{M}(t)$ where the flow solution is given by Lagrangian variables. Finally, there are two other surfaces, $z = \eta_1(x - ct, y)$ and $z = \eta_2(x - ct, y)$, that define the transition of the velocity field towards the bottom. Typical equatorial depth values for these layers are approximately 60 m for $\mathcal{L}(t)$, 120 m for $\mathcal{M}(t)$, 160 m for the beginning of the transitional layer and 200 m for the motionless layer. The governing equations for this flow are completed with boundary conditions on each of these interfaces. The pressure is assumed to be continuous throughout the fluid and across each interface in particular, which imposes a condition on each interface. In addition, the following

kinematic boundary conditions, as discussed in the first chapter, are required

$$w = \frac{\partial \eta_i}{\partial t} + u\frac{\partial \eta_i}{\partial x} + v\frac{\partial \eta_i}{\partial y}\,, \quad i = 0, 1, 2\,. \tag{2.4}$$

Now, taking into account that v vanishes in the fluid region, the kinematic boundary conditions are reduced to

$$w = \frac{\partial \eta_i}{\partial t} + u\frac{\partial \eta_i}{\partial x}\,, \quad i = 0, 1, 2\,. \tag{2.5}$$

It is important to note that the motion in the three deepest layers will be given by means of Eulerian variables therefore it is straightforward that the motion is dynamically possible in these layers once it satisfies the governing equations. The interesting point, and the focus of this chapter, will be the dynamics in the region $\mathcal{M}(t)$ described by the mapping from the Lagrangian labelling domain to three-dimensional fluid domain. Nevertheless, a brief description of the flow in the four different regions beneath $\mathcal{L}(t)$ is given in order to provide a comprehensive understanding of the whole situation. Further details are provided in [14].

2.3 Exact solution

The solution derived in [14] is given in each of the layers separately, beginning with the regions below the thermoline. These three first solutions are presented in the Eulerian framework and it is easy to check that they satisfy the governing equations and boundary conditions. Thus, their velocity field and pressure are provided only due to their importance in prescribing the exact and explicit solution in the layer above the thermocline.

The deep motionless water layer

The deepest layer is determined by the surface $z = \eta_2(x - ct, y) := -D + \frac{\beta}{4\Omega}y^2$ for some fixed equatorial depth D. For $z < \eta_2(x - ct, y)$, the water is in the hydrostatic state, i.e.,

$$u = v = w = 0\,,$$

and the pressure is of the form

$$P = P_0 - \rho_+ g z\,.$$

where P_0 is an integration constant.

The transitional layer

In this case, setting

$$z = \eta_1(x - ct, y) := -d + \frac{\beta}{4\Omega} y^2$$

for some equatorial depth $d < D$, together with the previous interface $\eta_2(x - ct, y)$, determines this transitional layer where the velocity flow is defined to be $v = w = 0$, and

$$u(x - ct, y) = \frac{c}{D - d} \left(z - \frac{\beta}{4\Omega} y^2 + D \right). \tag{2.6}$$

Therefore, the expression for the continuous pressure must be

$$P(x - ct, y, z) = P_0 - \rho_+ g z + \rho_+ \frac{\Omega c}{D - d} \left(z - \frac{\beta}{4\Omega} y^2 + D \right)^2. \tag{2.7}$$

It is worth noting that the interfaces given by η_1 and η_2 are parabolic in y agreeing with the trapped character of the flow considered.

The layer beneath the thermocline

The flow for $z \in (\eta_1(x - ct, y), \eta_0(x - ct, y))$ is considered to be uniform, with

$$u = c\,, \quad v = w = 0\,,$$

where the speed $c > 0$ will depend upon the flow above the thermocline by means of the dispersion relation (2.11). The pressure that satisfies (2.3) with $\rho = \rho_+$ and is continuous across η_1 is given by

$$P(x - ct, y, z) = P_0 - \rho_+ g z + 2\rho_+ \Omega c \Big(z - \frac{\beta}{4\Omega} y^2 \Big) + \Omega \rho_+ g c (D + d) \tag{2.8}$$

for all z in (η_1, η_0).

2.3.1 Solution above the thermocline

Attention is now focused on the layer $\mathcal{M}(t)$. The exact solution of the β-plane equations (2.3) was made explicit in [14] by using the Lagrangian framework. The

positions of the fluid particles at time t in terms of the labelling variables (q, s, r) are

$$\begin{cases} x(q,s,r;t) = q - \dfrac{1}{k} e^{-k(r+\zeta(s))} \sin[k(q-ct)] \\ \\ y(q,s,r;t) = s \\ \\ z(q,s,r;t) = -d_0 + r - \dfrac{1}{k} e^{-k(r+\zeta(s))} \cos[k(q-ct)] \end{cases} \tag{2.9}$$

where $k = 2\pi/L$ is the wavenumber for a given wavelength L, while $d_0 > 0$ fixes the mean depth of the thermocline at the equator to be $[d_0 - r_0]$. It is also assumed that the labelling variable r is such that

$$r \geq r^* := \min_{s \in [-s_0, s_0]} \{r_0(s)\} > 0\,, \tag{2.10}$$

where $r_0(s)$ is a continuous function of s. Hence, it attains its minimum in the compact set $[-s_0, s_0]$. Its implicit expression is given later on. The wave phase speed is subjected to the following dispersion relation

$$c = \frac{\rho_+ - \rho_0}{\rho_0} \cdot \frac{-\Omega + \sqrt{\Omega^2 + kg\dfrac{\rho_0}{\rho_+ - \rho_0}}}{k} > 0 \tag{2.11}$$

and the function ζ in (2.9) expressing the decay from the Equator is

$$\zeta(s) = \frac{\beta s^2}{2(kc - 2\Omega)}. \tag{2.12}$$

Looking at previous models [11, 13], it is suggested that if r can be expressed as a function of s, this allows to determine a surface with the property that a particle located initially on this surface remains there for all time, this fact being equivalent to the kinematic conditions (2.5). The pressure is assumed to be continuous through the interfaces. This condition is sufficient for obtaining the function $r_0(s)$ specifying the thermocline. Taking the following notation

$$\xi := k(r + \zeta(s))\,, \tag{2.13}$$

$$\theta := k(q - ct)\,. \tag{2.14}$$

The expression for the pressure in this region takes the form

$$P(q-ct,s,r)=\rho_0\frac{kc^2-2\Omega c}{2k}e^{-2\xi}-\rho_0 gr+\rho_0\frac{kc^2-2\Omega c+g}{k}e^{-\xi}\cos\theta+\tilde{P}_0\,, \quad (2.15)$$

where the constant $\tilde{P}_0$ results from the integration of the pressure satisfying the governing equations for the given solution (2.9). Then, the thermocline is the regular surface given parametrically by

$$(q,s)\mapsto\left(q-\frac{1}{k}e^{-k(r_0(s)+\zeta(s))}\sin\theta,\ s,-d_0+r_0(s)-\frac{1}{k}e^{-k(r_0(s)+\zeta(s))}\cos\theta\right)$$

where $r_0(s)$ is the unique solution to the nonlinear equation

$$\mathscr{F}(r)=P_0-\tilde{P}_0-\rho_+\frac{\beta c}{2}s^2+\rho_+ gd_0-\rho_+\Omega c(D+d-2d_0) \quad (2.16a)$$

with

$$\mathscr{F}(r):=\rho_0(kc^2-2\Omega c)\left[r+\frac{1}{2k}\exp\left(-2kr-\frac{k\beta}{kc-2\Omega}s^2\right)\right]. \quad (2.16b)$$

The upper boundary $z=\eta_+$ is obtained in the same manner, where $r_+(s)$ is the resulting implicit function.

2.4 Main result: flow dynamically possible

The main result of this chapter states that the motion throughout the layer $\mathcal{M}(t)$ is dynamically possible. In order to prove this, the map (2.9) from the labelling domain into the fluid domain needs to be a global diffeomorphism. First of all, the problem is simplified by showing that it is enough to show the result for a fixed time. Let that time be $t=0$, then the solution takes the form

$$\begin{cases} x=q-\dfrac{1}{k}e^{-k(r+\zeta(s))}\sin(kq) \\ \\ y=s \\ \\ z=-d_0+r-\dfrac{1}{k}e^{-k(r+\zeta(s))}\cos(kq)\,. \end{cases} \quad (2.17)$$

The following notation is introduced

$$(q,s,r) \in \mathscr{D} \longmapsto F(q,s,r) = (x(q,s,r;0), y(q,s,r;0), z(q,s,r;0))\,, \tag{2.18}$$

where x, y and z are given by (2.17) and

$$\mathscr{D} = \{(q,s,r) : q \in \mathbb{R}, s \in (-s_0, s_0),\, r \in (r_0, r_+)\}. \tag{2.19}$$

In order to analyse the diffeomorphic character of (2.9), it will be enough to study it for the operator F, which corresponds to the initial time $t = 0$, and then make use of the following change of variables and shift in the x variable,

$$F(q - ct, s, r) + (ct, 0, 0)\,,$$

to recover the solution (2.9) for any other time t. It is worth noting that, for every fixed r and s, z is $(2\pi/k)$-periodic in q and x is $(2\pi/k)$-periodic in q excepting a linear shift of $2\pi/k$. Therefore, we could restrict our study of the mapping (2.17) to the following domain

$$\mathscr{D}_L = \{(q,s,r) : q \in (0, L),\, s \in (-s_0, s_0),\, r \in (r_0, r_+)\}, \tag{2.20}$$

although the approach taken here elegantly avoids the explicit calculations given in the proof for Gerstner's wave contained in [7]. A schematic picture of the transformation is shown in Figure 2.2. The proof is structured in two lemmas and a final theorem. The main argument relies upon the application of the fundamental Invariance of Domain theorem. The result can be proven by algebraic-topological arguments or by means of Degree Theory, c.f. [115]. The proof given in [90] is provided in the Appendix A.

Theorem 2.4.1 (Invariance of Domain Theorem)**.** *If $U \subset \mathbb{R}^n$ is an open set and $f : U \to \mathbb{R}^n$ is a continuous one-to-one mapping, then $f(U)$ is open.*

Remark 2.4.1. *If $f : \mathbb{R}^n \to \mathbb{R}^n$ is a continuous one-to-one mapping then the mapping $f : \overline{U} \to f(\overline{U})$ is continuous and bijective. Furthermore, by the Invariance of Domain Theorem it follows that this mapping is also open. Indeed, for any open set B in the relative topology of $\overline{U}$*

$$B = A \cap \overline{U} \qquad \textit{where } A \textit{ is open in } \mathbb{R}^n\,.$$

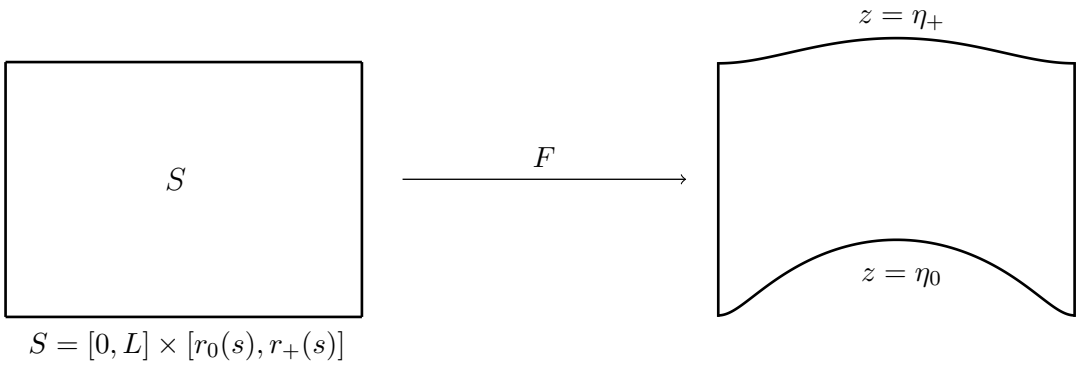

Figure 2.2: Mapping from the labelling domain corresponding to a fixed latitude $y = s$, a whole period $L = 2\pi/k$ for $r \in [r_0, r_+]$ to the fluid region contained between the thermocline and the upper boundary of $\mathcal{M}(t)$.

Now, from the injectivity of f, it follows that

$$f(B) = f(A \cap \overline{U}) = f(A) \cap f(\overline{U})$$

and from the Invariance of Domain Theorem $f(A)$ is open in $\mathbb{R}^n$. Thus, $f(B)$ is open in $f(\overline{U})$. It is noted here that for a bijective mapping f, f is continuous and open if and only if f is a homeomorphism and if and only if $f(\overline{U}) = \overline{f(U)}$ (see Theorem III.12.2 in [36]).

Therefore, it has been shown that the continuity and injectivity of f in $\mathbb{R}^n$ implies that $f : \overline{U} \to f(\overline{U}) = \overline{f(U)}$ is a homeomorphism.

Before making use of the Invariance of Domain, a first result regarding the regularity of the solution (2.9) is given.

Lemma 2.4.1. *F is a local diffeomorphism from $\mathscr{D}$ onto its image by F.*

Proof. The differential of F at (q, s, r) is given by the following Jacobian matrix

$$DF_{(q,s,r)} = \begin{pmatrix} 1 - e^{-k(r+\zeta(s))}\cos(kq) & f'(s)e^{-k(r+\zeta(s))}\sin(kq) & e^{-k(r+\zeta(s))}\sin(kq) \\ 0 & 1 & 0 \\ e^{-k(r+\zeta(s))}\sin(kq) & f'(s)e^{-k(r+\zeta(s))}\cos(kq) & 1 + e^{-k(r+\zeta(s))}\cos(kq) \end{pmatrix},$$

whose determinant is

$$\begin{vmatrix} 1 - e^{-k(r+\zeta(s))}\cos(kq) & e^{-k(r+\zeta(s))}\sin(kq) \\ e^{-k(r+\zeta(s))}\sin(kq) & 1 + e^{-k(r+\zeta(s))}\cos(kq) \end{vmatrix} = 1 - e^{-2k(r+\zeta(s))}.$$

By the requirement (2.10) and the expression for f given by (2.12), it follows that

$$-2k(r+\zeta(s)) < 0 \quad \text{for all} \quad s \in (-s_0, s_0) \quad \text{and} \quad r \in (r_0(s), r_+(s)). \tag{2.21}$$

Therefore,

$$1 - e^{-2k(r+\zeta(s))} > 0$$

and so the determinant is positive for all $(r,s) \in (-s_0, s_0) \times (r_0(s), r_+(s))$. It is easy to check that F has continuous partial derivatives in any neighbourhood of $(q,s,r) \in \mathscr{D}$. Hence, F is a continuously differentiable function with a non-zero Jacobian. By the Inverse Function Theorem, F has a local inverse that is differentiable and so it is a local diffeomorphism onto its range.

□

Lemma 2.4.2. *The map F is globally injective on $\overline{\mathscr{D}}$.*

We note here that the following proof actually shows that F is injective on $\mathbb{R}^3$.

Proof. Let (q_1, s_1, r_1) and (q_2, s_2, r_2) be two arbitrary points of $\mathbb{R}^3$. Assuming that

$$F(q_1, s_1, r_1) = F(q_2, s_2, r_2), \tag{2.22}$$

we will show that $(q_1, s_1, r_1) = (q_2, s_2, r_2)$. By hypothesis,

$$y(q_1, s_1, r_1) = y(q_2, s_2, r_2)\,,$$

so $s_1 = s_2$. Hence, we can fix s and focus on checking the injectivity on the x and z components. Once we have fixed $s \in (-s_0, s_0)$, writing F (in an abuse of notation) as

$$F(q,r) = (q, r - d_0) + h(q,r)\,, \tag{2.23a}$$

where

$$h(q,r) = -\frac{1}{k} e^{-k(r+\zeta(s))}(\sin(kq), \cos(kq))\,. \tag{2.23b}$$

Due to the regularity of h, it is possible to apply the mean-value inequality for functions of several variables contained in Appendix A, which in this case yields

$$|h(q_1, r_1) - h(q_2, r_2)| \leq \max_{\tau \in [0,1]} \|Dh_{\tau(q_1,r_1)+(1-\tau)(q_2,r_2)}\| \cdot |(q_1, r_1) - (q_2, r_2)|\,, \tag{2.24}$$

where $|\cdot|$ is the Euclidean norm and $\|\cdot\|$ is the matrix norm induced by the latter, i.e.

$$\|M\| = \sup\{|M(q,r)| : (q,r) \in \mathbb{R}^2 \quad \text{such as} \quad |(q,r)| = 1\}.$$

We have that

$$\begin{aligned}
|Dh_{(q,r)}(\sin(a),\cos(a))^T| &\leq e^{-k(r+\zeta(s))} \left| \begin{pmatrix} -\cos(kq) & \sin(kq) \\ \sin(kq) & \cos(kq) \end{pmatrix} \begin{pmatrix} \sin a \\ \cos a \end{pmatrix} \right| \\
&= e^{-k(r+\zeta(s))} \left| \begin{pmatrix} -\cos(kq)\sin a + \sin(kq)\cos a \\ \sin(kq)\sin a + \cos(kq)\cos a \end{pmatrix} \right| \\
&= e^{-k(r+\zeta(s))} \left| \begin{pmatrix} sin(kq-a) \\ \cos(kq-a) \end{pmatrix} \right| = e^{-k(r+\zeta(s))}\,,
\end{aligned}$$

where $\{(\sin(a),\cos(a))\}$ for $a \in [0,2\pi)$ characterises the unitary vectors for the Euclidean norm $|\cdot|$. It follows that

$$\|Dh_{(q,r)}\| = e^{-k(\tilde{r}+\zeta(s))}$$

for $\tilde{r} = \min\{r : r \in [r_0(s), r_+(s)],\ \text{for } s \text{ fixed}\}$ and so

$$\max_{\tau\in[0,1]} \|Dh_{\tau(q_1,r_1)+(1-\tau)(q_2,r_2)}\| \leq e^{-k(\tau r_1+(1-\tau)r_2+\zeta(s))} \leq e^{-k(r+\zeta(s))}\,,$$

where $r = \min\{r_1, r_2\}$. Therefore, from the expression of F in terms of h and (2.24), the following is obtained

$$\begin{aligned}
0 = |F(q_1,r_1) - F(q_2,r_2)| &\geq |(q_1-q_2, r_1-r_2)| - e^{-k(r+\zeta(s))}|(q_1,r_1)-(q_2,r_2)| \\
&= (1 - e^{-k(r+\zeta(s))})|(q_1-q_2, r_1-r_2)|\,.
\end{aligned}$$

Finally, as in the previous lemma, $1 - e^{-2k(r+\zeta(s))} > 0$. Thus

$$|(q_1-q_2, r_1-r_2)| \leq \frac{1}{1-e^{-2k(r+\zeta(s))}} |F(q_1,r_1) - F(q_2,r_2)| = 0\,.$$

The injectivity of F follows from the properties of the norm. □

The main theorem of this chapter is now presented. As mentioned, its proof relies on the Invariance of Domain theorem and on the the assumption (2.10) together with the choice (2.12) for ζ.

Theorem 2.4.2 (The motion is dynamically possible)**.** *The map defined by* (2.9) *is a global diffeomorphism from* $\{(q,s,r) : q \in \mathbb{R},\ s \in (-s_0, s_0), r \in (r_0, r_+)\}$ *into the fluid region* $\mathcal{M}(t)$ *that extends continuously to the boundaries.*

Proof. From Lemma (2.4.1) and Lemma (2.4.2), F is an injective local diffeomorphism from $\mathscr{D}$ into its range. By the Invariance of Domain Theorem and the Remark 2.4.1, F is a homeomorphism from $\overline{\mathscr{D}}$ into $\overline{\mathcal{M}(t)}$ (the fluid region between the thermocline and the layer $\mathcal{L}(t)$ including the boundaries). For any homeomorphism, $F(\partial\mathscr{D}) = \partial(F(\mathscr{D}))$ and therefore F maps boundaries into boundaries. In addition,

$$F : \mathscr{D} \subset \mathbb{R}^3 \mapsto F(\mathscr{D}) = \mathcal{M}(t) \subset \mathbb{R}^3$$

is a global diffeomorphism on the open set $\mathscr{D}$ as it is a bijective local diffeomorphism. □

The Invariance of Domain theorem offers an elegant alternative for proving the surjectivity of F onto the fluid region and the existence of a global inverse. Theorem 2.4.2, together with the derivation given in [14] of a pressure satisfying the governing equations, establishes that (2.9) provides a valid solution that results in a flow that is dynamically possible. Results similar to the one presented here were first given studied on Gerstner's wave [7,9,50] and more recently in [118] for geophysical surface waves. Moreover, we will show a similar result for a more challenging flow in Chapter 6.

As a technical remark, we may consider the natural complex extension of the operator F for a fixed s as given in (2.23). Let G be the complex domain given by

$$G = \{\vartheta \in \mathbb{C} : 0 < \Re(\vartheta) < 2\pi/k,\ r_0(s) < \Im(\vartheta) < r_+(s)\}$$

and Ψ the natural complex extension of F defined by

$$\begin{array}{rccl} \Psi: & G \subset \mathbb{C} & \longrightarrow & \mathbb{C} \\ & \vartheta & \longmapsto & \Psi(\vartheta) = \vartheta - i(d_0 - \dfrac{1}{k} e^{-k\zeta(s)} e^{-ik\overline{\vartheta}}), \end{array} \tag{2.25}$$

where $\vartheta = q + ir$, $\Re$ stands for the real part, $\Im$ for the imaginary part and $\overline{\vartheta}$ for the complex conjugate. It is possible to use this expression to prove that Ψ is a one-to-one function, in a similar way as it was shown for Gerstner's wave in [9]. However,

it is not possible to extend the result of this chapter in terms of the regularity of the map F. The map Ψ fails to satisfy the Cauchy-Riemann equations and therefore is not holomorphic, so the two-dimensional real function is not analytic. Hence, it is not possible to apply the Open Mapping theorem which is equivalent to the Invariance of Domain theorem in the Complex plane.

Remark 2.4.2. *The model considered in [14] also allows the incorporation of a constant underlying current in the region $\mathcal{M}(t)$, as was recently shown in [86]. Indeed, let c_0 be the constant accounting for the current strength, then it is possible to obtain the following Lagrangian flow map which satisfies the β-plane approximation equations*

$$\begin{cases} x = q - c_0 t - \dfrac{1}{k} e^{-k(r+\zeta(s))} \sin[k(q-ct)]\,, \\ \\ y = s\,, \\ \\ z = -d_0 + r - \dfrac{1}{k} e^{-k(r+\zeta(s))} \cos[k(q-ct)]\,, \end{cases} \tag{2.26}$$

where $q \in \mathbb{R}$, $s \in [-s_0, s_0]$ for some s_0 restricting the latitude to a narrow strip about the Equator, and $r \in [r_0(s), r_+(s)]$. As in the previous case, $r_0(s)$ and $r_+(s)$ prescribe the thermocline and the upper boundary of $\mathcal{M}(t)$ respectively. It follows that the speed c satisfies the dispersion relation

$$c = \frac{\rho_+ - \rho_0}{\rho_0} \frac{-\Omega + \sqrt{\Omega^2 + \dfrac{\rho_0 k(2\Omega c_0 + g)}{\rho_+ - \rho_0}}}{k} > 0\,,$$

resulting in eastward-propagating internal waves which decay from the equator by means of the function

$$\zeta(s) = \frac{\beta}{2(kc - 2\Omega)} s^2\,. \tag{2.27}$$

It is note here that is possible to prove that (2.26) *is dynamically possible. The derivation performed in [86] shows that this is a solution to the* β*-plane equations and corresponding boundary conditions. Regarding the diffeomorphic character of* (2.26)*, it is sufficient to consider the case* $t = 0$ *and use the fact that* (2.17) *is a global diffeomorphism. Then, considering the change of variables* $(q, s, r) \longmapsto (q - ct, s, r)$ *and the time shift by* $(c - c_0)t$ *in the* x *component, it is ensured that this Lagrangian description also establishes a global diffeomorphism between the labelling domain and the fluid domain.*

Chapter 3

Internal equatorial water waves and wave-current interactions in the f-plane

In this chapter a solution to the f-plane approximation of the governing equations incorporating not only a constant current in the zonal direction, but also a transverse current in the meridional direction is derived. Some of the ideas regarding this solution have been already published in [112].

The solution presented and analysed in Chapter 2 inspired many others in a pursuit of new ways of describing more difficult and realistic physical scenarios. Within the equatorially-trapped internal waves inspired by Gerstner's wave, there are those that incorporate current terms. Being able to accommodate a current term in the exact and explicit solution allows amongst other things to consider flows that no longer have particles moving in perfect circles. Furthermore, with the addition of a depth-invariant current, it is possible to obtain flows with a net mass transport over a period, a question that will be discussed in Chapter 4. The presence of currents in the equatorial Pacific is well documented and it has proven to be a key factor in the geophysical dynamics of the equator [24, 25, 33].

Exact Gerstner-like solutions for equatorial geophysical water waves incorporating a constant underlying mean current were presented firstly in [55]. This has led to a number of generalisations [77, 86]. We describe here an exact and explicit nonlinear solution for geophysical internal ocean waves in the equatorial region under the presence of a constant zonal current and a transverse-equatorial meridional current. This constitutes a purely three-dimensional fluid motion and the existence of such a solution relies on the application of the f-plane approximation. This is justified for oceanic equatorial flows within a narrow latitudinal ocean strip [12, 24, 33] although, it provides a poorer approximation than the one given by the β-plane

approximation equations (2.3). This is an interesting mathematical exercise on its own right, demonstrating the robust structure of the exact and explicit solution to the f-plane equations. However, this is not a purely mathematical exploration and its applicability and importance is confirmed by the presence of strong currents in the equatorial Pacific [24, 25, 33, 41, 123].

The addition of a variable transverse current was recently achieved in [87] for surface waves and in [58] for internal waves constituting a three-dimensional motion. Although remarkable, this was done for a simplified, hydrostatic model without a mean zonal current. In this chapter, both the constant mean zonal and the variable meridional currents are incorporated. At the same time a non-hydrostatic three-dimensional model which accommodates the oscillations of a thermocline over the infinite-depth motionless bottom is considered.

3.1 f-plane approximation at the Equator

The additional difficulty of the flow described here requires a further simplification in the governing equations (2.3). Namely, the order of the Taylor expansion (2.1) is reduced even more, taking the Coriolis parameters as constants. In other words, the β term is neglected, which is justified within a narrow equatorial strip. This approximation is known as f-plane approximation and it is given by the following equations

$$\begin{cases} u_t + uu_x + vu_y + wu_z + 2\Omega w = -\dfrac{1}{\rho}P_x\,, \\ \\ v_t + uv_x + vv_y + wv_z = -\dfrac{1}{\rho}P_y\,, \\ \\ w_t + uw_x + vw_y + ww_z - 2\Omega u = -\dfrac{1}{\rho}P_z - g\,, \end{cases} \tag{3.1}$$

while the continuity equation under the incompressibility condition remains as before

$$\nabla \cdot \mathbf{u} = 0\,.$$

3.2 Solution for the five-layer model

In this section, the derivation of the solution incorporating both a constant current in the zonal direction and a variable transverse current is detailed and also published in [112]. The solution satisfies the f-plane approximation of the Euler equations for an incompressible fluid. The five-layer model described in Figure 2.1 is considered so the transition from the oscillations of the thermocline to the motionless bottom is done in a relatively natural way. The situation allowing for the currents to be part of the solution is depicted in Figure 3.1

Apart from the thermocline, the model includes some other artificial boundaries where the appropriate boundary conditions have to be verified. The thermocline given by $z = \eta_0(x - ct, y)$ divides the flow into two regions of densities $\rho_0 < \rho_+$. There is a region above the thermocline, denoted by $\mathcal{M}(t)$, where the solution is presented in Lagrangian coordinates, incorporating a variable transverse current. This region has $z = \eta_+(x - ct, y)$ as its upper boundary, above which the motion is not addressed in this work and where wind is supposed to be the main mechanism of wave generation, being able to regard the effects of the internal wave in this region as a small perturbation of these wind waves. Beneath the thermocline, there are two other interfaces, $z = \eta_1(x-ct, y)$ and $z = \eta_2(x-ct, y)$, that help to accommodate the oscillations of the thermocline to the motionless bottom. On all these interfaces we require the kinematic boundary condition, given by (2.4). Furthermore, the pressure P is assumed to be continuous throughout the whole fluid region, which results in the corresponding conditions on each of the interfaces.

The flow is described layer by layer where the f-plane equations, the mass conservation and the corresponding boundary conditions must be satisfied. In the layer $\mathcal{M}(t)$ the exact and explicit solution is given in the Lagrangrian framework. Below the thermocline, the flow takes the form of a uniform velocity field $\mathbf{u} = (c-c_0, \mu, 0)$, followed by a transitional layer, after which the water is assumed to remain motionless. It follows a detailed description of this solution layer by layer.

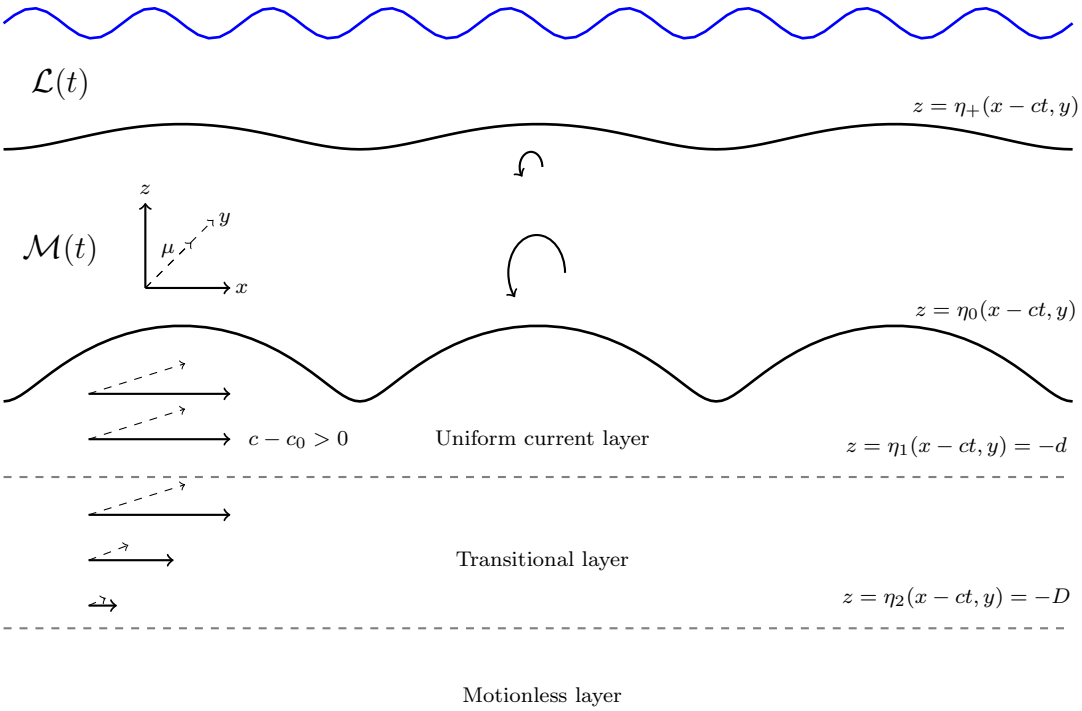

Figure 3.1: Depiction of the different layers in which the fluid motion is divided. The assumption of a two-dimensional flow will not be valid; therefore, this representation should be taken as an approximated sketch of the real situation for a fixed latitude. For both, a positive phase speed c and a positive current c_0 such that $c - c_0 > 0$, there is an underlying current in the upper part of $\mathcal{M}(t)$ which flows westward in the longitudinal direction, whereas close to the thermocline $z = \eta_0$, there is an uniform eastward current which fades out towards the motionless layer. The flow in the meridional direction will be determined by the current term μ.

3.2.1 Deepest layer

As water is assumed to be of infinite depth, this is an unbounded layer that is limited only by the upper boundary

$$z = \eta_2(x - ct, y) = -D,$$

for some fixed equatorial depth D. The water is motionless within this layer, i.e.

$$u = v = w = 0 \quad \text{for} \quad z \leq \eta_2(x - ct, y).$$

Therefore, the continuity equation and the kinematic boundary condition (2.4) are trivially satisfied, whereas from the equation (3.1), the pressure must be

$$P = P_0 - \rho_+ g z \quad \text{for} \quad z \leq -D,$$

where P_0 is an integration constant.

3.2.2 Transitional layer

This is the region enclosed by the previous plane $z = -D$ and the interface

$$z = \eta_1(x - ct, y) = -d,$$

where $d < D$ is another fixed equatorial depth. Let μ be a function which does not depend upon y and let $\mathbf{u}$ be defined by

$$\begin{cases} u = \dfrac{c - c_0}{D - d}(z + D), \\ \\ v = \dfrac{\mu}{D - d}(z + D), \qquad \text{for } -D \leq z \leq -d, \\ \\ w = 0. \end{cases}$$

Then, the velocity describes a linear transition from the motionless layer to a region with a uniform current of magnitude $c - c_0$ in the longitudinal direction and a current in the latitudinal direction given by μ. Due to μ being independent of y, the continuity equation is readily satisfied. On the other hand, if

$$\mu = \mu\Big(x - \frac{c - c_0}{D - d}(z + D)t, z\Big),$$

the pressure derived from the f-plane equation does not depend on x or y and it must satisfy

$$\frac{1}{\rho_+}P_z + g = 2\Omega u\,, \tag{3.2}$$

resulting in the following expression

$$P = \Omega\rho_+\frac{(c-c_0)}{D-d}(z+D)^2 - \rho_+ gz + \tilde{P}_0\,, \quad \text{for} \quad \eta_2(x-ct) \le z \le \eta_1(x-ct),$$

where $\tilde{P}_0$ is a constant. However, by requiring the continuity of the pressure on the interface $z = \eta_2(x-ct, y)$ it follows that $\tilde{P}_0 = P_0$. The kinematic boundary condition on $z = \eta_2(x-ct, y)$ is trivially satisfied. Finally, it is worth noting that for a non-constant function μ, the flow in this layer also presents a non-zero vorticity.

3.2.3 Uniform-flow layer

Let $z = \eta_0(x-ct, y)$ be the equation of the thermocline, for which an explicit expression will be determined in Section 3.2.4. For the region below the thermocline, the flow is defined by the following velocity field

$$\begin{cases} u = c - c_0, \\ \\ v = \mu(x-(c-c_0)t, z), \qquad \text{for } -d \le z \le \eta_0(x-ct, y), \\ \\ w = 0. \end{cases} \tag{3.3}$$

Although the case $c = c_0$ is still valid mathematically, the current c_0 is normally considered to be much smaller in absolute terms than the wave speed c, preventing the velocity u from vanishing . It follows that the pressure satisfies the equation (3.2), hence

$$P = 2\Omega\rho_+(c-c_0)z - \rho_+ gz + \hat{P}_0\,; \quad \text{for} \quad \eta_1(x-ct) \le z \le \eta_0(x-ct),$$

for an arbitrary constant $\hat{P}_0$. Now, for the pressure to be continuous on $z = -d$, we must require that

$$\hat{P}_0 = P_0 + \Omega\rho_+(c-c_0)(D+d)\,.$$

Thus, the pressure takes the form

$$P = P_0 - \rho_+ gz + \Omega\rho_+(c-c_0)(2z+D+d) \quad \text{for} \quad \eta_1(x-ct) \le z \le \eta_0(x-ct)\,. \tag{3.4}$$

3.2.4 Layer above the thermocline

The layer $\mathcal{M}(t)$ is the region above the thermocline $z = \eta_0(x - ct, y)$ and below the interface $z = \eta_+(x - ct, y)$. For this layer, the description of the flow is presented in the Lagrangian formulation (see Chapter 1). In particular, given labelling variables $(q, s, r) \in \mathbb{R} \times [-s_0, s_0] \times [r_0, r_+]$, the position of the fluid particles is

$$\begin{cases} x = q - c_0 t - \dfrac{1}{k} e^{-kr} \sin[k(q - ct)], \\ \\ y = s + \mu(q, r)t, \\ \\ z = r - d_0 - \dfrac{1}{k} e^{-kr} \cos[k(q - ct)], \end{cases} \tag{3.5}$$

where μ is now a smooth function representing the speed of a transverse current depending on the Lagrangian variables. The constant $d_0 > 0$ is introduced again in order to allow an adjustment of the mean depth of the thermocline. It will be shown that $r = r_0$ determines the thermocline and $r = r_+$ defines the interface η_+.

It is important to note that, from the solution (3.5), these waves will not be equatorially trapped in contrast to the solution presented in Chapter 2. However, the latitude is implicitly restricted once the f-plane approximation is adopted. The labelling variable r is required to satisfy

$$r \geq r_0 > 0 \tag{3.6}$$

for the region $\mathcal{M}(t)$. Under (3.6), the Jacobian of the transformation is always positive and so the Lagrangian description is valid, although it remains to be proven that the map (3.5) is a global diffeomorphism. The velocity of a particle, obtained by differentiating (3.5) with respect to time, is

$$\begin{cases} u = ce^{-kr} \cos\theta - c_0, \\ \\ v = \mu(q, r), \\ \\ w = -ce^{-kr} \sin\theta, \end{cases} \tag{3.7}$$

where θ is as in (2.14). The previous expression confirms the three-dimensional character of the flow, as opposed to the corresponding formulations with a vanishing meridional velocity [14, 55]. In general, the velocity field is discontinuous along the thermocline, being this a region of high shear and strong stratification. However, as long as the kinematic boundary condition (2.4) holds on the thermocline, the normal component of the velocity will be always continuous. The acceleration in the Lagrangian formulation for a fixed label (i.e. for a given particle) is given by

$$\begin{cases} \dfrac{du}{dt} = kc^2 e^{-kr} \sin\theta, \\ \dfrac{dv}{dt} = 0, \\ \dfrac{dw}{dt} = kc^2 e^{-kr} \cos\theta, \end{cases} \tag{3.8}$$

where the derivative is a partial derivative only when the label is fixed. On the other hand, the equations (3.1) can be reformulated using the convective derivative (which is simply the time derivative in the Lagrangian framework) as follows

$$\begin{cases} \dfrac{Du}{Dt} + 2\Omega w = -\dfrac{1}{\rho} P_x, \\ \dfrac{Dv}{Dt} = -\dfrac{1}{\rho} P_y, \\ \dfrac{Dw}{Dt} - 2\Omega u = -\dfrac{1}{\rho} P_z - g. \end{cases}$$

For the acceleration given by (3.8), we obtain a set of equations for the pressure

$$\begin{aligned} P_x &= -\rho_0 \Big[kc^2 - 2\Omega c e^{-kr} \Big] \sin\theta, \\ P_y &= 0, \\ P_z &= -\rho_0 \Big[kc^2 e^{-kr} \cos\theta - 2\Omega (c e^{-kr} \cos\theta - c_0) + g \Big]. \end{aligned}$$

By means of the following change of variables,

$$\begin{cases} P_q = P_x\dfrac{\partial x}{\partial q} + P_y\dfrac{\partial y}{\partial q} + P_z\dfrac{\partial z}{\partial q}, \\ \\ P_s = P_x\dfrac{\partial x}{\partial s} + P_y\dfrac{\partial y}{\partial s} + P_z\dfrac{\partial z}{\partial s}, \\ \\ P_r = P_x\dfrac{\partial x}{\partial r} + P_y\dfrac{\partial y}{\partial r} + P_z\dfrac{\partial z}{\partial r}, \end{cases}$$

the pressure can be expressed in terms of the labelling variables as

$$\begin{aligned} P_q &= -\rho_0\Big[kc^2 - 2\Omega(c-c_0) + g\Big]e^{-kr}\sin\theta, \\ P_s &= 0, \\ P_r &= -\rho_0\Big[(kc^2 - 2\Omega c)e^{-2kr} + (kc^2 - 2\Omega(c-c_0) + g)e^{-kr}\cos\theta + g + 2\Omega c_0\Big]. \end{aligned} \tag{3.9}$$

Integrating this expression (3.9), it follows that the pressure for the layer above the thermocline must take the form

$$P = \rho_0\frac{kc^2 - 2\Omega(c-c_0) + g}{k}e^{-kr}\cos\theta + \rho_0\frac{kc^2 - 2\Omega c}{2k}e^{-2kr} - \rho_0(g + 2\Omega c_0)r + Q, \tag{3.10}$$

for some constant Q. The thermocline is the parametric surface $\mathbf{S}(q,s)$ resulting from setting $r = r_0$ in (3.5), where r_0 is a solution of the nonlinear equation (3.15), i.e. the thermocline is parametrically given by

$$(q,s) \mapsto \left(q - c_0 t - \frac{1}{k}e^{-kr_0}\sin[k(q-ct)],\ s + \mu(q,r_0)t,\ r_0 - d_0 - \frac{1}{k}e^{-kr_0}\cos[k(q-ct)]\right) \tag{3.11}$$

for each time t. This is indeed a regular parametric surface: for any time t, $e^{-kr_0} < 1$ implies that

$$\mathbf{S}_q \times \mathbf{S}_r = (e^{-kr_0}\sin\theta, 0\,, -1 + e^{-kr_0}\cos\theta) \neq \mathbf{0}$$

and so,

$$\mathbf{n} = \frac{\mathbf{S}_q \times \mathbf{S}_r}{||\mathbf{S}_q \times \mathbf{S}_r||}$$

is well defined. The existence and choice of such r_0 is given by the nature of the problem. Firstly, the continuity of the pressure on the thermocline is required.

Therefore, the result of evaluating the expression (3.11) on (3.4) must be equal to (3.10). At the same time, assuming the pressure to be independent of time yields

$$kc^2 - 2\Omega(c - c_0) + g = \frac{\rho_+}{\rho_0}[g - 2\Omega(c - c_0)]\,, \tag{3.12}$$

which leads to the dispersion relation

$$c = \frac{-\Omega\tilde{\rho} \pm \sqrt{\Omega^2\tilde{\rho}^2 + k(\tilde{g} + 2\Omega\tilde{\rho}c_0)}}{k}\,, \tag{3.13}$$

where $\tilde{\rho} = \frac{\rho_+ - \rho_0}{\rho_0}$ has a typical value of $\tilde{\rho} \approx 6 \times 10^{-3}$, cf. [41] and $\tilde{g} = g\tilde{\rho}$. The dispersion relation (3.13) agrees with the one obtained in [86] and generalises the dispersion relation in [14], although here the use of the f-plane approximation allows negative velocities. In that sense, there are two cases in terms of the current c_0:

1. If $c_0 > 0$, the velocity c can take positive and negative values, unlike the case of the β-plane approximation. If c is taken positive, reasonable values for the wavenumber result in $c \approx \sqrt{\tilde{g}/k}$, which resembles the dispersion relation for deep water waves in the linear theory with g replaced with $\tilde{g}$. The current is normally assumed to be much smaller than c, therefore $c - c_0 > 0$ and $c - c_0 \approx \sqrt{\tilde{g}/k}$.

2. If $c_0 < 0$, the existence of a real velocity c requires $c_0 > -(\frac{g}{2\Omega} + \frac{\Omega}{2k}\tilde{\rho})$, whereas a positive speed c will be only possible if the current is such that $c_0 > -\frac{g}{2\Omega}$. Both conditions are satisfied for any reasonable current, due to the fact that $\frac{g}{2\Omega} = 1.344 \times 10^5\,\mathrm{m\,rad^{-1}\,s^{-1}}$. Thus, in any realistic scenario, a negative constant current c_0 will correspond to a real velocity c with opposite direction to c_0.

Returning to the discussion about the deduction of the thermocline, the continuity of the pressure on the thermocline is transformed using (3.12) in

$$\frac{1}{2k}\Lambda(c_0)e^{-2kr_0} + \Lambda(c_0)r_0 = \frac{1}{\rho_0}\Big[P_0 - Q - \rho_+\Omega(c - c_0)(D + d - 2d_0) - \rho_+ g d_0\Big], \tag{3.14}$$

where the following notation is adopted

$$\Lambda(c_0) := \tilde{g} + 2\Omega\tilde{\rho}c_0 - 2\Omega\frac{\rho_+}{\rho_0}c.$$

Finally, the justification for the existence of such $r = r_0$, which determines the thermocline, relies on finding the unique solution of the nonlinear equation

$$\mathscr{F}(r) = 0\,, \tag{3.15}$$

where

$$\mathscr{F}(r) := \frac{1}{2k}\Lambda(c_0)e^{-2kr} + \Lambda(c_0)r - \frac{1}{\rho_0}\Big[P_0 - Q - \rho_+\Omega(c-c_0)(D+d-2d_0) - \rho_+ g d_0\Big].$$

It follows that

$$\mathscr{F}'(r) = \Lambda(c_0)(1 - e^{-2kr})\,,$$

where $1 - e^{-2kr} > 0$ for $r > 0$. Then, the increasing behaviour of $\mathscr{F}(r)$ depends upon the sign of $\Lambda(c_0)$. For any reasonable current, $c_0 > \frac{\rho_+}{\rho_+ - \rho_0}c - \frac{1}{2\Omega}g$, which implies that $\Lambda(c_0) > 0$. Therefore, under this assumption, $\mathscr{F}(r)$ is strictly increasing with

$$\lim_{r\to\infty} \mathscr{F}(r) = \infty\,.$$

Provided that

$$P_0 - Q > \frac{\rho_0}{2k}\Lambda(c_0) + \rho_+\Omega(c-c_0)(D+d-2d_0) - \rho_+ g d_0 \tag{3.16}$$

holds, this then implies that

$$\mathscr{F}(0) < 0\,.$$

The existence of a unique solution $r_0 > 0$ for (3.14) has been transformed into a condition involving the arbitrary constants P_0 and Q, so the determination of the thermocline and the verification of (3.6) is concluded. In the same manner, the interface $z = \eta_+(x - ct, y)$ will be specified by fixing some constant $P^* > P_0 - Q$ and obtaining the unique solution $r = r_+ > r_0$ of the nonlinear problem

$$\mathscr{F}(r) := \frac{1}{2k}\Lambda(c_0)e^{-2kr} + \Lambda(c_0)r - \frac{1}{\rho_0}\Big[P^* - \rho_+\Omega(c-c_0)(D+d-2d_0) - \rho_+ g d_0\Big] = 0.$$

Remark 3.2.1. *A quantitative discussion can be done as follows. Let* $L = 300\,\mathrm{m}$ *be the wavelength of the wave, the dispersion relation* (3.13) *yields the approximative wave speed* $c \approx 1.676\,\mathrm{m\,s^{-1}}$ *for the case of a vanishing current* c_0*. The wave speed will be slightly affected by the value of a reasonable current* c_0*. However, as it has been already noticed, the physical scenario is hugely influenced by changes in* c_0 *(this will be make more explicit in the Chapter 4). The choices* $r_0 = 187\,\mathrm{m}$ *and* $d_0 = 307\,\mathrm{m}$ *ensure that the thermocline is placed* $120\,\mathrm{m}$ *below the surface, while* $r_+ = 247\,\mathrm{m}$*,* $d = 160\,\mathrm{m}$ *and* $D = 200\,\mathrm{m}$ *are suitable choices for the situation at the equator (cf. [14]).*

Chapter 4

Mean flow properties for equatorially-trapped internal waves

Continuing with the analysis of equatorially-trapped internal waves, the present chapter focus on some important features of ocean waves, namely the idea of mass transport and mass flux, for which adequate expressions of mean flow velocities are fundamental. In particular, mass flux and mean flow velocities will be given for the solution (3.5) derived in Chapter 3 and the solution (4.5) described in [77]. These results have been first published in [112] for the solution (3.5) and in [114] for the solution (4.5), where the mean flow velocities and mass transport induced by the oscillations of the thermocline under the effect of several currents are investigated.

The study of mass flux properties was part of the works of Stokes [119], who showed that particles in an irrotational gravity wave on an ideal fluid are transferred forwards with a constant velocity that decreases rapidly with depth. For those waves, there exists an additional motion apart from the oscillatory motion of the particles. In this sense, Stokes stated that individual particles in a progressive irrotational wave do not describe exactly closed paths possessing an additional nonlinear mean velocity. This was further investigated in [8, 9, 15, 28, 49, 51].

However, irrotational waves are not the only type of theoretically possible wave in a perfect fluid (cf. [47, 108]). As it has been shown, Gerstner's wave has a non-vanishing vorticity (1.24) and the particles describe circular orbits, therefore the mean Lagrangian velocity or mass-transport velocity vanishes. Furthermore, Dubreil-Jacotin [35] showed the existence of a family of waves having different vorticity distributions and mass transport velocities, in which both Stokes and Gerstner's waves were included as particular cases. Contrary to expectations, the concept of mean mass flux past a given recording station requires more information than the

mean velocity at that point. This is due to the difference between the Lagrangian and Eulerian descriptions. In order to make this idea precise and to provide manageable expressions, Longuet-Higgins established a general definition of the mass-transport velocity [93, 94], which defines the concept of Stokes drift velocity as a difference of Lagrangian and Eulerian mean velocities. Normally, in the study of ocean flows, the Eulerian description is the preferred choice and the techniques in [93, 94] are dedicated to obtain the Stokes drift velocity via Eulerian quantities. In this work, the flows are given in terms of Lagrangian variables and as a consequence, a different approach will be employed. Previously, an analysis of the flow characteristics in the absence of a background current was presented in [13, 20]. A more complicated scenario, derived in [55], incorporating an underlying current for the equatorially-trapped surface water wave was addressed in [70]. While the incorporation of current terms in these models could be viewed as a change in the Lagrangian flow map, it leads to important modifications in the underlying flow and rather interesting physical phenomena.

4.1 Mean flow velocity and Stokes drift

Following the works of Stokes [119], Longuet-Higgins [93, 94] studied the so-called mass-transport velocity, which more precisely defines the mean velocity of a marked particle. For a flow described in Eulerian coordinates, the behaviour of the mass flux passing a fixed point cannot be stated just by measuring the mean velocity at that point. There is an additional quantity, known as the Stokes drift, that must be considered. Following [93], if $\mathbf{x}_0$ denotes the position of a particle at time t_0 which moves to $\mathbf{x}_0 + \Delta\mathbf{x}$ at time t, the velocity at the new position can be given by the following Taylor approximation

$$\mathbf{u}(\mathbf{x}, t) \approxeq \mathbf{u}(\mathbf{x}_0, t) + (\Delta\mathbf{x} \cdot \nabla)\mathbf{u}(\mathbf{x}_0, t)\,. \tag{4.1}$$

Moreover, if the $\Delta\mathbf{x}$ is small compared to the local length scale of the velocity, it follows that

$$\Delta\mathbf{x} \approxeq \int_{t_0}^{t} \mathbf{u}(\mathbf{x}_0, \tau)\, d\tau\,. \tag{4.2}$$

Note that for the Lagrangian description, an exact expression for (4.2) can be obtained. Now, combining both (4.1) and (4.2) gives

$$\mathbf{u}(\mathbf{x},t) = \mathbf{u}(\mathbf{x}_0,t) + \left\{ \left[\int_{t_0}^{t} \mathbf{u}(\mathbf{x}_0,\tau)\, d\tau \right] \cdot \nabla \right\} \mathbf{u}(\mathbf{x}_0,t)\,,$$

Taking the average over one wave period yields the following expression for the mass-transport velocity given in [93]

$$\langle \mathbf{u} \rangle_L = \langle \mathbf{u} \rangle_E + \left\langle \left[\int \mathbf{u}\, dt \cdot \nabla \right] \mathbf{u} \right\rangle , \tag{4.3}$$

where $\langle \mathbf{u} \rangle_L = (\langle u \rangle_L, \langle v \rangle_L, \langle w \rangle_L)$ is the Lagrangian mean velocity, i.e. the mean velocity of the marked particle that at time $t = t_0$ was at $\mathbf{x}$. On the other hand, $\langle \mathbf{u} \rangle_E = (\langle u \rangle_E, \langle v \rangle_E, \langle w \rangle_E)$ refers to the Eulerian mean velocity. The remaining term

$$\mathbf{U}^S = (U^S, V^S, W^S) := \left\langle \left[\int \mathbf{u}\, dt \cdot \nabla \right] \mathbf{u} \right\rangle$$

is the aforementioned Stokes drift velocity which, up to order $\Delta\mathbf{x}$, is the difference of the Lagrangian and Eulerian mean velocities

$$\mathbf{U}^S = \langle \mathbf{u} \rangle_L - \langle \mathbf{u} \rangle_E \,. \tag{4.4}$$

When dealing with Lagrangian descriptions, obtaining the mass-transport velocity can be obtained exactly. However, flows given by the Lagrangian description are rare and their Eulerian description is not normally available. Thus, finding the Stokes drift for the flows studied in this thesis provides a good tool for comparing these flows with classical flows described in the ocean waves theory.

4.2 Internal wave in the β-plane

The flow derived by Hsu in [77] is presented here. This flow incorporates a constant current to the solution initially derived in [13], where a thermocline was considered, although in a simpler way than the model discussed in Chapter 2. A sketch of this physical model is presented in Figure 4.1. In particular, the flow described in [77]

is a solution to the β-plane equations (2.3) for a vanishing meridional velocity v. Following the description given for the exact solution (2.9), this solution specifies the position (x, y, z) of a fluid particle at some time t by

$$\begin{cases} x = q - c_0 t - \dfrac{1}{k} e^{-k[r+\zeta(s)]} \sin[k(q-ct)], \\ y = s, \\ z = r - \dfrac{1}{k} e^{-k[r+\zeta(s)]} \cos[k(q-ct)], \end{cases} \tag{4.5}$$

where $(q, s, r) \in \mathbb{R} \times [-s_0, s_0] \times [r_0(s), r_+(s)]$ are the labels of the fluid particles. When restricting the study to eastward-propagating waves, the following dispersion relation is obtained

$$c = \frac{\Omega + \sqrt{\Omega^2 + k\varsigma}}{k},$$

where

$$\varsigma = \tilde{g} - 2\Omega c_0 \qquad \text{for} \quad \tilde{g} = g\frac{\rho_+ - \rho_0}{\rho_0}\,. \tag{4.6}$$

The constant $\tilde{g}$ is usually known as reduced gravity and has a typical value of $6 \times 10^{-3}\mathrm{m} \cdot s^{-2}$ (cf. [41]). The function ζ determining the decay of the particle oscillations in the latitudinal direction away from the equator is now given by

$$\zeta(s) = \frac{c\beta}{2\varsigma} s^2\,. \tag{4.7}$$

It is worth noting that $2\Omega c_0$ is taken to be less then $\tilde{g}$, which is physically reasonable, in order to obtain $\varsigma > 0$. On the other hand, the velocity field, given by the time derivative of (4.5), is

$$\begin{cases} u = -c_0 + ce^{-\xi}\cos\theta, \\ v = 0, \\ w = -ce^{-\xi}\sin\theta. \end{cases} \tag{4.8}$$

where θ is given by (2.14) and ξ is given by (2.13) and where the expression for ζ is the one in (4.7).

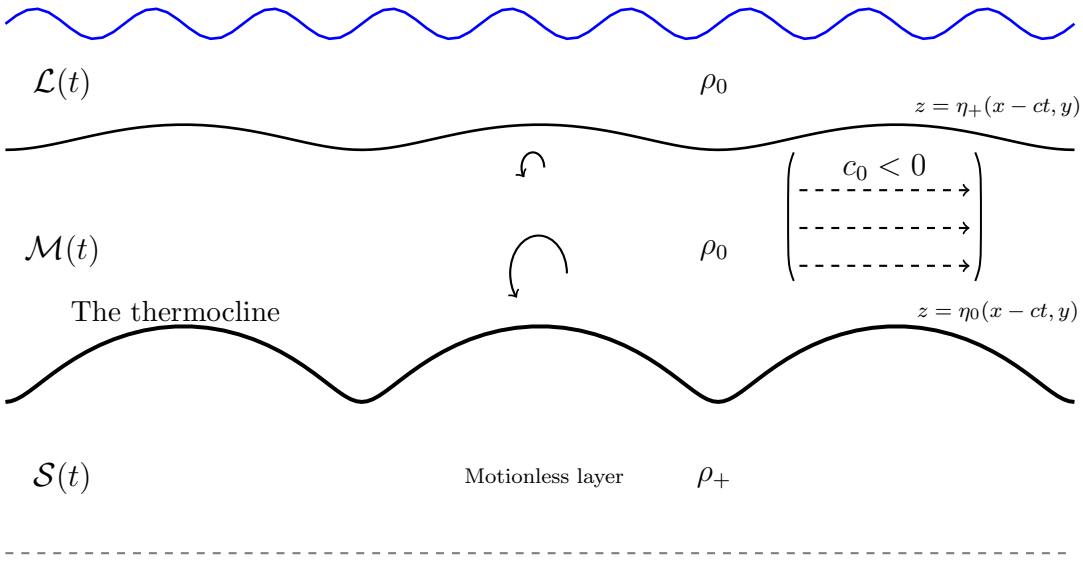

Figure 4.1: Depiction of the different flow regions for a fixed latitude y and a negative constant value of the underlying current c_0 in the layer $\mathcal{M}(t)$. In the absence of the current, the thermocline is specified by a trochoid propagating eastward at constant speed. The thermocline separates two layer of different densities $\rho_0 < \rho_+$ in a stable stratification with the denser fluid below.

In addition, the Jacobian matrix of the transformation (4.5) is given by

$$\left(\frac{\partial(x,y,z)}{\partial(q,s,r)}\right) = \begin{pmatrix} 1 - e^{-\xi}\cos\theta & 0 & e^{-\xi}\sin\theta \\ \zeta'(s)e^{-\xi}\sin\theta & 1 & \zeta'(s)e^{-\xi}\cos\theta \\ e^{-\xi}\sin\theta & 0 & 1 + e^{-\xi}\cos\theta \end{pmatrix}, \tag{4.9}$$

which, under the assumption that

$$r + \zeta(s) \geq r^* > 0 \tag{4.10}$$

has a non-vanishing determinant $1 - e^{-2\xi}$. Moreover, the determinant is time independent, assuring that the mass conservation equation for an incompressible fluid is satisfied. The flow satisfies the governing equations (2.3) and boundary conditions (2.4), as it can be shown by obtaining a compatible pressure.

On the other hand, a boundary condition of the type (2.4) allows the thermocline to be determined. Following the method used in [77], the determination of the thermocline is equivalent to finding the unique solution $r := r_0(s) > 0$ for every

fixed $s \in [-s_0, s_0]$ of

$$\mathscr{F}(r,s) := r + \frac{c_0}{c}(-2kr - \frac{k\beta c}{\varsigma}s^2) + \frac{1}{2k}\exp(-2kr - \frac{k\beta c}{\varsigma}s^2) - P_0^* = 0, \qquad (4.11)$$

where P_0^* is an arbitrary constant, $s_0 = \sqrt{\tilde{c}/\beta} \approx 250$ km is the so-called equatorial radius of deformation. The constant $\tilde{c}$ is a typical speed for the waves in the tropical region, which value is approximately 1.4 m s^{-1} (cf. [13, 33]). It follows from the Intermediate Value theorem and the properties of $\mathscr{F}(s,r)$ that

$$P_0^* > \frac{c_0\beta}{2\varsigma}s_0^2 + \frac{1}{2k}$$

is a sufficient condition for the existence and uniqueness of the solution of (4.11). Summarising, the thermocline $z = \eta_0(x - ct, y)$ is the surface given by

$$(q,s) \longrightarrow (q - c_0t - \frac{1}{k}e^{-k[r_0(s)+\zeta(s)]}\sin[k(q-ct)], s, r_0(s) - \frac{1}{k}e^{-k[r_0(s)+\zeta(s)]}\cos[k(q-ct)]),$$

where $r := r_0(s)$ is the unique solution of (4.11) for each given s. At this point, we take care of the physical implications of this mathematical model. Differentiating (4.11) with respect to s yields

$$r_0'(s) = \frac{\beta s}{\varsigma}\frac{ce^{-2\xi} - c_0}{1 - e^{-2\xi}}.$$

Hence, it is clear that the values of the current should be restricted to

$$c_0 < ce^{-2kr_0(s)} \qquad (4.12)$$

in order to ensure that $r_0(s)$ is a strictly increasing function for $|s| > 0$ and that as a consequence

$$s \longmapsto \exp(-2kr_0(s) - \frac{k\beta c}{\varsigma}s^2) \qquad (4.13)$$

is strictly decreasing for $|s| > 0$. Otherwise, the amplitude of the waves will grow exponentially with the distance from the equator, constituting an unrealistic model violating the equatorially-trapped nature of these waves. To complete the definition of this solution, the boundary delimiting the layers $\mathcal{M}(t)$ and $\mathcal{L}(t)$ must be specified. This is done by considering the same nonlinear equation (4.11) for another constant $\mathscr{P}_0 > P_0^*$. The unique solution of that equation for every given latitude $s \in [-s_0, s_0]$ will be denoted by $r_+(s)$, see [77] for a complete discussion.

4.2.1 Mean Lagrangian flow velocity

The mean Lagrangian flow velocity, also known as mass-transport velocity, provides a measure of the velocity of a fluid particle over a wave period. The horizontal mean Lagrangian velocity over a wave period T of the flow given by (4.5) is

$$\langle u \rangle_L = \frac{1}{T} \int_0^T u(q - ct, s, r)\, dt = -c_0\,, \tag{4.14}$$

which is independent of the initial location of the fluid particle considered. Therefore, it follows that the mean Lagrangian flow velocity has an absolute value given by c_0 and it is either westwards or eastwards, depending on whether c_0 is positive or negative respectively.

4.2.2 Mean Eulerian flow velocity

As it was mentioned before, obtaining an explicit solution for the equation describing ocean waves is an extraordinary achievement. In the present case, this was possible by means of the Lagrangian formulation. However, the scarcity of flows given in this manner makes it difficult to compare this solution with previous works. Therefore, an expression for the Stokes drift is given by means of the Eulerian velocity. Let us consider the crest and trough levels at a given latitude $y = s$ of the thermocline, which are given by

$$z_0^c(s) = r_0(s) + \frac{1}{k} e^{-k[r_0(s)+\zeta(s)]} \quad \text{and} \quad z_0^t(s) = r_0(s) - \frac{1}{k} e^{-k[r_0(s)+\zeta(s)]}\,.$$

Similarly, the crest and trough levels of $z = \eta_+(x - ct, y)$, i.e. of the upper boundary of $\mathcal{M}(t)$ as depicted in Figure 4.1, correspond to

$$z_+^c(s) = r_+(s) + \frac{1}{k} e^{-k[r_+(s)+\zeta(s)]} \quad \text{and} \quad z_+^t(s) = r_+(s) - \frac{1}{k} e^{-k[r_+(s)+\zeta(s)]}\,.$$

An expression relating the Lagrangian and Eulerian representations, for each fixed s, is obtained by the continuously differentiable map

$$\mathscr{G}_s(q - ct, r) := r - \frac{1}{k} e^{-k(r+\zeta(s))} \cos[k(q - ct)]\,.$$

For any fixed $\tilde{z} \in (z_0^c(s), z_+^t(s))$,

$$\mathscr{G}_s(\tilde{q} - ct, \tilde{r}) = \tilde{z}\,,$$

where $\tilde{r} \geq r^* > 0$. Also

$$\frac{\partial \mathscr{G}_s}{\partial r}(\tilde{q} - ct, \tilde{r}) = 1 + e^{-k(\tilde{r}+\zeta(s))} \cos[k(\tilde{q} - ct)] \neq 0$$

as long as (4.10) holds. Thus, it is possible to apply the Implicit Function theorem to conclude that there exists a function

$$r = R\,(q - ct; s, z)$$

and neighbourhoods of $\tilde{r}$ and $\tilde{q}$ for which

$$z = R - \frac{1}{k} e^{-\xi(R)} \cos\theta \tag{4.15}$$

at any given latitude s and for any $z \in (z_0^c(s), z_+^t(s))$ in the vertical direction. Furthermore, implicitly differentiating the previous relation with respect to q gives

$$0 = R_q + R_q e^{-\xi(R)} \cos\theta + e^{-\xi(R)} \sin\theta\,.$$

Rearranging yields

$$R_q = -\frac{e^{-\xi(R)} \sin\theta}{1 + e^{-\xi(R)} \cos\theta}\,, \tag{4.16}$$

where the denominator does not vanish in the neighbourhood of $\tilde{q}$ for which the Implicit Function theorem applies.

Let $y = s$ be a fixed latitude and let $z(s)$ be a depth between $z_0^c(s)$ and $z_+^t(s)$. The mean Eulerian flow velocity in the horizontal component is defined as

$$\langle u \rangle_E\,(s, z) = \frac{1}{T} \int_0^T [u(x - ct, y, z)]\; dt\,, \tag{4.17}$$

which after the change of variables given by the wave speed $x = ct$, is transformed into a spatial average

$$\langle u \rangle_E\,(s, z) = \frac{1}{L} \int_0^L [u(x - ct, y, z)]\; dx\,,$$

where the relation $c = L/T$ and the periodicity with respect x have been used. By adding the term c, the calculation is simplified as follows

$$c + \langle u \rangle_E\,(s, z) = \frac{1}{L} \int_0^L [c + u(x - ct, y, z)]\; dx = \frac{1}{L} \int_0^L [c + u(q - ct, s, z)] \frac{\partial x}{\partial q}\; dq\,.$$

It follows from the expression of the x-component of (4.5), the velocity (4.8) and the implicit relation (4.16) that

$$\begin{aligned} c + \langle u \rangle_E (s,z) &= \frac{1}{L}\int_0^L \left(c + ce^{-\xi(R)}\cos\theta - c_0\right)\left(1 + R_q e^{-\xi(R)}\sin\theta - e^{-\xi(R)}\cos\theta\right) dq \\ &= \frac{1}{L}\int_0^L \left(c + ce^{-\xi(R)}\cos\theta - c_0\right)\left(\frac{1 - e^{-2\xi(R)}}{1 + e^{-\xi(R)}\cos\theta}\right) dq \\ &= \frac{c}{L}\int_0^L \left[1 - e^{-2\xi(R)}\right] dq - \frac{c_0}{L}\int_0^L \frac{1 - e^{-2\xi(R)}}{1 + e^{-\xi(R)}\cos\theta}\, dq \\ &= c - \frac{c}{L}\int_0^L e^{-2\xi(R)}\, dq - \frac{c_0}{L}\int_0^L \frac{1 - e^{-2\xi(R)}}{1 + e^{-\xi(R)}\cos\theta}\, dq\,. \end{aligned}$$

Hence, the mean Eulerian flow velocity for a fixed latitude s and depth z is

$$\langle u \rangle_E (s,z) = -\frac{c}{L}\int_0^L e^{-2\xi(R)}\, dq - \frac{c_0}{L}\int_0^L \frac{1 - e^{-2\xi(R)}}{1 + e^{-\xi(R)}\cos\theta}\, dq. \tag{4.18}$$

4.2.3 Study of the Eulerian velocity in terms of the current

The direction of the mean Eulerian velocity will be affected by the current c_0 as can be seen in (4.18). In order to investigate this, a similar approach to the one taken in [70] is performed. Contrary to that situation, in the present flow the internal equatorially-trapped waves have an amplitude that decreases as moving upwards and the motion is restricted to the finite region $\mathcal{M}(t)$. The next inequalities are useful bounds for the discussion that follows,

$$\int_0^L \frac{1 - e^{-2\xi}}{1 + e^{-\xi}}\, dq \leq \int_0^L \frac{1 - e^{-2\xi}}{1 + e^{-\xi}\cos\theta}\, dq \leq \int_0^L \frac{1 - e^{-2\xi}}{1 - e^{-\xi}}\, dq, \tag{4.19}$$

Case I : Current $c_0 > 0$

The case of a positive current c_0 represents a westward current. From (4.19) and the sign of the current we have that

$$\frac{-c_0}{L}\int_0^L \frac{1 - e^{-2\xi}}{1 - e^{-\xi}}\, dq \leq \frac{-c_0}{L}\int_0^L \frac{1 - e^{-2\xi}}{1 + e^{-\xi}\cos\theta}\, dq \leq \frac{-c_0}{L}\int_0^L \frac{1 - e^{-2\xi}}{1 + e^{-\xi}}\, dq. \tag{4.20}$$

Furthermore, the positive value of the current is bounded by (4.12). Therefore, $c_0 < c$ for $r_0(s) > 0$ and the second inequality in (4.20) gives the upper bound

$$\begin{aligned}\langle u\rangle_E(s,z) &\le -\frac{c}{L}\int_0^L e^{-2\xi(R)}\,dq - \frac{c_0}{L}\int_0^L \frac{1-e^{-2\xi(R)}}{1+e^{-\xi(R)}}\,dq \\ &\le -\frac{c_0}{L}\int_0^L e^{-2\xi(R)}\,dq - \frac{c_0}{L}\int_0^L \frac{1-e^{-2\xi(R)}}{1+e^{-\xi(R)}}\,dq \\ &= -\frac{c_0}{L}\int_0^L \frac{1+e^{-3\xi(R)}}{1+e^{-\xi(R)}}\,dq < 0\end{aligned}$$

for a fixed latitude $s \in [-s_0, s_0]$ and a fixed depth $z(s) \in [z_0^c(s), z_+^t(s)]$. Similarly, a lower bound is obtained from the first inequality in (4.20),

$$\begin{aligned}\langle u\rangle_E(s,z) &\ge -\frac{c}{L}\int_0^L e^{-2\xi(R)}\,dq - \frac{c_0}{L}\int_0^L \frac{1-e^{-2\xi(R)}}{1-e^{-\xi(R)}}\,dq \\ &\ge -\frac{c}{L}\int_0^L e^{-2\xi(R)}\,dq - \frac{c}{L}\int_0^L \frac{1-e^{-2\xi(R)}}{1-e^{-\xi(R)}}\,dq \\ &= -\frac{c}{L}\int_0^L \frac{1-e^{-3\xi(R)}}{1-e^{-\xi(R)}}\,dq.\end{aligned} \tag{4.21}$$

Finally, the last integrand in (4.21) is a continuous function decreasing in terms of $r > 0$ and since $\xi \ge kR > kr^* > 0$, where r^* satisfies (4.10),

$$-\,c\,\frac{1-e^{-3kr^*}}{1-e^{-kr^*}} < \langle u\rangle_E(s,z) < 0.$$

It is concluded that the mean Eulerian velocity will be westward for all admissible values of current c_0. This agrees with the idea that the new current term only intensifies the effect of the adverse flow previously discussed in [13], where the current term c_0 is absent.

Case II : Current $c_0 < 0$

In this case, it is assumed that (4.18) is negative, i.e.

$$\langle u\rangle_E(s,z) < 0\,, \tag{4.22}$$

or equivalently

$$-\frac{c_0}{L}\int_0^L \frac{1-e^{-2\xi(R)}}{1+e^{-\xi(R)}\cos\theta}dq < \frac{c}{L}\int_0^L e^{-2\xi(R)}dq \tag{4.23}$$

and it is claimed then that

$$c_0 > -c \min_{q\in[0,L]} \frac{e^{-2\xi(R)}\left(1-e^{-\xi(R)}\right)}{1-e^{-2\xi(R)}} \tag{4.24}$$

is a sufficient condition for (4.22). Indeed, it follows from (4.24) that

$$-c_0 \max_{q\in[0,L]} \frac{1-e^{-2\xi(R)}}{1-e^{-\xi(R)}} < c \min_{q\in[0,L]} e^{-2\xi(R)},$$

and therefore

$$\begin{aligned}-\frac{c_0}{L}\int_0^L \frac{1-e^{-2\xi(R)}}{1+e^{-\xi(R)}\cos\theta}\,dq \le -\frac{c_0}{L}\int_0^L \frac{1-e^{-2\xi(R)}}{1-e^{-\xi(R)}}\,dq \le -c_0 \max_{q\in[0,L]} \frac{1-e^{-2\xi(R)}}{1-e^{\xi(R)}} \\ < c \min_{q\in[0,L]} e^{-2\xi(R)} \le \frac{c}{L}\int_0^L e^{-2\xi(R)}\,dq.\end{aligned}$$

On the contrary, if

$$\langle u\rangle_E(s,z) > 0\,, \tag{4.25}$$

this yields

$$-\frac{c_0}{L}\int_0^L \frac{1-e^{-2\xi(R)}}{1+e^{-\xi(R)}\cos\theta}\,dq > \frac{c}{L}\int_0^L e^{-2\xi(R)}\,dq.$$

In this case, it is sufficient that

$$c_0 < -c \max_{q\in[0,L]} \frac{e^{-2\xi(R)}\left(1+e^{-\xi(R)}\right)}{1-e^{-2\xi(R)}}, \tag{4.26}$$

in view of the following inequalities

$$\begin{aligned}-\frac{c_0}{L}\int_0^L \frac{1-e^{-2\xi(R)}}{1+e^{-\xi(R)}\cos\theta}\,dq \ge -\frac{c_0}{L}\int_0^L \frac{1-e^{-2\xi(R)}}{1+e^{-\xi(R)}}\,dq \ge -c_0 \min_{q\in[0,L]} \frac{1-e^{-2\xi(R)}}{1+e^{-\xi(R)}} \\ > c \max_{q\in[0,L]} e^{-2\xi(R)} \ge \frac{c}{L}\int_0^L e^{-2\xi(R)}\,dq.\end{aligned}$$

Finally, in the absence of current, the inequality (4.24) holds and the mean Eulerian flow is such that $\langle u\rangle_E \in (-c, 0)$ as it was shown in [13]. This means that the mean Eulerian flow is constantly westwards for $c_0 = 0$.

4.2.4 Stokes drift

Taking the approximate expression for the Stokes drift given by (4.4), it follows that

$$U^S(s,z) = -c_0 + \frac{c}{L}\int_0^L e^{-2\xi(R)}\,dq + \frac{c_0}{L}\int_0^L \frac{1-e^{-2\xi(R)}}{1+e^{-\xi(R)}\cos\theta}\,dq,$$

for fixed latitudes $s \in [-s_0, s_0]$ and depths $z_0^c(s) \leq z(s) \leq z_+^t(s)$. Furthermore, if $0 \leq c_0 < ce^{-2kr_0(s)} < c$ then

$$U^S(s,z) = \frac{1}{L}\int_0^L \left(ce^{-2\xi(R)} - c_0\right) dq + \frac{c_0}{L}\int_0^L \frac{1-e^{-2\xi(R)}}{1+e^{-\xi(R)}\cos\theta}\,dq > 0.$$

This shows that the Stokes drift for an westward current is eastwards. If $c_0 < 0$, then the mean Eulerian velocity is positive as long as (4.26) holds. Thus, under this condition the Stokes drift will be in the westward direction.

4.2.5 Mass flux for the constant current solution

Another insightful quantity is the mass flux through a given line $x = x_0$ (where x_0 is fixed) between two depths, which in this case will be given by the thermocline and the upper boundary of $\mathcal{M}(t)$. For a fixed latitude $y = s \in [-s_0, s_0]$, the mass flux between these two surfaces, depicted in Figure 4.2, is

$$m(x_0 - ct, s) = \int_{\eta_0(x_0-ct)}^{\eta_+(x_0-ct)} u(x_0 - ct, y, z)dz\,.$$

As the flow description is prescribed in Lagrangian coordinates, the integral is transformed into

$$m(x_0 - ct, s) = \int_{r_0(s)}^{r_+(s)} (-c_0 + ce^{-\xi}\cos\theta)\frac{\partial z}{\partial r}dr, \tag{4.27}$$

where the expression for the velocity (4.8) is used. On the other hand, the x-component of the solution (4.5) and the Implicit Function theorem ensures, for any fixed $x = x_0$, that

$$x_0 = q - c_0 t - \frac{1}{k}e^{-\xi}\sin\theta \tag{4.28}$$

provides a functional relationship $q = \kappa(r; s, t)$ between q and r (where the semicolon indicates that the latitude s and the time t are kept fixed). Furthermore, substituting this relationship in (4.28) and differentiating with respect r, it follows that

$$0 = \kappa_r + e^{-\xi}\sin\theta - \kappa_r e^{-\xi}\cos\theta,$$

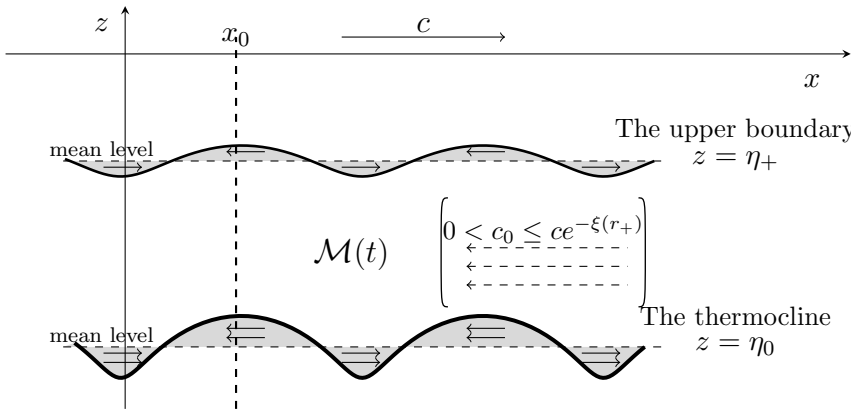

Figure 4.2: Depiction of the mass flux at any fixed latitude s within a narrow equatorial band in presence of a current such that $|c_0| \le ce^{k(r_+(s)+\zeta(s))}$. For every internal wave in the region $\mathcal{M}(t)$ the situation can be seen as a mass of water moving forward near the crest and backward near the trough as the wave passes, having a net result depending upon the current.

which gives

$$\kappa_r = -\frac{e^{-\xi}\sin\theta}{1 - e^{-\xi}\cos\theta}. \tag{4.29}$$

Then, from the expression of the z component in (4.5) and by means of the Implicit Function κ and its derivative with respect r, we obtain the derivative required in the change of variable (4.27), i.e.

$$\frac{\partial z}{\partial r} = 1 + e^{-\xi}\cos\theta + \kappa_r e^{-\xi}\sin\theta = \frac{1 - e^{-2\xi}}{1 - e^{-\xi}\cos\theta}.$$

Thus, the mass flux is written now in the form

$$m(x_0 - ct, s) = \int_{r_0(s)}^{r_+(s)} (-c_0 + ce^{-\xi}\cos\theta)\frac{1 - e^{-2\xi}}{1 - e^{-\xi}\cos\theta}\, dr. \tag{4.30}$$

Let us consider a current c_0 such that

$$|c_0| \le ce^{-k(r_+(s)+\zeta(s))}. \tag{4.31}$$

From the z-component of the solution (4.5), it follows that the crests correspond to $\cos\theta = -1$ and the troughs to $\cos\theta = 1$. Hence, restricting the analysis to the region $\mathcal{M}(t)$, the mass flux for waves within this layer is negative (backwards with respect the wave propagation direction) at the crests and positive (forwards with

respect the wave propagation direction) at the troughs as shown in Figure 4.2). This is similar to the case treated in [13]. The situation is completely different when

$$c_0 < -ce^{-k(r_+(s)+\zeta(s))},$$

obtaining a positive mass flux (4.30) going forwards at the crests and troughs of the internal wave for eastward-propagating waves. The scenario described here is the rather different from [13]. This is due to the addition of a constant current c_0.

Additionally, the time average of the mass flux over a wave period T in the case $c_0 = 0$ can provide some insight into its general behaviour. It is deduced from (4.28) that the function κ is now T-periodic. Moreover, if differentiating (4.28) with respect to time t,

$$\kappa_t = \frac{-ce^{-\xi}\cos\theta}{1 - e^{-\xi}\cos\theta}.$$

Therefore, the mass flux (4.30) is written now as

$$m(x_0 - ct, s) = \int_{r_0(s)}^{r_+(s)} -\kappa_t(1 - e^{-2\xi})dr\,.$$

As κ is T-periodic, it follows that the average of the mass flux over a period T is zero, which is consistent with the results of [13]. As previously, the current term c_0 changes the situation completely; its inclusion produces some net mass flux over a period in a direction that depends on the sign of c_0.

4.3 Internal wave in the f-plane

The analysis done in the previous section is now applied to the solution (3.5) derived in Chapter 3. Due to the incorporation of a meridional variable current, the study of the mean properties for this flow includes not only zonal but also meridional directions.

4.3.1 Mean Lagrangian flow velocity

The horizontal mean Lagrangian velocity over a wave period T in the region $\mathcal{M}(t)$ for the flow (3.5) matches the one already calculated in (4.14), i.e.

$$\begin{aligned}\langle u\rangle_L &= \frac{1}{T}\int_0^T u(q-ct,s,r)\,dt = \frac{1}{T}\int_0^T \left(ce^{-\xi}\cos\theta - c_0\right)dt \\ &= \frac{ce^{-\xi}}{T}\int_0^T \cos[k(q-ct)]dt + \frac{-c_0}{T}\int_0^T 1\,dt = -c_0\,.\end{aligned} \tag{4.32}$$

As before, the horizontal mean Lagrangian flow velocity is either westwards or eastwards, depending on whether the sign of c_0 is positive or negative respectively. This matches the previous case and observations made in [13, 14, 20].

On the other hand, the meridional mean Lagrangian velocity over a wave period T is given by

$$\langle v\rangle_L = \frac{1}{T}\int_0^T \mu(q,r)\,dt = \mu(q,r), \tag{4.33}$$

showing that the mass transport in this direction is governed by the transverse current μ. In either case, no mass is transported when these currents vanish. It is also interesting to study the mean velocity in the layer below the thermocline. It is possible to provide a Lagrangian description for the motion within this layer, indeed the following map

$$\begin{cases} x = q + (c-c_0)t\,, \\ \\ y = \mu(q,r)t\,, \\ \\ z = r\,, \end{cases}$$

has a simple inverse which allows to express the flow in both Lagrangian and Eulerian descriptions, where the velocity field is given by (3.3) when expressed in Eulerian coordinates. In the Lagrangian framework, the velocity takes the form

$$\begin{cases} u = c - c_0\,, \\ \\ v = \mu(q,r)\,, \\ \\ w = 0\,. \end{cases}$$

Thus, the horizontal mean Lagrangian velocity for a particle labelled by (q, s, r) in the layer below the thermocline is

$$\langle u \rangle_L = c - c_0 \,,$$

while the meridional mean Lagrangian velocity is

$$\langle v \rangle_L = \mu(q, r) \,,$$

which is expected as within this layer the currents completely define the motion.

4.3.2 Mean Eulerian flow velocity

The steps given in the previous section to obtain the expression (4.17) for the (horizontal) mean Eulerian velocity over a wave period T are now applied to the present case. For a given latitude y_0 and a fixed depth

$$z_0 = r - d_0 - \frac{1}{k} e^{-kr} \cos\theta$$

in the region $\mathcal{M}(t)$, the Implicit Function theorem establishes a functional relationship $r = \mathscr{R}(q,t) = \mathscr{R}(q - ct)$ between q and r. Hence, an implicit expression for the horizontal Eulerian mean velocity is obtained as follows

$$\begin{aligned}
c + \langle u \rangle_E &= \frac{1}{T} \int_0^T [c + u(x - ct, y_0, z_0)] \, dt = \frac{1}{L} \int_0^L [c + u(x - ct, y_0, z_0)] \, dx \\
&= \frac{1}{L} \int_0^L [c + u(q - ct, s, \mathscr{R}(q - ct)] \frac{\partial x}{\partial q} \, dq \\
&= \frac{1}{L} \int_0^L \left(c + c e^{-k\mathscr{R}} \cos\theta - c_0 \right) \left(1 + \mathscr{R}_q e^{-k\mathscr{R}} \sin\theta - e^{-k\mathscr{R}} \cos\theta \right) dq \\
&= \frac{c}{L} \int_0^L dq - \frac{c}{L} \int_0^L e^{-2k\mathscr{R}} \, dq - \frac{c_0}{L} \int_0^L \frac{1 - e^{-2k\mathscr{R}}}{1 + e^{-k\mathscr{R}} \cos\theta} \, dq \\
&= c - \frac{c}{L} \int_0^L e^{-2k\mathscr{R}} \, dq - \frac{c_0}{L} \int_0^L \frac{1 - e^{-2k\mathscr{R}}}{1 + e^{-k\mathscr{R}} \cos\theta} \, dq \,.
\end{aligned}$$

Therefore,

$$\langle u \rangle_E = -\frac{c}{L} \int_0^L e^{-2k\mathscr{R}} \, dq - \frac{c_0}{L} \int_0^L \frac{1 - e^{-2k\mathscr{R}}}{1 + e^{-k\mathscr{R}} \cos\theta} \, dq \tag{4.34}$$

for any x at a fixed latitude and depth in the region $\mathcal{M}(t)$. This formula is consistent with the mean velocities obtained in the previous section and the ones derived in [70, 114]. It is worth mentioning that for positive c and c_0, (4.34) shows the existence of a westward underlying current in the longitudinal direction and the same analysis done in the previous section in terms of the current c_0 applies here. On the other hand, the mean velocity in the meridional component for the layer $\mathcal{M}(t)$ is given by

$$\begin{aligned}\langle v\rangle_E &= \frac{1}{T}\int_0^T v(x-ct,y_0,z_0)\,dt = \frac{1}{L}\int_0^L v(x-ct,y_0,z_0)\,dx\\ &= \frac{1}{L}\int_0^L v(q-ct,s,\mathscr{R}(q-ct))\frac{\partial x}{\partial q}\,dq\\ &= \frac{1}{L}\int_0^L \mu(q-ct,\mathscr{R}(q-ct))\left(1+\mathscr{R}_q e^{-k\mathscr{R}}\sin\theta - e^{-k\mathscr{R}}\cos\theta\right)dq\\ &= \frac{1}{L}\int_0^L \mu(q-ct,\mathscr{R}(q-ct))\frac{1-e^{-2k\mathscr{R}}}{1+e^{-k\mathscr{R}}\cos\theta}\,dq\,.\end{aligned} \tag{4.35}$$

In addition, the Eulerian mean velocities in the layer below the thermocline are included. The velocity field defined by (3.3) in terms of Eulerian coordinates is

$$\mathbf{u}(x,y,z,t) = \Big(c-c_0,\ \mu(x-(c-c_0)t,z),\ 0\Big)\,.$$

Hence, the horizontal mean velocity over a period T in the uniform layer is given by

$$\langle u\rangle_E = c - c_0\,.$$

The mean meridional Eulerian velocity for a fixed depth z_0 over the period T is

$$\langle v\rangle_E = \frac{1}{T}\int_0^T \mu(x-(c-c_0)t,z_0)\,dt\,,$$

where the nonlinear term $\frac{1-e^{-2k\mathscr{R}}}{1+e^{-k\mathscr{R}}\cos\theta}$ is not longer present and the mean velocity only depends upon μ.

4.3.3 Stokes drift

The Stokes drift is obtained from the expressions of the mean velocities derived in the previous section by means of the formula (4.4). For the layer $\mathcal{M}(t)$, the Stokes

drift in the horizontal and meridional directions are

$$U^S = \frac{1}{L}\int_0^L (ce^{-2k\mathscr{R}} - c_0)\, dq + \frac{c_0}{L}\int_0^L \frac{1-e^{-2k\mathscr{R}}}{1+e^{-k\mathscr{R}}\cos\theta}\, dq$$

and

$$V^S = \mu(q,r) - \frac{1}{L}\int_0^L \mu(q-ct, \mathscr{R}(q-ct))\frac{1-e^{-2k\mathscr{R}}}{1+e^{-k\mathscr{R}}\cos\theta}\, dq\,.$$

respectively. For the layer below the thermocline,

$$U^S = 0$$

in the zonal direction and

$$V^S = \mu(q,r) - \frac{1}{T}\int_0^T \mu(x-(c-c_0)t, z_0)\, dt$$

in the meridional direction.

4.3.4 Mass flux for the transverse current

The study of mean flow properties is concluded with the analysis of the mass flux past a fixed reference. In this case this reference is the portion of a fixed plane $x = x_0$ contained between two given latitudes y_1 and y_2 in the region $\mathcal{M}(t)$. It is necessary to consider a fixed plane, instead of the fixed line as in (4.27), because the flow has now a purely three dimensional description. At a given time t, the relative mass flux crossing

$$S := \{x = x_0\,, \quad y \in [y_1, y_2]\,, \quad z \in [\eta_0(x-ct, y), \eta_+(x-ct, y)]\}\,,$$

where $z = \eta_0(x-ct, y)$ is prescribes the thermocline and $z = \eta_+(x-ct, y)$ the upper interface, is given by

$$\begin{aligned} m(x_0 - ct) &= \iint_S \mathbf{u}\cdot\mathbf{n}\, dS \\ &= \iint_{[y_1,y_2]\times[\eta_0,\eta_+]} (u,v,w)\cdot(1,0,0)\, dy\, dz \\ &= \iint_{[y_1,y_2]\times[\eta_0,\eta_+]} u(x_0-ct, y, z)\, dy\, dz \end{aligned} \tag{4.36}$$

where $\mathbf{n}$ is the unit normal to the surface S. From (3.5),

$$x_0 = q - \frac{1}{k} e^{-kr} \sin[k(q - ct)]$$

and it follows that there exists a functional dependence $q = Q(r)$, whose derivative is given by

$$Q'(r) = -\frac{e^{-kr} \sin\theta}{1 - e^{-kr}\cos\theta} \,. \tag{4.37}$$

Now, for the two fixed latitudes y_1 and y_2,

$$s_1(r) = y_1 - \mu(Q(r), r)t$$

and

$$s_2(r) = y_2 - \mu(Q(r), r)t$$

at any given time t. Subsequently, by (4.37), Fubini's theorem and the corresponding change of variables, the mass flux becomes

$$\begin{aligned}
m(x_0 - ct) &= \int_{[\eta_0,\eta_+]\times[y_1,y_2]} u(x_0 - ct, y, z)\, dydz \\
&= \int_{r_0}^{r_+} \int_{s_1(r)}^{s_2(r)} (ce^{-kr}\cos\theta - c_0) \begin{vmatrix} y_r & y_s \\ z_r & z_s \end{vmatrix} ds\, dr \\
&= -\int_{r_0}^{r_+} \int_{s_1(r)}^{s_2(r)} (ce^{-kr}\cos\theta - c_0)(1 + e^{-kr}\cos\theta + Q'(r)e^{-kr}\sin\theta)\, ds\, dr \\
&= -\int_{r_0}^{r_+} \int_{s_1(r)}^{s_2(r)} (ce^{-kr}\cos\theta - c_0)\left(1 + e^{-kr}\cos\theta - \frac{e^{-2kr}\sin^2\theta}{1 - e^{-kr}\cos\theta}\right) ds\, dr \\
&= -\int_{r_0}^{r_+} \int_{s_1(r)}^{s_2(r)} (ce^{-kr}\cos\theta - c_0)\frac{1 - e^{-2kr}}{1 - e^{-kr}\cos\theta}\, ds\, dr \\
&= -\int_{r_0}^{r_+} (ce^{-kr}\cos\theta - c_0)\frac{1 - e^{-2kr}}{1 - e^{-kr}\cos\theta}(s_2(r) - s_1(r))\, dr \\
&= (y_1 - y_2)\int_{r_0}^{r_+} (ce^{-kr}\cos\theta - c_0)\frac{1 - e^{-2kr}}{1 - e^{-kr}\cos\theta}\, dr \,.
\end{aligned}$$

This expression resembles (4.30) with the addition of the latitude terms accounting for the meridional behaviour. When μ is not constant, the wave motion is three-dimensional. However, due to the simplification offered by the f-plane approximation, the z-component of the solution (3.5) does not depend upon s. Therefore, the

mass flux for a fixed plane $x = x_0$ depends on the width given by the latitudes y_1 and y_2, but not on the function μ. Thus, the mass flux at the crests and troughs can be analysed in the same way as the previous case in terms of conditions such as (4.31).

Finally, for the same region $\mathcal{M}(t)$, fixing the plane $y = y_0$ results in the following mass flux

$$\begin{aligned} m(y_0) &= \int_{[0,\frac{2\pi}{L}]\times[z_0,z_+]} (u,v,w)\cdot(0,1,0)\; d(x,z) = \int_0^{\frac{2\pi}{L}} \int_{z_0}^{z_+} v(x-ct,y_0,z)\; dx\; dz \\ &= \int_0^{\frac{2\pi}{L}} \int_{r_0}^{r_+} \mu(q,r) \begin{vmatrix} x_q & x_r \\ z_q & z_r \end{vmatrix} dq\, dr = \int_0^{\frac{2\pi}{L}} \int_{r_0}^{r_+} \mu(q,r)(1-e^{-2kr})\; dq\, dr \\ &\leq \int_0^{\frac{2\pi}{L}} \int_{r_0}^{r_+} \mu(q,r)\; dq\, dr. \end{aligned}$$

Chapter 5

Hydrodynamic stability of geophysical Lagrangian flows

5.1 Introduction

This chapter focuses on the hydrodynamic stability of the non-hydrostatic internal geophysical waves (2.9) presented in Chapter 2 and the solution (5.18) for the modified β-plane equations described in [61].

In order to properly describe flows from a physical point of view, it is important not only to obtain a flow satisfying the governing equations but also that such flow is stable as it evolves from an initial state. Moreover, it is of great interest to know when and why a particular flow is transformed into something radically different as a consequence of the lack of such stability. This is addressed by what is known as hydrodynamic stability and its definition is far from being trivial, leading to several mathematical approaches. The first important contributions to this area were given by Helmholtz, Rayleigh, Kelvin and Reynolds amongst others. It was Reynolds' experiments which pointed out the necessity of a more rigorous study of hydrodynamic stability, raising the question of whether a given flow is stable or unstable and how it breaks down into turbulence.

In general, equations describing fluid motions are nonlinear PDEs. As a consequence, the methods employed in determining the stability of rigid bodies cannot be simply translated into this case, restricting the hydrodynamic stability studies to just a few particular cases. Those cases are mostly laminar flows with some planar, axial or spherical symmetry.

From a purely physical perspective, the mechanisms of instability are generally due to an imbalance of the equilibrium of external forces, inertia and viscous effects

within a fluid. Even when just one of these mechanisms is taken into account, it is not clear what can be said about the stability. For instance; it is known that, for a large viscosity, any bounded flow is stable. Therefore, the viscosity seems to have a stabilising influence. However, viscosity can also have the effect of diffusing momentum, making some flows that were originally stable under the inviscid hypothesis unstable. The proper balance between inertial forces and viscous forces is given by Reynolds number

$$R = (UL)/\nu\,,$$

which provides some insight into the transition from laminar to turbulent flows, where U and L are respectively some characteristic velocity and length for each particular problem and ν is the kinematic viscosity of the fluid. However, it is not the aim of this chapter to present a complete description of all the physical phenomena involved in hydrodynamical instability. We limit ourselves to introduce some mathematical tools that study this phenomenon and to analyse the geophysical flows presented in the previous chapters.

The analysis of stability usually starts by considering what is called a basic flow, a flow for which some description of its velocity is known as well as the pressure and maybe some other quantities as the temperature. This flow is such that satisfies the governing equations and boundary conditions that apply to each particular case of interest. Once the basic flow is identified, it is disturbed (in some particular way yet to be described) and the evolution of the disturbances characterises its stability. Broadly speaking, a disturbance can fade away, persist as a disturbance of the same order of magnitude, or grow transforming the flow in something completely different from the basic flow.

5.2 Instability of geophysical flows

The linear theory (see [34] for a complete discussion) suggests that studying the spectrum of differential operators provides some insight about stability. However, this is far from trivial for general flows. Nevertheless, as it was proven by Friedlander & Vishik through several papers summarised in [44], a sufficient condition for instability can be obtained in terms of an "energy norm". Using the Lagrangian approach

and the concept of Lyapunov exponents from dynamical system theory, the stability is related with the exponential growth rate along infinitely close trajectories of the fluid velocity. This relation between instability and the use of Lyapunov exponents was described by Bayly in [3], Lifschitz & Hameiri in [92], and Friedlander & Vishik in [43]. Then, Leblanc [91] intelligently implemented this technique for studying the stability of Gerstner's waves and Constantin [20] applied it for more general three-dimensional geophysical flows. The same approach was also employed in obtaining a sufficient condition for instability of equatorial water waves with an underlying current [46]. We are going to make use of the short-wavelength instability method to obtain an instability criterion for the non-hydrostatic internal geophysical waves (2.9) and the solution (5.18) for the modified β-plane equations. A survey of the short-wavelength stability method can be found in [82].

As often occurs with mathematical descriptions, the exact solution given by (2.9) is not likely to appear as such in the ocean or in laboratory experiments. However, from its analysis we are able to study more realistic flows resulting from perturbations of the initial exact and explicit solution. Hence, analysing the stability of the exact solution becomes fundamental. The instability result is then translated into a steepness threshold for these waves, exceeding which the waves are unstable to short-wavelength transverse perturbations.

5.3 Short-wavelength instability method

The short-wavelength method sets a rigorous framework for analysing the instability of geophysical flows described in Lagrangian coordinates, with or without stratification [20, 46, 64, 73, 74, 79–82, 84]. This method developed independently in [3, 42, 92] makes use of perturbations in the form of Wentzel-Kramers-Brillouin-Jeffreys (WKBJ) approximate solutions. Subsequently, the time evolution of the amplitude of these perturbations is regarded as the indicator of the stability, which for the case analysed in this chapter, leads to the study of a system of ODEs. In its most general form, this instability method can be applied to a fluid with variable density, provided the flow is barotropic, i.e. that the density is a function of the pressure only.

It is noted here that, once the barotropic property of the flow has been proven, the governing equations can be rewritten in the following manner. Incompressibility (1.4) is expressed in terms of the pressure as

$$\frac{\partial P}{\partial t} + (\mathbf{u}\cdot\nabla)P = 0\,, \tag{5.1}$$

whereas the momentum equation is given by

$$\frac{D\mathbf{u}}{Dt} + L\mathbf{u} = -\frac{1}{h(P)}\nabla P + \mathbf{F}\,, \tag{5.2a}$$

where

$$L = \begin{pmatrix} 0 & -\beta y & 2\Omega \\ \beta y & 0 & 0 \\ -2\Omega & 0 & 0 \end{pmatrix}. \tag{5.2b}$$

We derive the method for the flow governed by the equations (5.2) and (5.1). This will then also be applied to the case of constant density. The choice of the disturbance for the velocity is

$$\mathbf{u}(\mathbf{X},t) = \Big[\mathbf{A}(\mathbf{X},t) + \varepsilon\,\boldsymbol{\mathcal{A}}(\mathbf{X},t)\Big]\exp\Big[\frac{i}{\varepsilon}\,\Phi(\mathbf{X},t)\Big] + \varepsilon\,\mathbf{u}_{rem}(t,\mathbf{X},\varepsilon)\,, \tag{5.3a}$$

where the amplitude terms $\mathbf{A}(\mathbf{X},t)$, $\boldsymbol{\mathcal{A}}(\mathbf{X},t)$ and the remainder term $\mathbf{u}_{rem}(t,\mathbf{X},\varepsilon)$ are vector functions. The function $\Phi(\mathbf{X},t)$ is a scalar such that $\Phi_t \not\equiv 0$ and $\mathbf{X}$ is the trajectory of the basic flow with velocity field $\mathbf{U}$. In addition, the disturbance of the pressure is taken to be

$$p(\mathbf{X},t) = \Big[B(\mathbf{X},t) + \varepsilon\,\mathscr{B}(\mathbf{X},t)\Big]\exp\Big[\frac{i}{\varepsilon}\,\Phi(\mathbf{X},t)\Big] + \varepsilon\,p_{rem}(t,\mathbf{X},\varepsilon)\,, \tag{5.3b}$$

where $B(\mathbf{X},t)$, $\mathscr{B}(\mathbf{X},t)$ and $p_{rem}(t,\mathbf{X},\varepsilon)$ are all scalar functions. These disturbances are of the form of the ones considered in [80] where the expression for the exponential in terms of the small parameter ε suits well the governing equations and it is key in maintaining the transversality condition of the wave vector with respect to the amplitude term. It follows that the short-wavelength instability method can be applied in a similar manner. Let us consider the flow which results from perturbing

the basic flow $\mathbf{U}$ with the previous disturbances, i.e. a flow with velocity and pressure given respectively by

$$\begin{aligned} \mathscr{U} &= \mathbf{U} + \mathbf{u}\,, \\ \mathscr{P} &= P + p\,. \end{aligned} \tag{5.4}$$

and assuming the following linear approximation

$$\frac{1}{h(P+p)} = \frac{1}{h(P)} - \frac{h'(P)}{h^2(P)}p\,,$$

the linearised version of the incompressibility condition for a barotropic fluid (5.1), the mass conservation for an incompressible fluid and the momentum equation for the modified β-plane approximation (5.2) for the perturbed flow (5.4) are obtained as

$$p_t + (\mathbf{u}\cdot\nabla)P + (\mathbf{U}\cdot\nabla)p = 0\,, \tag{5.5a}$$

$$\nabla\cdot\mathbf{u} = 0\,, \tag{5.5b}$$

$$\mathbf{u}_t + (\mathbf{U}\cdot\nabla)\mathbf{u} + (\mathbf{u}\cdot\nabla)\mathbf{U} + L\mathbf{u} = -\nabla\Big(\frac{p}{h(P)}\Big)\,, \tag{5.5c}$$

where it has been taken into account that the basic flow $\mathbf{U}$ satisfies the governing equations.

Substituting the choice of disturbance (5.3) into the equations (5.5) and taking the resultant equations in terms of powers of ε yields a system of ODEs describing the evolution of the short-wavelength perturbations. First, from (5.5b), up to order ε,

$$\mathbf{A}\cdot\nabla\Phi = 0 \tag{5.6}$$

$$\nabla\cdot\mathbf{A} + i\,\boldsymbol{\mathcal{A}}\cdot\nabla\Phi = 0\,.$$

Second, from (5.5c)

$$\Big(\Phi_t + \mathbf{U}\cdot\nabla\Phi\Big)\mathbf{A} = -\frac{B}{h(P)}\nabla\Phi \tag{5.7}$$

and

$$\mathbf{A}_t + (\mathbf{U}\cdot\nabla)\mathbf{A} + (\mathbf{A}\cdot\nabla)\mathbf{U} + L\mathbf{A} + i\Big(\Phi_t + \mathbf{U}\cdot\nabla\Phi\Big)\boldsymbol{\mathcal{A}} = -\Big[\nabla\Big(\frac{B}{h(P)}\Big) + i\frac{\mathscr{B}}{h(P)}\nabla\Phi\Big]\,. \tag{5.8}$$

Combining (5.6) and (5.7), yields

$$\Phi_t + \mathbf{U}\cdot\nabla\Phi = 0\,, \quad \text{for all } \mathbf{A} \neq \mathbf{0}\,, \tag{5.9}$$

and

$$B = 0\,, \quad \text{for all } \nabla\Phi \neq \mathbf{0}\,. \tag{5.10}$$

Hence, (5.8) becomes

$$\mathbf{A}_t + (\mathbf{U}\cdot\nabla)\mathbf{A} + (\mathbf{A}\cdot\nabla)\mathbf{U} + L\mathbf{A} = -i\frac{\mathscr{B}}{h(P)}\nabla\Phi\,.$$

Finally, from (5.5a) together with (5.9) and (5.10)

$$\mathbf{A}\cdot\nabla P = 0\,.$$

Therefore, the evolution of the short-wavelength perturbations at leading order in powers of ε is governed by

$$\Phi_t + \mathbf{U}\cdot\nabla\Phi = 0\,, \tag{5.11}$$

which after taking the gradient becomes

$$\frac{D}{Dt}\Big\{\nabla\phi\Big\} = -\nabla\mathbf{U}[\nabla\phi] \tag{5.12}$$

and

$$\mathbf{A}_t + (\mathbf{U}\cdot\nabla)\mathbf{A} + (\mathbf{A}\cdot\nabla)\mathbf{U} + L\mathbf{A} = -i\frac{\mathscr{B}}{h(P)}\nabla\Phi\,,$$

together with the initial conditions

$$\Phi(0,\mathbf{X}) = \Phi_0(\mathbf{X})\,,$$
$$\mathbf{A}(0,\mathbf{X}) = \mathbf{A}_0(\mathbf{X})\,,$$

such that $\mathbf{A}_0\cdot\nabla\Phi_0 = 0$. Moreover, it can be shown that

$$\mathscr{B} = i\frac{h(P)}{||\nabla\Phi||^2}\big[\nabla\Phi\cdot\{2(\mathbf{A}\cdot\nabla)\mathbf{U} + L\mathbf{A}\}\big] \tag{5.13}$$
$$\boldsymbol{\mathcal{A}} = i\frac{1}{||\nabla\Phi||^2}(\mathbf{A}\cdot\nabla)\nabla\Phi\,.$$

Summarising B is zero whereas $\mathscr{B}$ and $\boldsymbol{\mathcal{A}}$ can be expressed in terms of $\mathbf{A}$ and $\nabla\Phi$. Furthermore, note that Φ_t can be obtained from (5.11). The remainder terms, of order ε, satisfy the following system of equations

$$(\mathbf{u}_{rem})_t + (\mathbf{U}\cdot\nabla)\mathbf{u}_{rem} + (\mathbf{u}_{rem}\cdot\nabla)\mathbf{U} + L\mathbf{u}_{rem} + \nabla\Big(\frac{p_{rem}}{h(P)}\Big) = \boldsymbol{\mathcal{T}}\,,$$
$$\nabla\cdot\mathbf{u}_{rem} = -(\nabla\cdot\boldsymbol{\mathcal{A}})\exp\Big[\frac{i}{\varepsilon}\Phi\Big]\,,$$

where

$$\boldsymbol{\mathcal{T}} = -\left\{\boldsymbol{\mathcal{A}}_t + (\mathbf{U}\cdot\nabla)\boldsymbol{\mathcal{A}} + (\boldsymbol{\mathcal{A}}\cdot\nabla)\mathbf{U} + L\boldsymbol{\mathcal{A}} + \nabla\Big(\frac{\mathscr{B}}{h(P)}\Big)\right\}\exp\Big[\frac{i}{\varepsilon}\Phi\Big]\,.$$

It can be proven, in the same way as in [79, 80], that $\mathbf{u}_{rem}(t,\mathbf{X},\varepsilon)$ and $p_{rem}(t,\mathbf{X},\varepsilon)$ are bounded in the L^2-norm, for any time t, by functions that can depend on t but are independent of ε. Therefore, the remainder terms are negligible as ε approaches to zero on any finite time interval. If we denote the wavevector by $\boldsymbol{k} = \nabla\Phi$; then, for an arbitrary particle with a trajectory passing through $\mathbf{X}_0$ at a given time, the evolution of $\mathbf{X}$, $\boldsymbol{k}$ and $\mathbf{A}$ at leading order in the expansion in powers of ε is given by the following system of ODEs

$$\begin{cases} \dfrac{D\mathbf{X}}{Dt} = \mathbf{U}(\mathbf{X},t)\,, \\[2ex] \dfrac{D\boldsymbol{k}}{Dt} = -\nabla\mathbf{U}[\boldsymbol{k}]\,, \\[2ex] \dfrac{D\mathbf{A}}{Dt} = -(\mathbf{A}\cdot\nabla)\mathbf{U} - L\mathbf{A} + \dfrac{\boldsymbol{k}\cdot\big[2(\mathbf{A}\cdot\nabla)\mathbf{U} + L\mathbf{A}\big]}{||\boldsymbol{k}||^2}\boldsymbol{k}\,, \end{cases} \tag{5.14a}$$

with initial conditions

$$\mathbf{X} = \mathbf{X}_0\,, \qquad \boldsymbol{k} = \boldsymbol{k}_0\,, \qquad \mathbf{A} = \mathbf{A}_0 \quad \text{such that} \quad \mathbf{A}_0\cdot\nabla\Phi_0 = 0\,. \tag{5.14b}$$

For the case of constant density, the incompressibility condition is trivially satisfied. However, it is pointed out here that this does not simplify the equations describing the evolution of the wavevector and the amplitude for the perturbations. The only difference, as indicated in [82], is in the the pressure term (5.13) which is no longer multiplied by $h(P)$. Moreover, the modification of the body force introduced by (5.16) does not affect the previous perturbation method neither. Therefore,

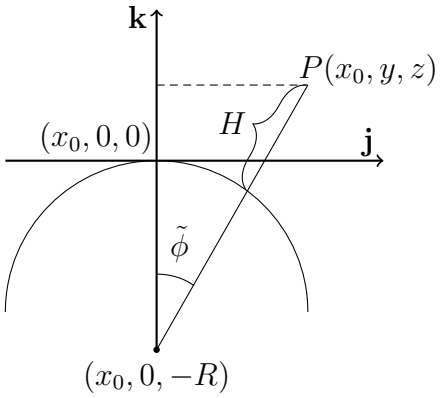

Figure 5.1: For a fixed x_0, the height H corrects the deviation of the curved Earth's surface from the tangent plane considered in the β-plane approximation.

the following criterion for the instability of geophysical water waves satisfying the modified β-plane approximation equations for a barotropic fluid, which can also be applied to the standard β-plane approximation equations is presented.

Theorem 5.3.1 (Criterion for Instability)**.** *A barotropic fluid satisfying the geophysical governing equations (either the modified or the standard β-plane approximation) is unstable in the L^2-norm along the trajectory of a given particle passing through $\mathbf{X}_0$ if, for some $\boldsymbol{k}_0$ and $\mathbf{A}_0$ such that $\boldsymbol{k}_0 \cdot \mathbf{A}_0 = 0$, the amplitude $\mathbf{A}$ given by the solution of* (5.14a) *grows without bound in time.*

5.4 Instability for the modified β-plane approximation

The different versions of the geophysical governing equations used so far have been based upon the choice of a local system of coordinates on the Earth's surface which simplifies the geometry and assumes the Earth is locally flat. This approach essentially involves working in a plane tangent to the surface of the Earth, which results in a miscalculation of the body force due to gravity that can be seen in Figure 5.1. The correction of the body force used in the β-plane approximation equations done in [61] is considered here. For the β-plane approximation equations derived in Chapter 2, the body force was given by the three-dimensional vector $(0, 0, -g)$,

while in this case

$$\mathbf{F} = -\nabla\Gamma\,,$$

where $\Gamma(x, y, z) = Hg$. From Figure 5.1, it follows that

$$H = \frac{R+z}{\cos\tilde{\phi}} - R = \frac{1}{\cos\tilde{\phi}}\Big[R(1-\cos\tilde{\phi}) + z\Big] = \frac{1}{\cos\tilde{\phi}}\Big[2R\sin^2\Big(\frac{\tilde{\phi}}{2}\Big) + z\Big]\,.$$

Using the same considerations as in the Taylor approximation (2.1) about the zero latitude, H is approximated as

$$H \approx R\,\frac{\tilde{\phi}^2}{2} + z\,.$$

Similar to the derivation of the β-plane equations, $\tilde{\phi} = y/R$ for latitudes within a narrow ocean strip about the equator, so

$$H \approx z + \frac{y^2}{2R}\,. \tag{5.15}$$

Therefore, the body force for what it will be referred to as the modified equatorial β-plane equations is given by

$$\mathbf{F} = (0, -\frac{y}{R}g, -g)\,. \tag{5.16}$$

These modified β-pane equations are then given by

$$\begin{cases} u_t + uu_x + vu_y + wu_z + 2\Omega w - \beta yv &= -\dfrac{1}{\rho}P_x\,, \\[2ex] v_t + uv_x + vv_y + wv_z + \beta yu &= -\dfrac{1}{\rho}P_y - \dfrac{g}{R}y\,, \\[2ex] w_t + uw_x + vw_y + ww_z - 2\Omega u &= -\dfrac{1}{\rho}P_z - g\,, \end{cases} \tag{5.17}$$

where the new body force has been incorporated into the original β-plane equations (2.3).

5.4.1 Solution for the modified β-plane equations

The exact solution for the modified β-plane equations (5.16) derived in [61] is now presented. This solution is given in Lagrangian coordinates, where the position of a fluid particle labelled by $(q, s, r) \in (-\infty, \infty) \times [-s_0, s_0] \times (-\infty, r_0)$, for $r_0 < 0$ and at time t is given by

$$\begin{cases} x(q,s,r,t) = q - c_0 t - \dfrac{1}{k} e^{k[r-\zeta(s)]} \sin[k(q-ct)]\,, \\ \\ y(q,s,r,t) = s\,, \\ \\ z(q,s,r,t) = r + \dfrac{1}{k} e^{k[r-\zeta(s)]} \cos[k(q-ct)]\,. \end{cases} \tag{5.18}$$

The function ζ expressing a decay in fluid motion away from the equator is now given by

$$\zeta(s) = \frac{c\beta}{2\hat{g}} s^2$$

where

$$\hat{g} = g + 2\Omega c_0\,.$$

The validity of (5.18) leads to the following dispersion relation [61],

$$c = \frac{-\Omega + \sqrt{\Omega^2 + k\hat{g}}}{k}\,. \tag{5.19}$$

By calculating the time derivative of (5.18), it follows that the velocity field is

$$(u, v, w) = (-c_0 + ce^{\xi} \cos\theta, 0, ce^{\xi} \sin\theta)\,, \tag{5.20}$$

where θ is as in (2.14) and

$$\overline{\xi} := k[r - \zeta(s)]\,. \tag{5.21}$$

Furthermore, the acceleration is obtained from (5.18) by differentiating again with respect to time to give

$$\left(\frac{du}{dt}, \frac{dv}{dt}, \frac{dw}{dt}\right) = (kc^2 e^{\xi} \sin\theta, 0, -kc^2 e^{\xi} \cos\theta)\,.$$

Finally, the velocity gradient tensor in terms of the position variables (x, y, z) is given by

$$\nabla \mathbf{u} = \begin{pmatrix} u_x & v_x & w_x \\ u_y & v_y & w_y \\ u_z & v_z & w_z \end{pmatrix} = \frac{kce^{\overline{\xi}}}{1-e^{2\overline{\xi}}} \begin{pmatrix} -\sin\theta & 0 & \cos\theta + e^{\overline{\xi}} \\ \zeta_s(e^{\overline{\xi}} - \cos\theta) & 0 & -\zeta_s \sin\theta \\ -e^{\overline{\xi}} + \cos\theta & 0 & \sin\theta \end{pmatrix}. \tag{5.22}$$

This gradient matrix is obtained by the change of variables that relates the Lagrangian and Eulerian coordinates, which is well defined since $\overline{\xi} \leq r_0$ and r_0 was taken to be negative; see [61] for more details.

Variable density case

It was proven in [61] that, in absence of the current c_0, it is possible to accommodate a variable density and obtain an exact solution of the form (5.18) for the modified β-plane equations. This section is devoted to prove that such flow description is barotropic, i.e, that the density is a function of the pressure only.

Lemma 5.4.1. *The flow given by* (5.18) *for* $c_0 = 0$ *is barotropic, i.e.,*

$$\rho = h(P) \quad \textit{where} \quad h'(P) \neq 0\,. \tag{5.23}$$

Proof. The proof is based upon the analysis of the corresponding vorticity equation. The vorticity $\boldsymbol{\omega} = (w_y - v_z, u_z - w_x, v_x - u_y)$ is computed using (5.22), resulting in

$$\boldsymbol{\omega} = \left(-s\frac{kc^2\beta\, e^{\xi}\sin\theta}{g(1-e^{2\xi})}, -\frac{2kce^{2\xi}}{1-e^{2\xi}}, s\frac{kc^2\beta}{g}\frac{e^{\xi}\cos\theta - e^{2\xi}}{1-e^{2\xi}} \right). \tag{5.24}$$

On the other hand, differentiating the third equation in (5.17) with respect to y and subtracting the derivative of the second equation with respect z,

$$\frac{D\omega_1}{Dt} - (\boldsymbol{\omega}\cdot\nabla)u - 2\Omega u_y - \beta y u_z = \frac{1}{\rho^2}(\boldsymbol{\nabla}\rho \times \boldsymbol{\nabla}P)_1\,,$$

where the incompressibility condition has been considered. In the same way, differentiating the first equation in (5.17) with respect to z and subtracting the derivative of the third equation with respect to x gives

$$\frac{D\omega_2}{Dt} - (\boldsymbol{\omega}\cdot\nabla)v - 2\Omega w_z - \beta y v_z + 2\Omega u_x = \frac{1}{\rho^2}(\boldsymbol{\nabla}\rho \times \boldsymbol{\nabla}P)_2\,.$$

Finally, differentiating the second equation with respect to x and subtracting the derivative of the first equation with respect to y results in

$$\frac{D\omega_3}{Dt} - (\omega \cdot \nabla)w - 2\Omega w_y + \beta y u_x + \beta y v_y + \beta v = \frac{1}{\rho^2}(\boldsymbol{\nabla}\rho \times \boldsymbol{\nabla}P)_3 \,.$$

Therefore, using the incompressibility condition again and taking into account that the meridional component of the velocity (5.20) vanishes, the following set of equations is obtained

$$\begin{cases} \dfrac{D\omega_1}{Dt} - (\boldsymbol{\omega} \cdot \nabla)u - 2\Omega u_y - \beta s u_z = \dfrac{1}{\rho^2}(\boldsymbol{\nabla}\rho \times \boldsymbol{\nabla}P)_1 \,, \\ \qquad\qquad\qquad\qquad \dfrac{D\omega_2}{Dt} = \dfrac{1}{\rho^2}(\boldsymbol{\nabla}\rho \times \boldsymbol{\nabla}P)_2 \,, \\ \dfrac{D\omega_3}{Dt} - (\omega \cdot \nabla)w - 2\Omega w_y + \beta s w_z = \dfrac{1}{\rho^2}(\boldsymbol{\nabla}\rho \times \boldsymbol{\nabla}P)_3 \,. \end{cases} \tag{5.25}$$

However, the left hand side of the equations (5.25) are all zero. For the second equation, it is enough to check that the second component in (5.24) is time independent. For the other two components, it follows from the expressions in (5.22), (5.24) and the dispersion relation in the absence of current, that

$$kc^2 + 2\Omega c - g = 0 \,.$$

Thus,

$$\boldsymbol{\nabla}\rho \times \boldsymbol{\nabla}P = \mathbf{0} \,.$$

It follows that the density can be expressed as a function of the form (5.23). □

5.5 Short-wavelength instability for the modified β-plane approximation

The first instability result is obtained for the flow solution (5.18). Thus, the basic flow velocity field considered here is given by

$$(U, V, W) = (-c_0 + ce^{\overline{\xi}} \cos\theta, 0, ce^{\overline{\xi}} \sin\theta) \,, \tag{5.26}$$

where capital letters are used to emphasise that this is the undisturbed flow, $\overline{\xi}$ is given by (5.21) and θ by (2.14). The velocity gradient tensor in terms of the position

variables (X, Y, Z) is given by

$$\nabla \mathbf{U} = \begin{pmatrix} U_X & V_X & W_X \\ U_Y & V_Y & W_Y \\ U_Z & V_Z & W_Z \end{pmatrix} = \frac{kce^{\bar{\xi}}}{1-e^{2\bar{\xi}}} \begin{pmatrix} -\sin\theta & 0 & \cos\theta + e^{\bar{\xi}} \\ \zeta_s(e^{\bar{\xi}} - \cos\theta) & 0 & -\zeta_s \sin\theta \\ -e^{\bar{\xi}} + \cos\theta & 0 & \sin\theta \end{pmatrix}. \tag{5.27}$$

It has been shown in Theorem 5.3.1 that in order to obtain an instability criterion it is enough to find an initial disturbance for which the amplitude $\mathbf{A}$ grows without bound. Accordingly, the following initial disturbance is chosen

$$\boldsymbol{k}_0 = \begin{bmatrix} 0 \\ 1 \\ 0 \end{bmatrix}, \qquad \mathbf{A}_0 = \begin{bmatrix} A_{01} \\ 0 \\ A_{02} \end{bmatrix}, \tag{5.28}$$

whose scalar product is zero. It follows from the second equation in (5.14a) and the velocity gradient (5.27) that

$$\boldsymbol{k}(t) = \begin{bmatrix} 0 \\ 1 \\ 0 \end{bmatrix} \qquad \text{for all} \quad t \geq 0\,,$$

whereas the amplitude equation turns into the nonautonomous differential system

$$\begin{cases} \dot{A}_1 = \beta s A_2 - 2\Omega A_3 + \dfrac{kce^{\bar{\xi}}\sin\theta}{1-e^{2\bar{\xi}}} A_1 - \dfrac{kc\zeta_s e^{\bar{\xi}}(e^{\bar{\xi}} - \cos\theta)}{1-e^{2\bar{\xi}}} A_2 + \dfrac{kce^{\bar{\xi}}(e^{\xi} - \cos\theta)}{1-e^{2\bar{\xi}}} A_3\,, \\ \dot{A}_2 = 0\,, \\ \dot{A}_3 = 2\Omega A_1 - \dfrac{kce^{\bar{\xi}}(e^{\bar{\xi}} + \cos\theta)}{1-e^{2\bar{\xi}}} A_1 + \dfrac{kc\zeta_s e^{\bar{\xi}}\sin\theta}{1-e^{2\xi}} A_2 - \dfrac{kce^{\bar{\xi}}\sin\theta}{1-e^{2\bar{\xi}}} A_3\,, \end{cases}$$

which, under the initial condition (5.28) for the amplitude, is reduced to the two-dimensional system

$$\begin{cases} \dot{A}_1 = -2\Omega A_3 + \dfrac{kce^{\bar{\xi}}\sin\theta}{1-e^{2\bar{\xi}}} A_1 + \dfrac{kce^{\bar{\xi}}(e^{\bar{\xi}} - \cos\theta)}{1-e^{2\bar{\xi}}} A_3 \\ \dot{A}_3 = 2\Omega A_1 - \dfrac{kce^{\bar{\xi}}(e^{\bar{\xi}} + \cos\theta)}{1-e^{2\bar{\xi}}} A_1 - \dfrac{kce^{\bar{\xi}}\sin\theta}{1-e^{2\bar{\xi}}} A_3\,. \end{cases}$$

Furthermore, this is expressed in a matrix form as

$$\dot{\mathbf{A}} = \frac{kce^{\bar{\xi}}}{1-e^{2\bar{\xi}}} M\mathbf{A} + \Big(2\Omega - \frac{kce^{2\bar{\xi}}}{1-e^{2\bar{\xi}}}\Big) R\mathbf{A}$$

where

$$M = \begin{pmatrix} \sin\theta & -\cos\theta \\ -\cos\theta & -\sin\theta \end{pmatrix}, \qquad R = \begin{pmatrix} 0 & -1 \\ 1 & 0 \end{pmatrix}, \qquad \mathbf{A} = \begin{pmatrix} A_1 \\ A_3 \end{pmatrix}.$$

However, M depends upon t so, in order to obtain an autonomous system, the system is transformed by means of the matrix

$$P = \begin{pmatrix} \cos(\frac{kct}{2}) & \sin(\frac{kct}{2}) \\ -\sin(\frac{kct}{2}) & \cos(\frac{kct}{2}) \end{pmatrix},$$

into the following autonomous system of ODEs

$$\frac{d\tilde{\mathbf{A}}}{dt} = Q\tilde{\mathbf{A}} \qquad \text{for} \quad \tilde{\mathbf{A}} = P^{-1}\mathbf{A} \tag{5.29}$$

where

$$Q = \begin{pmatrix} \frac{kce^{\bar{\xi}}}{1-e^{2\bar{\xi}}}\sin(kq) & -\frac{kce^{\bar{\xi}}}{1-e^{2\bar{\xi}}}\cos(kq) - 2\Omega + \frac{kce^{2\bar{\xi}}}{1-e^{2\bar{\xi}}} - \frac{kc}{2} \\ -\frac{kce^{\bar{\xi}}}{1-e^{2\bar{\xi}}}\cos(kq) + 2\Omega - \frac{kce^{2\bar{\xi}}}{1-e^{2\bar{\xi}}} + \frac{kc}{2} & -\frac{kce^{\bar{\xi}}}{1-e^{2\bar{\xi}}}\sin(kq) \end{pmatrix}.$$

Thus, the asymptotic behaviour of $\tilde{\mathbf{A}}(t)$ is now characterised by the eigenvalues of Q. In general, λ is an eigenvalue of Q if and only if satisfies the equation

$$\lambda^2 = \frac{(3kc+4\Omega)^2 e^{2\bar{\xi}} - (kc+4\Omega)^2}{4(1-e^{2\bar{\xi}})}.$$

Therefore, $\tilde{\mathbf{A}}(t)$ will grow exponentially as t goes to infinity if and only if there exists a positive real eigenvalue, which from the last expression is equivalent to

$$e^{\xi} > \frac{4\Omega + kc}{4\Omega + 3kc}. \tag{5.30}$$

Finally, due to the time periodicity of the matrix P, the amplitude A given by (5.29) will grow exponentially when $\tilde{\mathbf{A}}(t)$ does, which occurs when (5.30) is satisfied.

5.5.1 Instability in terms of the wave steepness

The result given by (5.30) is interpreted here in physical terms. We make use of a quantity often considered in the study of water waves, the steepness of the wave profile. This is defined as the amplitude of the wave times the wavenumber.

Constant density

In the case of constant density, the dispersion relation (5.19) allows to express the instability criterion (5.30) in terms of just three relevant physical parameters; the wavenumber k, the rotational speed of the Earth Ω and the gravitational term $\hat{g}$ (which includes the current c_0). The flow (5.18) for constant density is unstable if and only if

$$e^{\bar{\xi}} > \frac{3\Omega + \sqrt{\Omega^2 + k\hat{g}}}{\Omega + 3\sqrt{\Omega^2 + k\hat{g}}}\,. \tag{5.31}$$

Whereas the steepness of the wave (5.18) along the equator is e^{kr_0}. It is important to point out that for typical ocean wavelengths, the fraction in (5.31) is approximately $1/3$ due to the fact that $\Omega^2 \ll k\hat{g}$. Thus, the equatorial trapped wave is unstable when the steepness is greater than $1/3$ for an initial disturbance satisfying (5.28).

Variable density

The same choice (5.28) for the initial wavevector and amplitude yields the same two-dimensional ODE for the amplitude $\mathbf{A}$ in the case of a variable density without the constant current term c_0. Repeating the process described before, it follows that the amplitude will grow exponentially if and only if (5.30) is satisfied. Therefore, the dispersion relation (5.19) establishes now the following instability criterion

$$e^{\bar{\xi}} > \frac{3\Omega + \sqrt{\Omega^2 + kg}}{\Omega + 3\sqrt{\Omega^2 + kg}}\,, \tag{5.32}$$

for the variable density in absence of the constant current where $\hat{g}$ became g. Therefore, as long as the flow is barotropic, the instability threshold (5.32) is the same as (5.31) when $c_0 = 0$, which is the same as the one originally derived in [20].

These results show that, at the same order in the disturbances, the incorporation of the term correcting the deviation of the β-plane approximation from the

curved Earth's surface does not affect the instability threshold already derived for the stratified case in [80] and for the case with current in [46].

5.6 Short-wavelength instability of the internal wave above the thermocline

The instability of the exact solution (2.9) described in Chapter 2 is performed in this section. This analysis, published in [113], is focused on the layer $\mathcal{M}(t)$, where the solution is explicit in terms of Lagrangian variables. The velocity of the solution (2.9) given in Lagrangian coordinates is

$$\mathbf{U} = (U, V, W) = (ce^{-\xi}\cos\theta, 0, -ce^{-\xi}\sin\theta)\,. \tag{5.33}$$

where ξ is given by (2.13) and θ by (2.14). By differentiating, it follows that the acceleration is given by

$$\left(\frac{dU}{dt}, \frac{dV}{dt}, \frac{dW}{dt}\right) = (kc^2e^{-\xi}\sin\theta, 0, kc^2e^{-\xi}\cos\theta)\,.$$

In addition, the gradient matrix of the velocity for the Eulerian variables (X, Y, Z) is

$$\nabla\mathbf{U} = \frac{kce^{-\xi}}{1-e^{-2\xi}}\begin{pmatrix} -\sin\theta & 0 & -\cos\theta - e^{-\xi} \\ f_s(e^{-\xi}-\cos\theta) & 0 & f_s\sin\theta \\ e^{-\xi}-\cos\theta & 0 & \sin\theta \end{pmatrix}. \tag{5.34}$$

The process employed in the previous section is applied to the flow given by (5.33). In order to apply the instability criterion (5.3.1), the initial disturbance (5.28) is chosen. It follows from the second equation in (5.14a) and the velocity gradient (5.34) that

$$\boldsymbol{k}(t) = \begin{bmatrix} 0 \\ 1 \\ 0 \end{bmatrix} \qquad \text{for all} \quad t \geq 0\,.$$

Now, the amplitude equation turns into the nonautonomous differential system

$$\begin{cases} \dot{A}_1 = -2\Omega A_3 + \dfrac{kce^{-\xi}\sin\theta}{1-e^{-2\xi}}A_1 - \dfrac{kc\zeta_s e^{-\xi}(e^{-\xi}-\cos\theta)}{1-e^{-2\xi}}A_2 - \dfrac{kce^{-\xi}(e^{-\xi}-\cos\theta)}{1-e^{-2\xi}}A_3\,, \\ \dot{A}_2 = 0\,, \\ \dot{A}_3 = 2\Omega A_1 + \dfrac{kce^{\xi}(e^{-\xi}+\cos\theta)}{1-e^{-2\xi}}A_1 - \dfrac{kc\zeta_s e^{-\xi}\sin\theta}{1-e^{-2\xi}}A_2 - \dfrac{kce^{-\xi}\sin\theta}{1-e^{-2\xi}}A_3\,, \end{cases}$$

which, under the initial condition (5.28) is reduced to the two-dimensional system

$$\begin{cases} \dot{A}_1 = -2\Omega A_3 + \dfrac{kce^{-\xi}\sin\theta}{1-e^{-2\xi}}A_1 - \dfrac{kce^{-\xi}(e^{-\xi}-\cos\theta)}{1-e^{-2\xi}}A_3 \\ \dot{A}_3 = 2\Omega A_1 + \dfrac{kce^{-\xi}(e^{-\xi}+\cos\theta)}{1-e^{-2\xi}}A_1 - \dfrac{kce^{-\xi}\sin\theta}{1-e^{-2\xi}}A_3\,. \end{cases}$$

Writing the system in terms of the matrices

$$N = \begin{pmatrix} \sin\theta & \cos\theta \\ \cos\theta & -\sin\theta \end{pmatrix}, \qquad R = \begin{pmatrix} 0 & -1 \\ 1 & 0 \end{pmatrix},$$

as

$$\dot{\mathbf{A}} = \frac{kce^{-\xi}}{1-e^{-2\xi}}N\mathbf{A} + \Big(2\Omega + \frac{kce^{-2\xi}}{1-e^{-2\xi}}\Big)R\mathbf{A}\,, \tag{5.35}$$

where N depends upon t and $\mathbf{A} = [A_1, A_3]$ refers to the two-dimensional amplitude vector. This system can be transformed into an autonomous system by the change of variables given by the matrix

$$P = \begin{pmatrix} \cos(\frac{kct}{2}) & -\sin(\frac{kct}{2}) \\ \sin(\frac{kct}{2}) & \cos(\frac{kct}{2}) \end{pmatrix}.$$

The system (5.35) is equivalent to the autonomous ODE system

$$\frac{d\tilde{\mathbf{A}}}{dt} = Q\tilde{\mathbf{A}} \qquad \text{for} \quad \tilde{\mathbf{A}} = P^{-1}\mathbf{A}\,,$$

where

$$Q = \begin{pmatrix} \frac{kce^{-\xi}}{1-e^{-2\xi}}\sin(kq) & \frac{kce^{-\xi}}{1-e^{-2\xi}}\cos(kq) - 2\Omega - \frac{kce^{-\xi}}{1-e^{-2\xi}} + \frac{kc}{2} \\ \frac{kce^{-\xi}}{1-e^{-2\xi}}\cos(kq) + 2\Omega + \frac{kce^{-\xi}}{1-e^{-2\xi}} - \frac{kc}{2} & -\frac{kce^{-\xi}}{1-e^{-2\xi}}\sin(kq) \end{pmatrix}.$$

Thus, the asymptotic behaviour of $\tilde{\mathbf{A}}(t)$ is characterised by the eigenvalues of Q. In general, λ is an eigenvalue of Q if and only if it satisfies the equation

$$\lambda^2 = \frac{[(3kc-4\Omega)^2 + (kc-4\Omega)^2]e^{-2\xi} - (3kc-4\Omega)^2e^{-4\xi} - (kc-4\Omega)^2}{4(1-e^{-2\xi})^2}\,.$$

Therefore, $\tilde{\mathbf{A}}(t)$ grows exponentially as t goes to infinity if and only if

$$\frac{(3kc-4\Omega)^2 e^{-2\xi} - (kc-4\Omega)^2}{4(1-e^{-2\xi})} > 0\,,$$

where $1-e^{-2\xi}$ is positive, ensuring the local diffeomorphic character of the flow map (see Chapter 2). It is noted here that kc is greater than 4Ω for any wavelength less than 2000 km (see section 3 in [14] for details). Therefore, within that range, the amplitude will grow exponentially if

$$e^{-\xi} > \frac{kc-4\Omega}{3kc-4\Omega}\,. \tag{5.36}$$

It follows from the dispersion relation (2.11), that the previous condition can be written as

$$e^{-\xi} > \frac{\sqrt{(\Omega\tilde{\rho})^2 + kg\tilde{\rho}} - \Omega\tilde{\rho} - 4\Omega}{3\sqrt{(\Omega\tilde{\rho})^2 + kg\tilde{\rho}} - 3\Omega\tilde{\rho} - 4\Omega}\,. \tag{5.37}$$

where $\tilde{\rho}$ is as in (3.13).

5.6.1 Instability in terms of the steepness of the internal wave

Regarding the solution given by (2.9), the steepness of the internal wave along the equator is given by e^{-kr_0}, since the difference in elevation between crest and trough is $2e^{-kr_0}/k$, as shown in Figure 5.2. Therefore, a steepness greater that the right-hand side of (5.37) will lead to instability. For typical ocean wavelengths kc dominates and the ratio on the right-hand side of (5.37) approaches 1/3 as the wavelength decreases, as illustrated in Table 5.1.

Finally, it is noted that the non-hydrostatic internal wave model considered here describes a complicated flow, which results in the intricate dispersion relation (2.11). The nature of the solution allows to derive an instability criterion by means of the short-wavelength method. Despite the intricate dispersion relation, it is possible to obtain an instability threshold for the steepness of the non-hydrostatic internal wave in terms of physically relevant parameters. For small wavelengths, the threshold for the wave steepness is slightly less than 1/3, which is similar to the situation described in [64].

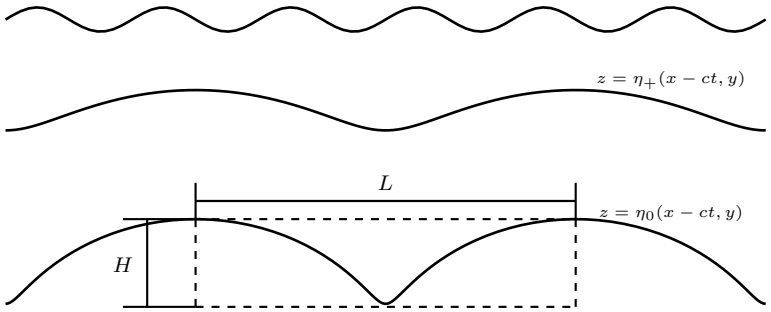

Figure 5.2: At the Equator, the internal wave height is $H = \frac{2}{k}e^{-kr_0}$ and the steepness of the internal wave is given by $\tau = e^{-kr_0}$, where $k = \frac{2\pi}{L}$.

Wavelength L (metres)	**Steepness**	**Instability threshold**
200	0.0028	0.3318
300	0.0199	0.3315
400	0.0530	0.3312
500	0.0954	0.3309
600	0.1411	0.3307
700	0.1867	0.3305
800	0.2302	0.3303
900	0.2710	0.3301
1000	0.3088	0.3299
1100	0.3436	0.3298
1200	0.3756	0.3296

Table 5.1: Comparison of the steepness and corresponding instability threshold for internal waves of different wavelengths with a thermocline whose equatorial-mean depth is 120 m.

This is a characteristic of internal waves in contrast to surfaces waves [20, 46] where the threshold was slightly greater that 1/3. Furthermore, the non-hydrostatic model stresses the difference between the two densities in the dispersion relation, see (5.37). It follows that, as the wavelength increases, the threshold decreases faster than for the hydrostatic case. This can be seen in Table 5.1 for the case when the thermocline is approximately about 120 m deep, which is typical in the mid-Pacific, cf. [41]. In addition, the Coriolis effects still play an important role by means of the terms involving Ω.

Chapter 6

Dynamical analysis of Pollard's solution

It is the aim of this chapter to show that the generalisation of Pollard's solution [26] is dynamically possible. More precisely, it is shown that the Lagrangian flow map (6.2) is a global diffeomorphism. This ensures that the map constitutes a purely three-dimensional motion of the whole fluid body where all particles describe inertial circles slightly tilted with respect to the vertical and with radius decreasing with depth at each latitude. Furthermore, the particles do not collide while filling the infinite water region below the free surface. The results that follow, published in [111], make use of the approach employed in Chapter 2 although this new solution requires the use of several conditions on the physical parameters given in [26] and its purely three-dimensional character is more mathematically demanding. Furthermore, the fact that the validity of the solution holds only when some of these parameters satisfy certain conditions shows the value of a mathematically rigorous study.

Gerstner's solution discussed in Chapter 1 has inspired new flow solutions such as those presented in Chapters 2 and 3. Another interesting result is the solution given by Pollard [107]. This flow solution extends Gerstner's description to an incompressible vertically-stratified fluid in a rotating system. The Lagragian flow map describes circular particle paths that lie on a plane slightly tilted in a certain angle dependent on Earth's latitude.

Recently, Constantin & Monismith [26] performed a Lagrangian analysis of the nonlinear Pollard's surface waves with the additional complication of incorporating a zonal current while maintaining the effects of Earth's rotation. The incorporation of the current is a remarkable achievement and it allows the generalisation of the waves obtained by Pollard. However, a rigorous mathematical analysis of the exact solution derived in [26] and of Pollard's solution itself is not yet given.

6.1 The generalised Pollard's solution

A brief describes of the solution to the f-plane equations constructed in [26] is provided. The approximation of the geophysical equations, introduced in (3.1) for the equator, will now be used for describing flows in a narrow ocean strip at any latitude.

6.1.1 The governing equations

The flow solution derived in [26] describes surface water waves propagating zonally, for which the effects of the Earth's rotation are significant. Consequently, the Coriolis forces must be taken into account, leading to the Euler equations for geophysical ocean waves (1.29). The waves propagate in a narrow ocean strip and so the Coriolis parameters $f = 2\Omega \sin\phi$ and $\hat{f} = 2\Omega \cos\phi$ are taken as constants resulting in the f-plane approximation of the Euler equations

$$\begin{cases} u_t + uu_x + vu_y + wu_z + \hat{f}w - fv = -\dfrac{1}{\rho}P_x\,, \\ \\ v_t + uv_x + vv_y + wv_z + fu = -\dfrac{1}{\rho}P_y\,, \\ \\ w_t + uw_x + vw_y + ww_z - \hat{f}u = -\dfrac{1}{\rho}P_z - g\,. \end{cases} \tag{6.1}$$

It is pointed out here that the constant values of f and $\hat{f}$ will depend upon the latitude taken as a reference for the fixed narrow ocean strip considered in each case. For example, the Coriolis parameter f vanishes along the Equator, as previously assumed in (3.1), while $f = \hat{f} \approx 10^{-4}\,\mathrm{s}^{-1}$ for a latitude of 45° North. Equation (6.1) is coupled with the mass conservation equation for an incompressible fluid (1.5) The dynamic and kinematic boundary conditions for deep water waves (1.9) and (1.7) are required. Finally, the fluid motion at the bottom of the ocean is taken to be negligible.

6.1.2 Exact and explicit solution

The solution derived by Constantin and Monismith [26] is given by means of the Lagrangian framework. As proven in [26], it constitutes an exact and explicit solution to the governing equations (6.1) for nonlinear waves propagating zonally with a constant current c_0 and under the effects of Earth's rotation. The position at each time t of a particle labelled by (q, s, r) is given by

$$\begin{cases} x(q,s,r,t) = q - c_0\, t - b\, e^{mr} \sin[k(q-ct)] \\ \\ y(q,s,r,t) = s - l\, e^{mr} \cos[k(q-ct)] \\ \\ z(q,s,r,t) = r + a\, e^{mr} \cos[k(q-ct)]\,, \end{cases} \tag{6.2}$$

where the label (q, s, r) belongs to the set $\mathbb{R} \times (-s_0, s_0) \times (-\infty, r_0(s))$, for a given s_0 and $r_0(s) < 0$. Two examples of the trajectories of fluid particles are depicted in Figure 6.1. Checking that (6.2) is a solution of the previous governing equations is based on obtaining a compatible continuous pressure. This requires the establishment of certain relations involving the real parameters a, b, l, m, as well as the wavenumber k and the wave speed c. A complete analysis and determination of the conditions on these parameters is given in full detail in [26]; however, in order to be self-contained, we indicate here the most relevant relations for our purposes. First, the dynamic boundary condition (1.9) requires that

$$b^2 = a^2 + l^2\,. \tag{6.3}$$

Second, in order to maintain the mass conservation the Jacobian of the solution (6.2) in terms of the labelling variables must be independent of time. This Jacobian is given by

$$(am - bk)e^{mr}\cos[k(q-ct)] + 1 - abmke^{2mr}$$

which implies that

$$am = bk\,. \tag{6.4}$$

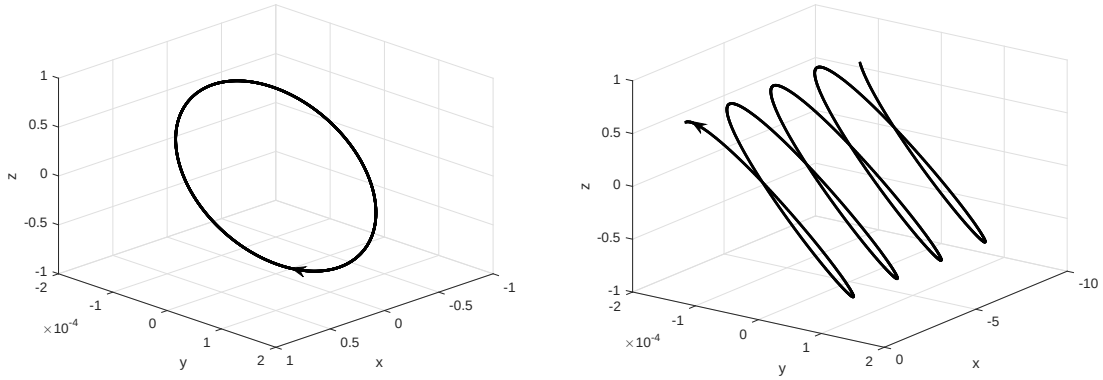

(a) $c_0 = 0\,\mathrm{m\,s^{-1}}$ (b) $c_0 = 0.3\,\mathrm{m\,s^{-1}}$

Figure 6.1: Particle paths on the free surface at a latitude $\phi = 60°\mathrm{N}$ for $a = 2\,\mathrm{m}$ and $L = 100\,\mathrm{m}$.

In particular, an approximation of the parameter m for mid-latitudes was obtained in [26] as follows

$$|m| \approx \frac{g}{fc_0}k\,, \qquad \text{when} \quad c_0 \neq 0\,,$$
$$|m| \approx \frac{g}{g - \hat{f}c}k\,, \qquad \text{when} \quad c_0 = 0\,,$$

where both $\frac{g}{fc_0}$ and $\frac{g}{g-\hat{f}c}$ are greater than 1, so $m > k > 0$. At the Equator $m = k$ and the solution with $c_0 = 0$ particularises to Gerstner's solution. In general,

$$m \geq k\,. \tag{6.5}$$

An example of the free surface is depicted in Figure 6.2. This surface, below which the infinite fluid region lies, can be obtained as a parametric surface, with parameters q and s, by utilising the Lagrangian description (6.2) and the boundary conditions on the pressure.

6.2 Dynamically-possible flow

Following Chapter 2, it is rigorously shown that the fluid motion given by (6.2) is dynamically possible according to Definition 1.2.1. This is summarised in Theorem 6.2.1.

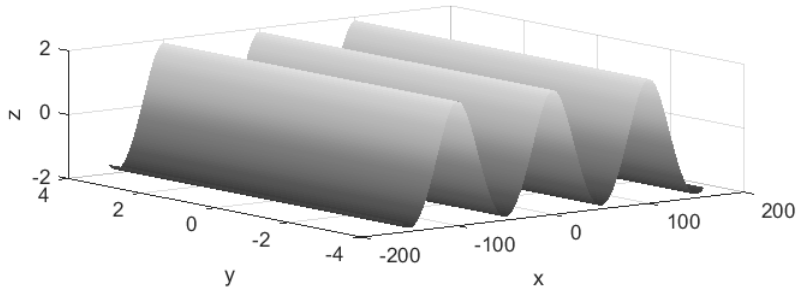

Figure 6.2: Free surface at the Equator ($\phi = 0$) for $a = 10\,\mathrm{m}$ and $L = 100\,\mathrm{m}$.

First, the case of an arbitrary time $t \geq 0$ follows from the case $t = 0$, for which (6.2) takes the form

$$\begin{cases} x = q - be^{mr}\sin(kq) \\ \\ y = s - le^{mr}\cos(kq) \\ \\ z = r + ae^{mr}\cos(kq)\,. \end{cases} \tag{6.6}$$

If the following notation

$$(q,s,r) \in \mathscr{D} \longmapsto \mathscr{F}(q,s,r) = \begin{bmatrix} q - be^{mr}\sin(kq) \\ s - le^{mr}\cos(kq) \\ r + ae^{mr}\cos(kq) \end{bmatrix} \tag{6.7}$$

is introduced, where

$$\mathscr{D} = \{(q,s,r) : q \in \mathbb{R}\,,\ s \in (-s_0, s_0)\,,\ r \in (-\infty, r_0(s))\}\,, \tag{6.8}$$

then the general case (6.2) can be recovered by the following change of variables and shift in the x-component

$$\mathscr{F}(q - ct, s, r) + \begin{bmatrix} (c - c_0)t \\ 0 \\ 0 \end{bmatrix}.$$

Furthermore, it is noted that the map (6.6) is periodic in q with period $L = 2\pi/k$ for both the y and the z-component, while being "quasi" periodic in the x component, for which it experiences a shift of $2\pi/k$ that does not affect the diffeomorphic character of the map in the whole real line. Therefore, showing that (6.2) is a global diffeomorphism in $\mathscr{D}$ can be reduced to proving that the map $\mathscr{F}$ is a global diffeomorphism from the domain

$$\mathscr{D}_L = \{(q, s, r) : q \in \left(0, \frac{2\pi}{k}\right), s \in (-s_0, s_0), r \in (-\infty, r_0(s))\} \tag{6.9}$$

into the fluid domain below the free surface. The use of the Invariance of Domain Theorem, together with a clever choice of a norm allows to prove the main result without having to restrict the analysis to this set and avoiding the tedious process of showing the surjectivity of the Lagrangian flow map directly. Before proving the main Theorem 6.2.1, some preliminary results are needed.

Local regularity

The first proposition, previously outlined in [26], establishes the local regularity of the map $\mathscr{F}$.

Proposition 6.2.1. *Under the condition*

$$ame^{mr_0(s)} < 1\,,$$

the map $\mathscr{F}$ is a local diffeomorphism from $\mathscr{D}$ onto its image, the fluid region below the free surface.

Proof. The Jacobian matrix of $\mathscr{F}$ is given by

$$D\mathscr{F}_{(q,s,r)} = \begin{pmatrix} 1 - bke^{mr}\cos(kq) & 0 & -bme^{mr}\sin(kq) \\ kle^{mr}\sin(kq) & 1 & -lme^{mr}\cos(kq) \\ -ake^{mr}\sin(kq) & 0 & 1 + ame^{mr}\cos(kq) \end{pmatrix},$$

whose determinant is

$$\begin{vmatrix} 1 - bke^{mr}\cos(kq & -bme^{mr}\sin(kq) \\ -ake^{mr}\sin(kq) & 1 + ame^{mr}\cos(kq) \end{vmatrix} = 1 - abmke^{2mr} + (am - bk)e^{mr}\cos(kq).$$

From (6.4), it follows that the determinant is reduced to

$$1 - a^2 m^2 e^{2mr}.$$

Thus, under the hypothesis that $1 > ame^{mr_0(s)}$, the determinant of the Jacobian matrix does not vanish for any $s \in (-\infty, r_0(s))$. On the other hand, $\mathscr{F}$ has continuous partial derivatives in any open set contained in $\mathscr{D}$. Hence, $\mathscr{F}$ is a continuously differentiable map with a Jacobian that is strictly positive, so $\mathscr{F}$ is a local diffeomorphism from $\mathscr{D}$ into its range due to the Inverse Function Theorem. □

Sufficient condition for injectivity

The globally injectivity of the map $\mathscr{F}$ is studied. The difficulty of this solution requires dealing with the three-dimensional map, which greatly complicates the situation with respect to the solution analysed in Chapter 2.

Proposition 6.2.2. *If*

$$bme^{mr_0(s)} < 1\,, \tag{6.10}$$

then $\mathscr{F}$ is globally injective in $\mathbb{R}^3$.

Proof. Let us write $\mathscr{F}$ in the following form

$$\mathscr{F}(q,s,r) = (q,s,r) + \mathscr{G}(q,s,r)\,,$$

where

$$\mathscr{G}(q,s,r) = -e^{mr}\Big(b\sin(kq), l\cos(kq), -a\cos(kq)\,.\Big)$$

is a continuously differentiable map and satisfies the following mean-value-theorem type of inequality (which is proven in Appendix A)

$$|\mathscr{G}(q,s,r) - \mathscr{G}(\tilde{q},\tilde{s},\tilde{r})|_2 \leq \max_{\tau\in[0,1]} \|D\mathscr{G}_{\tau(q,s,r)+(1-\tau)(\tilde{q},\tilde{s},\tilde{r})}\|_2 \cdot |(q,r,s) - (\tilde{q},\tilde{s},\tilde{r}))|_2 \tag{6.11}$$

in any convex set of $\mathbb{R}^3$, where

$$D\mathscr{G}_{\tau(q,s,r)+(1-\tau)(\tilde{q},\tilde{s},\tilde{r})} \quad \text{for } \tau \in [0,1]$$

is the Jacobian matrix at any point of the segment joining (q, s, r) and $(\tilde{q}, \tilde{s}, \tilde{r})$, $|\cdot|_2$ is the Euclidean norm in $\mathbb{R}^3$ and $\|\cdot\|_2$ is the operator norm induced by the previous norm $|\cdot|_2$. In general, $\|\cdot\|_2$ is defined for an arbitrary 3×3 matrix M by

$$\|M\|_2 = \sup\{|M(q,s,r)|_2 : (q,s,r) \in \mathbb{R}^3 \quad \text{such that} \quad |(q,s,r)|_2 = 1\}\,.$$

However, for this particular case, the matrix norm $\|\cdot\|_2$ is the same as the so-called spectral matrix norm [75]. The choice of this norm allows a bound for the map $\mathscr{F}$ to be obtained. The spectral norm of a matrix M is the square root of the largest eigenvalue of the positive-semidefinite matrix M^*M, i.e.

$$\|M\|_2 = \sqrt{\lambda_{max}(M^*M)}\,, \tag{6.12}$$

where M^* is the conjugate transpose of M. The Jacobian matrix of $\mathscr{G}$ is given by

$$D\mathscr{G}_{(q,s,r)} = \begin{pmatrix} -bke^{mr}\cos(kq) & 0 & -bme^{mr}\sin(kq) \\ lke^{mr}\sin(kq) & 0 & -lme^{mr}\cos(kq) \\ -ake^{mr}\sin(kq) & 0 & ame^{mr}\cos(kq) \end{pmatrix}.$$

which gives that

$$\begin{aligned} &D\mathscr{G}^*_{(q,s,r)} D\mathscr{G}_{(q,s,r)} = \\ &= e^{2mr} \begin{pmatrix} b^2k^2\cos^2(kq) + (l^2+a^2)k^2\sin^2(kq) & 0 & (b^2-l^2-a^2)km\sin(kq)\cos(kq) \\ 0 & 0 & 0 \\ (b^2-l^2-a^2)km\sin(kq)\cos(kq) & 0 & b^2m^2\sin^2(kq) + (l^2+a^2)m^2\cos^2(kq) \end{pmatrix} \\ &= e^{2mr} \begin{pmatrix} b^2k^2 & 0 & 0 \\ 0 & 0 & 0 \\ 0 & 0 & b^2m^2 \end{pmatrix} \\ &= b^2e^{2mr} \begin{pmatrix} k^2 & 0 & 0 \\ 0 & 0 & 0 \\ 0 & 0 & m^2 \end{pmatrix}, \end{aligned}$$

where the second equality follows from (6.3). Hence,

$$\{0,\, b^2k^2e^{2mr},\, b^2m^2e^{2mr}\}$$

is the set of eigenvalues of $D\mathscr{G}^T_{(q,s,r)}D\mathscr{G}_{(q,s,r)}$. The maximum of this set is $b^2m^2e^{2mr}$ from the inequality (6.5). Consequently,

$$\|D\mathscr{G}_{(q,s,r)}\|_2 = \sqrt{b^2m^2e^{2mr}} = bme^{mr}$$

On the other hand,

$$\max_{\tau\in[0,1]} \|D\mathscr{G}_{\tau(q,s,r)+(1-\tau)(\tilde{q},\tilde{s},\tilde{r})}\|_2 = bme^{mr_{max}}\,,$$

where r_{max} is the maximum of r-component of the points (q,s,r) and $(\tilde{q},\tilde{s},\tilde{r})$. In particular, $r_{max} \leq r_0(s)$. Now by (6.11),

$$|\mathscr{G}(q,s,r) - \mathscr{G}(\tilde{q},\tilde{s},\tilde{r})|_2 \leq bme^{mr_{max}}|(q,s,r) - (\tilde{q},\tilde{s},\tilde{r}))|_2\,.$$

Returning to the function $\mathscr{F}$, the previous inequality yields

$$\begin{aligned}
|\mathscr{F}(q,s,r) - \mathscr{F}(\tilde{q},\tilde{s},\tilde{r})|_2 &= |(q,s,r) - (\tilde{q},\tilde{s},\tilde{r}) + \mathscr{G}(q,s,r) - \mathscr{G}(\tilde{q},\tilde{s},\tilde{r})|_2 \\
&= |(q,s,r) - (\tilde{q},\tilde{s},\tilde{r}) - (\mathscr{G}(\tilde{q},\tilde{s},\tilde{r}) - \mathscr{G}(q,s,r))|_2 \\
&\geq |(q,s,r) - (\tilde{q},\tilde{s},\tilde{r})|_2 - |\mathscr{G}(q,s,r)) - \mathscr{G}(\tilde{q},\tilde{s},\tilde{r})|_2 \\
&\geq |(q,s,r) - (\tilde{q},\tilde{s},\tilde{r})|_2 - bme^{mr_{max}}|(q,s,r) - (\tilde{q},\tilde{s},\tilde{r})|_2 \\
&= (1 - bme^{mr_{max}})|(q,s,r) - (\tilde{q},\tilde{s},\tilde{r})|_2\,.
\end{aligned}$$

Finally, by the hypothesis (6.10),

$$1 - bme^{mr_{max}} \geq 1 - bme^{mr_0(s)} > 0\,,$$

therefore

$$|(q,s,r) - (\tilde{q},\tilde{s},\tilde{r})|_2 \leq \frac{1}{1 - bme^{mr_{max}}}|\mathscr{F}(q,s,r) - \mathscr{F}(\tilde{q},\tilde{s},\tilde{r})|_2 \tag{6.13}$$

which, by means of the properties of the norm, proves that the map $\mathscr{F}$ is globally injective in $\mathbb{R}^3$. □

Necessary condition for injectivity

Showing the injectivity of $\mathscr{F}$ required imposing a new condition on some of the parameters used to describe the exact solution. It seems appropriate to analyse the injectivity more deeply and to obtain a necessary condition for the injectivity of $\mathscr{F}$. Together with the previous results, this will provide a mathematical characterisation and a bound for the physical parameters involved.

Proposition 6.2.3. *If $\mathscr{F}$ is injective, then it follows that*

$$bke^{mr_0(s)} \leq 1\,. \tag{6.14}$$

Proof. Let us focus on the first component of $\mathscr{F}$. We prove that the nonlinear equation

$$\mathscr{H}(q) := q - be^{mr}\sin(kq) = 0 \tag{6.15}$$

has more than one solution. Let us assume that (6.14) does not hold, i.e.

$$bke^{mr_0(s)} > 1\,. \tag{6.16}$$

We have that $\mathscr{H}'(q) = 0$ if and only if

$$q = \frac{1}{k}\arccos\left(\frac{1}{bke^{mr}}\right),$$

which is well-defined by (6.16). Moreover, it is possible to find a unique $q_0 \in \left(0, \frac{\pi}{2k}\right)$ such that q_0 is a minimum for $\mathscr{H}$ and $\mathscr{H}(q_0) < 0$. It follows that

$$\mathscr{H}''(q_0) = k\sqrt{b^2k^2e^{2mr} - 1} > 0.$$

In addition, $\mathscr{H}(0) = 0$ and $\mathscr{H}' < 0$ in a neighbourhood of 0. Thus, $\mathscr{H}'$ takes negative values to the right of 0. Furthermore,

$$\mathscr{H}(q) \to \infty \quad \text{as} \quad q \to \infty\,.$$

Therefore, it follows that there exists a strictly positive solution of (6.15). If α is such a solution, then it follows that $-\alpha$ is also a solution. A sketch of the situation is depicted in Figure 6.3. Hence, the mapping $\mathscr{F}$ is not injective, as the points

$$(q_1, s_1, r_1) = (\alpha, s, r)$$
$$(q_2, s_2, r_2) = (-\alpha, s, r)$$

are such that

$$\mathscr{F}(q_1, s_1, r_1) = \mathscr{F}(q_2, s_2, r_2)\,.$$

□

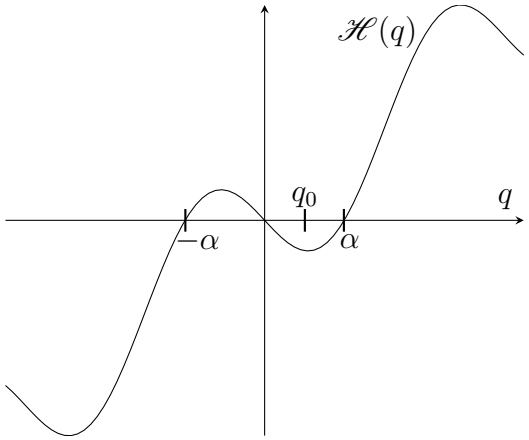

Figure 6.3: A Sketch of the graph of $\mathscr{H}$. Here q_0 is a local minimum for $\mathscr{H}$ and $\mathscr{H}(\alpha) = \mathscr{H}(-\alpha) = 0$.

It is interesting to compare both the necessary and the sufficient conditions for the injectivity of $\mathscr{F}$ given in Propositions 6.2.3 and 6.2.2, as well as the condition for the local regularity given in Proposition 6.2.1. Taking into account that both a and b are positive, together with the condition (6.3), it follows that

$$b \geq a\,,$$

which yields

$$1 - bme^{mr} \leq 1 - ame^{mr}\,, \quad \text{for all} \quad m > 0.$$

Therefore, in general, the sufficient condition (6.10) for the global injectivity of $\mathscr{F}$ implies the condition for the local diffeomorphic character of $\mathscr{F}$. In particular, along the Equator, $a = b$ and $m = k$. Therefore, the necessary condition for injectivity (6.14) and the sufficient condition (6.10) coincide. Moreover, they also match the condition establishing the diffeomorphic character of $\mathscr{F}$, see Proposition (6.2.1). However, outside the Equator m is strictly greater than k and therefore the condition for global injectivity (6.10) is stronger than the condition for the local diffeomorphic character of $\mathscr{F}$. In this case, it is possible to find a set of values for the parameters a, b, m, and k producing a solution to the governing equations (3.1) such that $1 > ame^{mr_0(s)}$ whereas $1 < bme^{mr_0(s)}$. Therefore, it is possible to have that $\mathscr{F}$ is a local diffeomorphism (which does not preserve the orientation) such that is not globally injective.

Global diffeomorphism flow map

The result anticipated at the beginning of this chapter is now presented.

Theorem 6.2.1. *If $bme^{mr_0(s)} < 1$, then the map $\mathscr{F}$ is a global diffeomorphism from $\mathscr{D}$ into the fluid region below the free surface. Therefore, the Lagrangian flow map* (6.2) *is a global diffeomorphism from $\mathscr{D}$ into the fluid domain and maps $\partial\mathscr{D}$ onto the free surface.*

As it has been mentioned, the proof of this result follows the approach taken in Chapter 2. This was approach was first used in [50] and then in [110, 118].

Proof of Theorem 6.2.1. It has been proven in Proposition 6.2.2 that, when the hypothesis in Theorem 6.2.1 holds, i.e., when

$$bme^{mr_0(s)} < 1\,, \tag{6.17}$$

the map $\mathscr{F}$ is globally injective. In addition, $\mathscr{F}$ is continuous. Therefore, by the Invariance of Domain Theorem and the Remark 2.4.1, the map

$$\mathscr{F} : \overline{\mathscr{D}} \to \mathscr{F}(\overline{\mathscr{D}})$$

is a homeomorphism. In particular, $\mathscr{F}(\partial\mathscr{D}) = \partial\mathscr{F}(\mathscr{D})$ and $\overline{\mathscr{F}(\mathscr{D})} = \mathscr{F}(\overline{\mathscr{D}})$. Thus, $\mathscr{F}$ maps the labelling domain continuously and surjectively onto the fluid domain below the free surface. Also, $\mathscr{F}$ is globally bijective in the interior of $\mathscr{D}$. On the other hand, the condition (6.17) implies that

$$ame^{mr_0(s)} < 1\,.$$

Hence, by Proposition 6.2.1, $\mathscr{F}$ is a local diffeomorphism. Finally, it follows that $\mathscr{F}$ is a local diffeomorphism which is globally bijective, therefore $\mathscr{F}$ is a global diffeomorphism. □

Chapter 7

Dispersion relations for steady periodic gravity water waves of fixed mean-depth

This final chapter focuses on the study of small-amplitude two-dimensional steady periodic water waves propagating over a flat bed located at a fixed mean-depth from the surface. The main objective is the derivation of a dispersion relation for these type of waves for a discontinuous piecewise constant vorticity of the form depicted in Figure 7.1.

The consideration of flows with vorticity has been a constant throughout this thesis as it is present in Gerstner-like waves. Its role in modelling wave-current interactions and other complex phenomena was shown in [9, 105, 121]. The choice of vorticity distribution utilised in this chapter assumes two layers of non-zero vorticity. This can model a flow whose surface layer is affected by wind-generated rotational waves (cf. [104, 106]) together with a current in the near-bed layer generated, for instance, by sediment transport. The type of waves described in this chapter were rigorously analysed by Constantin and Strauss [27,29] for the case of fixed mass-flux. Its regularity was analysed by Escher in [38] and [19, 31, 40, 52, 72]. Moreover, the study of symmetry was performed by Constantin and Escher in [17, 18], and others in [16, 67, 102]. Important investigations regarding stability, stratification and the presence of stagnation points and critical layers were accomplished in [30–32, 37, 39, 39, 66, 68, 69, 97, 103, 124–126].

It is important to notice that in [27] the mass-flux is assumed to be a fixed quantity that can result in a variation of the mean-depth throughout the continuum of solutions which are obtained as bifurcations from laminar-flow solutions, as shown in [88, 89]. This is a result of the mathematical construction used to obtain these small-amplitude waves. From a physical perspective this does not seem reasonable

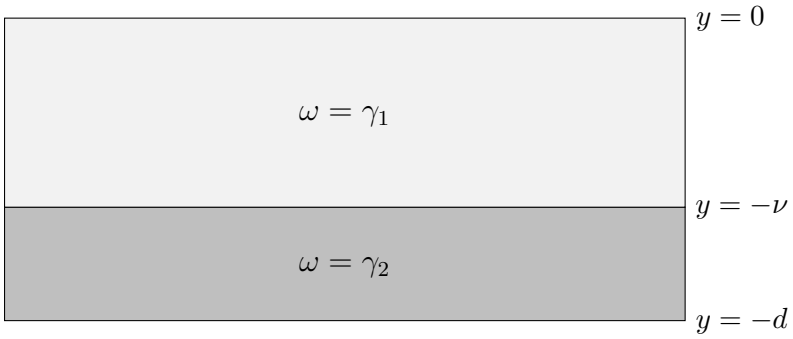

Figure 7.1: Depiction of the two-layer vorticity model for a period L

as for the same vorticity the mean water depth should not change. Therefore, one should start by assuming that the mean depth is a fixed quantity. Precisely this was proposed by Henry [56, 57] and some of the ideas supporting the existence of small-amplitude waves in this scenario will outlined herein. However, the priority is to obtain the dispersion relation for the small-amplitude waves, within the mean-depth fixed assumption, arising from a particular choice of vorticity distribution, namely a discontinuous piecewise constant vorticity. This generalises those derived in [53, 54] where one of the layers was considered to be irrotational and it offers a fixed mean-depth counterpart to the studies [10, 29, 95–99, 101]. where the quantity fixed was the mass flux.

The dispersion relation has already been derived and discussed in this thesis. These formulae are important from a physical standpoint as they relate several parameters such as the wavelength, wave speed and others such as the mean depth of the flow, the location of the jump in vorticity. Moreover, in this case, the dispersion relation is also important from a functional analytical perspective, as it provides a condition for the bifurcation from the laminar flows to occur.

This chapter is concluded by an analysis of the stability of the laminar flow solutions in the fixed mean-depth framework is included. To perform the aforementioned analysis we employ and adapt to our setting, in which the mean-depth is kept fixed, the variational formulation of the water waves equations that was devised in [30]. It is worth noting that variational formulations were recently employed in the study of rotational water waves allowing for a constant or piecewise constant vorticity in [21–23, 83].

7.1 Fixed-depth formulation for steady periodic waves

This chapter focuses on two-dimensional periodic travelling surface waves propagating over a flat bed of fixed depth ($d > 0$), while allowing for piecewise constant vorticity. The approach taken here follows the one described in Chapter 3 of [9]. The water is taken as an incompressible and inviscid fluid, so the mass conservation and momentum equations are given by (1.5) and (1.6) respectively. Furthermore, the kinematic boundary conditions on the free surface and the flat bed are provided by (1.7) and (1.8). Let us now particularise this to the present type of waves. First, the motion is two dimensional, with the X axis pointing in the direction of wave propagation and the Y axis pointing upwards. Second, if the waves are travelling at a constant speed $c > 0$, then the velocity field (u, v), the pressure P and the free surface $X \to \eta(X, t)$ show a dependence of the form $X - ct$. Thus, after the following change of coordinates

$$x := X - ct, \qquad y := Y\,, \tag{7.1}$$

the governing equations for two-dimensional, periodic travelling waves propagating at the free surface of a fluid with a bed situated at a depth $-d$ are given. Explicitly, these equations are the Euler equations

$$\begin{cases} (u-c)u_x + vu_y &= -P_x \\ \\ (u-c)v_x + vv_y &= -P_y - g\,, \end{cases} \tag{7.2a}$$

and the continuity equation for an incompressible fluid

$$u_x + v_y = 0\,. \tag{7.2b}$$

The kinematic boundary conditions take the form

$$v = (u-c)\eta_x \qquad \text{on} \quad y = \eta(x)\,, \tag{7.2c}$$

$$v = 0 \qquad \text{on} \quad y = -d\,, \tag{7.2d}$$

and the dynamic boundary condition

$$P = P_{atm} \quad \text{on } y = \eta(x)\,. \tag{7.2e}$$

These waves require the horizontal velocity to satisfy

$$u(x,y) < c \quad \text{for all} \quad (x,y) \in D_\eta = \{(x,y) : -L \le x \le L;\ -d \le y \le \eta(x)\}\,. \tag{7.3}$$

This assumption will be proven to be fundamental for the existence of such waves and it states that there are no stagnation points within the flow. We are going to study how to incorporate a particular vorticity distribution into this model. Thus, it is noted that, as in (1.24), the vorticity is defined as the only non-zero term of the curl of the vector $(u, 0, v)$, i.e.

$$\omega = u_y - v_x\,.$$

In addition, taking the wavelength of the waves to be L, a scaling of the variables involved in the problem is given by

$$(x, y, t, g, \eta, u, v, P, c, \omega) \longmapsto (k\,x, \kappa\,y, k\,t, \frac{g}{k}, k\,\eta, u, v, P, c, \omega/k)\,. \tag{7.4}$$

The scaled variables satisfy the governing equations (7.2) replacing g by g/k. Thus, the scaled problem is considered in the following. Furthermore, for an incompressible two-dimensional motion, there exists a stream function, ψ, which satisfies

$$\begin{cases} \psi_y = u - c, \\ \psi_x = -v, \end{cases} \tag{7.5}$$

and results in the following proposition.

Proposition 7.1.1. *The stream function $\psi(x,y)$ is a L-periodic in x function which is constant on the free surface $y = \eta(x)$ and on the flat bed $y = -d$.*

By choosing $\psi(x, \eta(x)) = 0$, it is inferred that $\psi(x, -d) = -p_0$, where

$$p_0 = \int_{-d}^{\eta(x)} (u(x,y) - c)\ dy < 0$$

is the relative mass flux. The governing equations (7.2) can be reformulated in terms of the stream function (cf. [9, 27]) as

$$\begin{cases} \Delta\psi = \gamma(\psi) & \text{for } y \in (-d, \eta(x))\,, \\ |\nabla\psi|^2 + 2g(y+d) = Q & \text{on } y = \eta(x)\,, \\ \psi = 0 & \text{on } y = \eta(x)\,, \\ \psi = -p_0 & \text{on } y = -d\,, \end{cases} \tag{7.6}$$

where Q is a constant that can be found through Bernoulli's formula, $\omega = \gamma(\psi)$ will be referred to as the vorticity function. It is not the purpose of this chapter to provide a complete derivation of the equations (7.6), although the existence of γ as a function of ψ is briefly justified. Indeed, by the Helmholtz's theorem for an incompressible fluid,

$$\frac{D\boldsymbol{\omega}}{Dt} = (\boldsymbol{\omega}\cdot\nabla)\mathbf{u}. \tag{7.7}$$

Moreover, for a two-dimensional motion, the previous equation (7.7) becomes the scalar equation

$$\frac{D\omega}{Dt} = 0.$$

Furthermore, after the change of coordinates (7.1), the motion can be seen as steady with respect to the moving axis and thus (7.7) is reduced to

$$(\mathbf{u}\cdot\nabla)\omega = 0\,,$$

showing that the vorticity is constant along streamlines. From the definition of vorticity and stream function, it follows that

$$\omega = \Delta\psi\,,$$

where Δ is the Laplace operator. Finally, from the fact that streamlines are precisely the curves along which the stream function is constant, the vorticity can be expressed as a function of the streamlines, or equivalently, as a function of the stream function, i.e.

$$\omega = \gamma(\psi).$$

7.1.1 Hodograph transformation

In order to avoid dealing with the unknown free surface, Dubreil-Jacotin [35] introduced the Hodograph transformation. In [9] this was used for transforming the governing equations (7.6) under the assumption that the mass flux p_0 was fixed. However, we are interested in a formulation for which the mean depth of the flat bed is fixed. This is more physically reasonable and its formulation was devised by Henry in [56, 57] in the context of continuous vorticity. This was subsequently extended to the discontinuous vorticity case by Henry and Sastre-Gómez [71] and by Henry, Martin and Sastre-Gómez [65]. Hence, the following change of variables is chosen

$$(q,p) = (q(x,y), p(x,y)) := \Big(x, \frac{\psi(x,y)}{p_0}\Big)\,. \tag{7.8}$$

Due to (7.3), it follows that (7.8) is a diffeomorphism

$$(x,y) \in D_\eta \longrightarrow (q,p) \in R := [-\pi,\pi] \times [-1,0].$$

Also from the non-stagnation condition, the function defined by

$$\phi(y) = \frac{1}{p_0}\psi(x,y) \quad \text{for any given } x$$

is invertible. Thus, it is possible to define the key function

$$h(q,p) = \frac{\phi^{-1}(p)}{d} - p. \tag{7.9}$$

and express the governing equations (7.6) in terms of this function and its derivatives

$$\begin{cases} \Big(\frac{1}{d^2} + h_q^2\Big)h_{pp} - 2h_q(h_p+1)h_{pq} + (h_p+1)^2 h_{qq} + \frac{\gamma(p)}{p_0}(h_p+1)^3 = 0 & \text{in } R\,, \\ \\ \frac{1}{d^2} + h_q^2 + \frac{h_p+1}{p_0^2}[2gd(h+1) - Q] = 0 & p = 0\,, \\ \\ h = 0 & p = -1\,, \end{cases} \tag{7.10}$$

where the vorticity function $\omega = \gamma(p)$ is now expressed in terms of the new variables. The assumption (7.3) is equivalent to

$$h_p + 1 > 0\,.$$

The system (7.10) consists of a uniformly elliptic quasilinear PDE with oblique nonlinear boundary conditions that can be expressed [71] in the form

$$\begin{cases} \left\{\dfrac{1+d^2h_q^2}{2d^2(1+h_p)} - \dfrac{\Gamma(p)}{2d^2}\right\}_p - \left\{\dfrac{h_q}{1+h_p}\right\}_q = 0 & \text{for } p \in (-1,0)\,, \\ \dfrac{1+d^2h_q^2}{2d^2(1+h_p)^2} + \dfrac{gd(h+1)}{p_0^2} = \dfrac{Q}{2p_0^2} & \text{on } p = 0\,, \\ h = 0 & \text{on } p = -1\,, \end{cases} \tag{7.11}$$

where

$$\Gamma(p) = 2\int_0^p \frac{d^2\gamma(s)}{p_0}\, ds \quad -1 \le p \le 0\,. \tag{7.12}$$

The solutions of (7.11) are understood as functions $h \in W^{2,r}_{per}(R) \subset C^{1,\alpha}_{per}(\overline{R})$ for $r > 2/(1-\alpha)$ with $\alpha \in (1/3, 1)$, allowing for a discontinuous vorticity function. For solutions of (7.11) which are independent of q, laminar flows whose streamlines are horizontal are obtained. Thus, if

$$\Gamma_{\min} = \min_{p\in(-1,0)} \Gamma(p)\,,$$

then there is a family of laminar flows for (7.11), parametrised by $\lambda \in (-\Gamma_{\min}, Q)$, given by the following expression

$$\mathbb{H}(p;\lambda) = \int_0^p \frac{1}{\sqrt{\lambda + \Gamma(p)}}\, ds + \frac{1}{2gd}\Big[Q - \frac{p_0^2}{d^2}\lambda\Big] - (p+1), \quad -1 < p \le 0. \tag{7.13}$$

Furthermore, the parameter λ is related with the velocity at the flat surface $y = 0$ by

$$\sqrt{\lambda} = \frac{1}{\mathbb{H}_p + 1}\bigg|_{p=0} = \frac{d(u-c)}{p_0}\bigg|_{y=0}. \tag{7.14}$$

Finally, the authors in [71] showed that small amplitude waves, which are perturbations of these laminar flows exist, if and only if there exists a nontrivial solution

$M \in C^{1,\alpha}_{per}(-1,0)$ for the Sturm-Liouville-like problem

$$\begin{cases} (a^3 M_p)_p = d^2 a M & -1 < p < 0\,, \\ \\ a^3 M_p = \dfrac{gd^3}{p_0^2} M & p = 0\,, \\ \\ M = 0 & p = -1\,, \end{cases} \tag{7.15}$$

where $a(p;\lambda) = \dfrac{1}{\mathbb{H}_p + 1} = \sqrt{\lambda + \Gamma(p)} \in C^{2,\alpha}_{per}(-1,0)$.

7.2 Two-layer vorticity model

In this section, a piecewise constant vorticity function is chosen. The existence of solutions for (7.15) with this particular choice is transformed into an algebraic problem.

(7.16) is chosen and the analysis of the existence of solutions for (7.15) with this particular choice is transformed into an algebraic problem.

7.2.1 The Sturm-Liouville Problem

Let $y = -\nu$ indicate an intermediate depth within the fluid region whose bed is at $y = -d$. If γ_1 denotes the vorticity in the layer adjacent to the free surface and γ_2 the vorticity in the layer near the bed, the choice of vorticity function is

$$\omega(x,y) = \begin{cases} \gamma_1 & -\nu < y < 0\,, \\ \\ \gamma_2 & -d < y < -\nu\,. \end{cases} \tag{7.16}$$

By denoting

$$p_1 := \frac{\psi(x,-\nu)}{p_0}\,, \tag{7.17}$$

the same expression in terms of the variables (q,p) is obtained,

$$\omega(q,p) = \begin{cases} \gamma_1 & p_1 < p < 0\,, \\ \\ \gamma_2 & -1 < p < p_1\,. \end{cases} \tag{7.18}$$

In particular, for laminar flows whose vertical velocity vanishes, it follows that $\omega = u_y$. Hence, from (7.14)

$$c - u(y) = \begin{cases} \dfrac{-p_0\sqrt{\lambda}}{d} - \gamma_1 y & -\nu < y < 0\,, \\ \\ \dfrac{-p_0\sqrt{\lambda}}{d} + \nu\gamma_1 - \gamma_2(y+\nu) & -d < y < -\nu\,. \end{cases} \tag{7.19}$$

In order to describe the Sturm-Liouville problem for the given vorticity, the following expression for $\Gamma(p)$ is needed, for $p_1 < p < 0$ it follows that

$$\Gamma(p) = -2\frac{d^2}{p_0}\int_p^0 \gamma_1\, ds = -2\frac{d^2}{p_0}\int_p^0 \gamma_1\, ds = 2\frac{d^2\gamma_1}{p_0}p$$

whereas for $-1 < p < p_1$,

$$\Gamma(p) = -2\frac{d^2}{p_0}\left[\int_p^{p_1} \gamma_2\, ds + \int_{p_1}^0 \gamma_1\, ds\right] = 2\frac{d^2}{p_0}\Big[\gamma_2 p + p_1(\gamma_1 - \gamma_2)\Big]\,.$$

Therefore,

$$\Gamma(p) = \begin{cases} 2\dfrac{d^2\gamma_1}{p_0}p & p_1 < p < 0\,, \\ \\ 2\dfrac{d^2}{p_0}\Big[\gamma_2 p + p_1(\gamma_1 - \gamma_2)\Big] & -1 < p < p_1\,, \end{cases} \tag{7.20}$$

which yields

$$a(p;\lambda) = \begin{cases} \sqrt{\lambda + 2\dfrac{d^2\gamma_1}{p_0}p} & p_1 < p < 0\,, \\ \\ \sqrt{\lambda + 2\dfrac{d^2}{p_0}\Big[\gamma_2 p + p_1(\gamma_1 - \gamma_2)\Big]} & -1 < p < p_1\,. \end{cases} \tag{7.21}$$

The Sturm-Liouville problem (7.15) for the vorticity function (7.18) is now specified by $a(p;\lambda)$. Thus, we seek a solution of this problem on both layers separately. For the near-surface layer, we look for a solution of the form

$$\begin{cases} (a^3 m_p)_p = d^2 a m & p_1 < p < 0\,, \\ a^3 m_p = \dfrac{g d^3}{p_0^2} m & p = 0\,, \end{cases} \tag{7.22}$$

where $a(p;\lambda)$ is given by (7.21) for $p \in (p_1, 0)$. For this first part we take the following ansatz

$$m(p) = \frac{1}{a(p)}\left[c_1 \sinh\left(\frac{p_0\,, a(p)}{d\gamma_1}\right) + c_2 \cosh\left(\frac{p_0\,, a(p)}{d\gamma_1}\right)\right],$$

for constants c_1, $c_2 \in \mathbb{R}$ and λ has been dropped from the expression of $a(p;\lambda)$ for simplicity. Regarding the other layer,

$$\begin{cases} (a^3\tilde{m}_p)_p = d^2 a\tilde{m} & -1 < p < p_1\,, \\ \\ \tilde{m} = 0 & p = -1\,, \end{cases} \tag{7.23}$$

where $a(p;\lambda)$ is given by (7.21) for $p \in (-1, p_1)$. The solution in this layer will be of the form

$$\tilde{m}(p) = \frac{C}{a(p)} \sinh\left(\frac{p_0[a(p) - a(-1)]}{d\gamma_2}\right), \qquad \text{for} \quad C := \frac{c_3}{\cosh\left(\frac{p_0\, a(-1)}{d\gamma_2}\right)},$$

where c_3 is another constant. Setting

$$M(p) := \begin{cases} m(p) & \text{if} \quad p \in [p_1, 0], \\ \tilde{m}(p) & \text{if} \quad p \in [-1, p_1] \end{cases} \tag{7.24}$$

as the solution in the whole domain. In order to simplify the calculations, the following notation is adopted

$$\begin{aligned} \theta_1 &= \frac{p_0\, a(p_1)}{d\gamma_1}, \\ \theta_2 &= \frac{p_0[a(p_1) - a(-1)]}{d\gamma_2}. \end{aligned} \tag{7.25}$$

By assuming the continuity of M at $p = p_1$, a first condition involving the unknown constants c_1, c_2 and C is obtained

$$c_1 \sinh(\theta_1) + c_2 \cosh(\theta_1) = C \sinh(\theta_2). \tag{7.26}$$

Secondly, from the continuity of the first derivative of M at $p = p_1$, it follows that

$$\begin{aligned} \frac{-Cd\gamma_2}{p_0} \sinh(\theta_2) + Ca(p_1)\cosh(\theta_2) = &- \frac{d\gamma_1}{p_0}\Big[c_1 \sinh(\theta_1) + c_2 \cosh(\theta_1)\Big] \\ &+ a(p_1)\Big[c_1 \cosh(\theta_1) + c_2 \sinh(\theta_1)\Big]. \end{aligned} \tag{7.27}$$

Making use of (7.26) gives

$$c_1 \cosh(\theta_1) + c_2 \sinh(\theta_1) = \frac{1}{a(p_1)} \frac{Cd}{p_0} (\gamma_1 - \gamma_2) \sinh(\theta_2) + C \cosh(\theta_2)\,. \tag{7.28}$$

Writing (7.26) and (7.27) as a system of equations

$$\begin{cases} c_1 \sinh(\theta_1) + c_2 \cosh(\theta_1) = C \sinh(\theta_2)\,, \\ \\ c_1 \cosh(\theta_1) + c_2 \sinh(\theta_1) = \dfrac{1}{a(p_1)} \dfrac{dC}{p_0} (\gamma_1 - \gamma_2) \sinh(\theta_2) + C \cosh(\theta_2), \end{cases} \tag{7.29}$$

which will be solved for c_1 and c_2 in terms of C. Imposing the boundary condition for $p = 0$,

$$a^3(0) m_{p|_{p=0}} = \frac{gd^3}{p_0^2} m(0).$$

After some algebra, it follows that the existence of a non-trivial solution of the Sturm-Liouville problem (7.15) is ensured if and only if the algebraic equation

$$\begin{aligned} & p_0^2 \left[\cosh\left((\theta_2 - \theta_1 + \frac{p_0\sqrt{\lambda}}{d\gamma_1} \right) + \frac{d}{p_0\, a(p_1)} (\gamma_1 - \gamma_2) \sinh(\theta_2) \cosh\left(\frac{p_0\sqrt{\lambda}}{d\gamma_1} - \theta_1 \right) \right] \lambda \\ & - \left[\sinh\left(\theta_2 - \theta_1 + \frac{p_0\sqrt{\lambda}}{d\gamma_1} \right) + \frac{d}{p_0\, a(p_1)} (\gamma_1 - \gamma_2) \sinh(\theta_2) \sinh\left(\frac{p_0\sqrt{\lambda}}{d\gamma_1} - \theta_1 \right) \right] p_0 d\gamma_1 \sqrt{\lambda} \\ & = \left[\sinh\left(\theta_2 - \theta_1 + \frac{p_0\sqrt{\lambda}}{d\gamma_1} \right) + \frac{d}{p_0\, a(p_1)} (\gamma_1 - \gamma_2) \sinh(\theta_2) \sinh\left(\frac{p_0\sqrt{\lambda}}{d\gamma_1} - \theta_1 \right) \right] gd^2 \end{aligned} \tag{7.30}$$

has a unique positive solution λ^*.

Remark 7.2.1. *If the matching conditions* (7.26) *and* (7.27) *are satisfied, they ensure that* $M \in C^1([-1, 0])$. *By utilizing Schauder-type estimates* cf. [48] *it can be argued along the lines of* [65] *and obtain that* $M \in C^{1,\alpha}([-1, 0])$ *as required for the existence of small-amplitude water waves that are perturbations of the laminar flow solutions* (7.13).

7.2.2 The algebraic equation

In order to study the existence of small-amplitude water waves, the equation (7.30) is considered. However, the current form of this equation provides little insight in terms

of the physical parameters describing the two-layer vorticity model. Therefore, first (7.30) is rewritten in pursuit of an expression that resembles a dispersion relation. Let us begin by integrating the velocity expression (7.19),

$$\begin{aligned}
-p_0 &= \int_{-d}^{0}(c-u)\,dy = \int_{-d}^{-\nu}(c-u)\,dy + \int_{-\nu}^{0}(c-u)\,dy \\
&= \int_{-d}^{-\nu}\left[\frac{-p_0\sqrt{\lambda}}{d} + \nu\gamma_1 - \gamma_2(y+\nu)\right]dy + \int_{-\nu}^{0}\left[\frac{-p_0\sqrt{\lambda}}{d} - \gamma_1 y\right]dy \\
&= \left(\frac{-p_0\sqrt{\lambda}}{d}y + \nu\gamma_1 y - \gamma_2\frac{(y+\nu)^2}{2}\right)\Bigg]_{-d}^{-\nu} + \left(-\frac{p_0\sqrt{\lambda}}{d}y - \gamma_1\frac{y^2}{2}\right)\Bigg]_{-\nu}^{0} \\
&= \frac{p_0\sqrt{\lambda}}{d}(\nu-d) + \nu\gamma_1(d-\nu) + \gamma_2\frac{(d-\nu)^2}{2} - \frac{p_0\sqrt{\lambda}}{d}\nu + \gamma_1\frac{\nu^2}{2} \\
&= -p_0\sqrt{\lambda} + \frac{\gamma_2}{2}(d-\nu)^2 - \frac{\gamma_1}{2}(d-\nu)^2 + \frac{\gamma_1}{2}d^2\,.
\end{aligned}$$

Hence, it follows that

$$p_0(\sqrt{\lambda}-1) = \frac{\gamma_2-\gamma_1}{2}(d-\nu)^2 + \frac{\gamma_1}{2}d^2\,. \tag{7.31}$$

Using (7.17), the assumption $\psi(0) = 0$ and the definition of the stream function yields

$$-p_1\,p_0 = \psi(0) - \psi(-\nu) = \int_{-\nu}^{0}(u-c)\,dy = \left(\frac{p_0\sqrt{\lambda}}{d}\nu - \frac{\gamma_1}{2}\nu^2\right).$$

Thus,

$$\frac{\gamma_1}{2p_0}\nu^2 - \frac{\sqrt{\lambda}}{d}\nu - p_1 = 0\,, \tag{7.32}$$

which, as a polynomial in ν, has roots

$$\nu = \frac{\sqrt{\lambda} \pm \sqrt{\lambda + 2\dfrac{\gamma_1 d^2 p_1}{p_0}}}{\dfrac{d\gamma_1}{p_0}}. \tag{7.33}$$

It is claimed that only a minus sign is possible in the previous expression (7.33) in order to keep ν positive as assumed at the beginning of this section. Indeed, if the choice of a positive sign is made, then any positive value of γ_1 implies that ν is

negative because $p_0 < 0$. On the contrary, if a minus sign is chosen then, (7.33) is positive regardless the sign of γ_1. On the one hand, if $\gamma_1 > 0$, both the numerator $\sqrt{\lambda} - \sqrt{\lambda + 2\frac{\gamma_1 d^2 p_1}{p_0}}$ and the denominator $\frac{d\gamma_1}{p_0}$ are negative, giving $\nu > 0$. On the contrary, if $\gamma_1 < 0$ then both the numerator and denominator in (7.33) are positive, again resulting in $\nu > 0$. Therefore, after making the choice in sign

$$\nu = \frac{\sqrt{\lambda} - \sqrt{\lambda + 2\dfrac{\gamma_1 d^2 p_1}{p_0}}}{\dfrac{d\gamma_1}{p_0}} = \frac{a(0) - a(p_1)}{\dfrac{d\gamma_1}{p_0}},$$

and from (7.25)

$$\theta_1 = \frac{p_0\sqrt{\lambda}}{d\gamma_1} - \nu. \tag{7.34}$$

In order to obtain an expression of the same kind for θ_2, we start by considering (7.31) as a polynomial in d, written in the following form

$$\gamma_2 d^2 + 2\nu(\gamma_1 - \gamma_2)d - (\gamma_1 - \gamma_2)\nu^2 - 2p_0(\sqrt{\lambda} - 1) = 0\,.$$

Multiplying by γ_2 and rearranging terms gives

$$\Big(\gamma_2 d + \nu(\gamma_1 - \gamma_2)\Big)^2 = \nu^2\gamma_1(\gamma_1 - \gamma_2) + 2p_0\gamma_2(\sqrt{\lambda} - 1)\,,$$

which after multiplying by d^2/p_0^2 , yields

$$\frac{d^2}{p_0^2}\Big(\gamma_2 d + \nu(\gamma_1 - \gamma_2)\Big)^2 - \frac{2d^2}{p_0}\gamma_2\sqrt{\lambda} + \frac{2d^2}{p_0}\gamma_2 = \frac{\nu^2 d^2}{p_0^2}\gamma_1(\gamma_1 - \gamma_2)\,. \tag{7.35}$$

Then, by (7.21) and (7.32)

$$a^2(-1;\lambda) = \lambda - \frac{2d^2}{p_0}\gamma_2 + \frac{\nu^2 d^2}{p_0^2}\gamma_1(\gamma_1 - \gamma_2) - \frac{2\nu d}{p_0}(\gamma_1 - \gamma_2)\sqrt{\lambda}\,.$$

Replacing the third term on the right-hand side by the expression given on the left hand side of (7.35), it follows that

$$a^2(-1;\lambda) = \left\{\frac{d}{p_0}\Big(\gamma_2 d + \nu(\gamma_1 - \gamma_2)\Big) - \sqrt{\lambda}\right\}^2. \tag{7.36}$$

In order to choose the correct sign, it is noted that $c - u(y)$ is positive for all y in $[-d, 0]$. In particular, for $y = -d$,

$$c - u(-d) = -\frac{p_0\sqrt{\lambda}}{d} + \nu(\gamma_1 - \gamma_2) + \gamma_2 d > 0\,,$$

which holds if and only if

$$\frac{d}{p_0}\Big(\gamma_2 d + \nu(\gamma_1 - \gamma_2)\Big) - \sqrt{\lambda} < 0.$$

Therefore,

$$a(-1;\lambda) = \sqrt{\lambda} - \frac{d}{p_0}\Big(\gamma_2 d + \nu(\gamma_1 - \gamma_2)\Big). \tag{7.37}$$

Hence, the expression for θ_2 is

$$\theta_2 = \frac{p_0}{d\gamma_2}\Big(a(p_1) - a(-1)\Big) = \frac{p_0}{d\gamma_2}\Big(a(p_1) - a(0)\Big) + \frac{p_0}{d\gamma_2}\Big(a(0) - a(-1)\Big) = d - \nu.$$

Thus, by means of the previous identities, summarised here

$$\begin{cases} \theta_1 = \dfrac{p_0\sqrt{\lambda}}{d\gamma_1} - \nu\,, \\ \theta_2 = d - \nu\,, \\ \theta_2 - \theta_1 + \dfrac{p_0\sqrt{\lambda}}{d\gamma_1} = d\,, \end{cases} \tag{7.38}$$

the equation (7.30) is rewritten as

$$\begin{aligned} &p_0^2\{p_0\, a(p_1)\cosh(d) + d(\gamma_1 - \gamma_2)\sinh(d-\nu)\cosh(\nu)\}\lambda \\ &- \{p_0\, a(p_1)\sinh(d) + d(\gamma_1 - \gamma_2)\sinh(d-\nu)\sinh(\nu)\}p_0 d\gamma_1\sqrt{\lambda} \\ &- \{p_0\, a(p_1)\sinh(d) + d(\gamma_1 - \gamma_2)\sinh(d-\nu)\sinh(\nu)\}gd^3 = 0\,. \end{aligned} \tag{7.39}$$

Then, (7.25) and (7.38) yield

$$p_0\, a(p_1) = p_0\sqrt{\lambda} - d\nu\gamma_1\,.$$

Finally, the following equation is obtained

$$\begin{aligned} &p_0^3\cosh(d)\,\lambda^{3/2} \\ &+ p_0^2\left\{-d\nu\gamma_1\cosh(d) + d(\gamma_1 - \gamma_2)\sinh(d-\nu)\cosh(\nu) - d\gamma_1\sinh(d)\right\}\lambda \\ &+ p_0\left\{d^2\nu\gamma_1^2\sinh(d) + d^2\gamma_1(\gamma_1 - \gamma_2)\sinh(d-\nu)\sinh(\nu) - gd^2\sinh(d)\right\}\lambda^{1/2} \\ &+ \{gd^3\nu\gamma_1\sinh(d) - gd^3(\gamma_1 - \gamma_2)\sinh(d-\nu)\sinh(\nu)\} = 0, \end{aligned} \tag{7.40}$$

which can be seen as a dispersion relation that relates the vorticity in the different layers, together with the depth of these layers, with the velocity at the surface. More precisely, provided (7.40) has a unique positive solution, it gives the relative speed at the free surface of the laminar solution.

7.3 Analysis of the dispersion relation

The problem of finding small-amplitude waves for the vorticity (7.16) has been transformed into an algebraic problem. The attention is focused on the different choices for parameters that produce a unique positive solution of (7.40). In this case, those parameters are the fixed mean depth of the flow, the location of the jump in vorticity, the vorticity distribution itself and the wavelength. Note that the wavelength is not explicit but can be recovered by means of the dimension variables prior to the scaling (7.4).

Particularly, it has been shown that non-laminar small-amplitude waves due to bifurcation exist if and only if (7.40) holds, i.e. if and only if there is a unique root $\sqrt{\lambda}$ of (7.40) compatible with (7.3). If such a root exists, the velocity at the surface is recovered via (7.14). This motivates the following change of variables

$$x := c - u(0) = -\frac{p_0\sqrt{\lambda}}{d} \quad (>0)\,, \tag{7.41}$$

which, after dividing by $-d^3$, transforms (7.40) into

$$\begin{aligned} p(x) := \cosh(d)\,x^3 &+ \Big\{\nu\gamma_1\cosh(d) - (\gamma_1-\gamma_2)\sinh(d-\nu)\cosh(\nu) + \gamma_1\sinh(d)\Big\}\,x^2 \\ &+ \Big\{\nu\gamma_1^2\sinh(d) - \gamma_1(\gamma_1-\gamma_2)\sinh(d-\nu)\sinh(\nu) - g\sinh(d)\Big\}\,x \\ &+ g\Big\{-\nu\gamma_1\sinh(d) + (\gamma_1-\gamma_2)\sinh(d-\nu)\sinh(\nu)\Big\} = 0\,. \end{aligned} \tag{7.42}$$

Note that the equation (7.42) coincides with the one derived in [99] for the fixed mass-flux setting, that in turn generalises the cases derived in [10] and [29] which dealt with two-layer flows including one irrotational layer. This suggests the possibility that the differences in the two approaches will be perceptible in waves of large amplitude, cf. [56, 65]. The existence of a unique positive solution of (7.42) that is compatible with (7.3) is now discussed in terms of the vorticity. The results given in [99] are derived here for the fixed mass-flux scenario. Moreover, these results are

extended in order to cover all the different combinations in terms of the sign of the constant vorticity layers.

Lemma 7.3.1. *If γ_1 and γ_2 are both positive, then there exists a unique positive root of* (7.42)*. Therefore, local bifurcation always occurs.*

Proof. Let $p(x)$ be the polynomial given by (7.42) and let σ be the function defined by

$$\sigma(\nu) = \sinh(d)\nu - \sinh(d-\nu)\sinh(\nu)\,.$$

This function has the following properties

$$\begin{aligned}\sigma(0) &= 0\,,\\ \sigma'(\nu) &= \sinh(d) - \sinh(d-2\nu) > 0 \quad \text{for all } \nu > 0\,.\end{aligned}$$

Furthermore, this function has a unique critical point at $\nu = 0$, which is a minimum since $\sigma''(\nu) > 0$ for all ν. Hence, $\sigma(\nu) > 0$ for all $\nu > 0$. Therefore, it follows that

$$-p(0) = g\Big[\nu\gamma_1\sinh(d) - (\gamma_1-\gamma_2)\sinh(d-\nu)\sinh(\nu)\Big] > g\gamma_1\sigma(\nu) > 0\,.$$

Thus, $p(0) < 0$ and there exists at least one positive root of the polynomial because p approaches infinity as x goes to infinity. It is claimed that this root is unique and the bifurcation occurs. If it is assumed the existence of another positive root, Viète's formula (A.11a) and the fact that

$$-\frac{p(0)}{\cosh(d)} > 0$$

would imply that there exists three real positive roots. However, by Viète's formula (A.11b), this is not possible because the coefficient of the second-order term in (7.42) is positive. Indeed,

$$\begin{aligned}&\frac{1}{\cosh(d)}\Big\{\nu\gamma_1\cosh(d) - (\gamma_1-\gamma_2)\sinh(d-\nu)\cosh(\nu) + \gamma_1\sinh(d)\Big\}\\ &> \frac{\gamma_1}{\cosh(d)}\Big\{\nu\cosh(d) - \sinh(d-\nu)\cosh(\nu) + \sinh(d)\Big\}\\ &= \frac{\gamma_1}{\cosh(d)}\Big\{\nu\cosh(d) - \sinh(d-\nu)\cosh(\nu) + \sinh(d)\big[\cosh^2(\nu) - \sinh^2(\nu)\big]\Big\}\\ &= \frac{\gamma_1}{\cosh(d)}\Big\{\nu\cosh(d) + \sinh(\nu)\cosh(d-\nu)\Big\} > 0\,.\end{aligned}$$

□

The next situation assumes two layers with constant vorticity of opposite sign.

Lemma 7.3.2. *Let γ_1 be negative and γ_2 be positive. There exists a unique positive root of the dispersion relation* (7.42) *satisfying the non-stagnation condition* (7.3) *if and only if*

$$\frac{g}{\gamma_1^2} > \nu^2 \frac{\cosh(\nu)}{\sinh(\nu)} - \nu\,. \tag{7.43}$$

Proof. In this case, a necessary and sufficient condition for (7.3) to hold for all $y \in [-d, 0]$ is

$$-p_0 \frac{\sqrt{\lambda}}{d} + \gamma_1 \nu = x + \gamma_1 \nu > 0\,.$$

This suggests the change of variables

$$\tilde{x} = -\frac{1}{\gamma_1} x - \nu.$$

The polynomial (7.42) in the variable y is given by

$$q(\tilde{x}) = A\,\tilde{x}^3 + B\,\tilde{x}^2 + C\,\tilde{x} + D\,, \tag{7.44}$$

where

$$\begin{aligned}
A &= \cosh(d)\,,\\
B &= \Big\{ 2\nu\cosh(d) - \sinh(\nu)\cosh(d-\nu) - \frac{\gamma_2}{\gamma_1}\sinh(d-\nu)\cosh(\nu) \Big\}\,,\\
C &= \Big\{ \nu^2\cosh(d) - \sinh(d-\nu)\sinh(\nu) + \nu\Big[\sinh(d-\nu)\cosh(\nu) - \sinh(\nu)\cosh(d-\nu) \Big] +\\
&\quad + \frac{\gamma_2}{\gamma_1}\sinh(d-\nu)\Big[\sinh(\nu) - 2\nu\cosh(\nu) \Big] - \frac{g}{\gamma_1^2}\sinh(d) \Big\}\,,\\
D &= \sinh(d-\nu)\Big\{ \frac{g\gamma_2}{\gamma_1^3}\sinh(\nu) - \frac{g}{\gamma_1^2}\sinh(\nu) + \Big(\nu^2\cosh(\nu) - \nu\sinh(\nu) \Big)\Big(1 - \frac{\gamma_2}{\gamma_1} \Big) \Big\}\,.
\end{aligned}$$

It is important to notice that x is a positive root of (7.42) that satisfies the non-stagnation condition (7.3) if and only if y is a positive root of $q(y)$. The polynomial q at 0 is such that

$$\begin{aligned}
q(0) &= \sinh(d-\nu)\Big\{ \frac{g}{\gamma_1^2}\Big(\frac{\gamma_2}{\gamma_1} - 1 \Big)\sinh(\nu) + \Big(1 - \frac{\gamma_2}{\gamma_1} \Big)\Big(\nu^2\cosh(\nu) - \nu\sinh(\nu) \Big) \Big\}\\
&= \Big(1 - \frac{\gamma_2}{\gamma_1} \Big)\sinh(d-\nu)\Big\{ \nu^2\cosh(\nu) - \nu\sinh(\nu) - \frac{g}{\gamma_1^2}\sinh(\nu) \Big\}
\end{aligned}$$

Since $1-\frac{\gamma_2}{\gamma_1}$ and $\sinh(d-\nu)$ are positive, it follows that $q(0) < 0$ if and only if (7.43) holds. Moreover,

$$\begin{aligned} B &= \left\{2\nu\cosh(d) - \sinh(\nu)\cosh(d-\nu) - \frac{\gamma_2}{\gamma_1}\sinh(d-\nu)\cosh(\nu)\right\} \\ &> 2\nu\cosh(d) - \sinh(\nu)\cosh(d-\nu) \\ &> 0\,, \end{aligned}$$

where the last inequality follows from the fact that the function

$$\tilde{\sigma}(\nu) = 2\nu\cosh(d) - \sinh(\nu)\cosh(d-\nu)$$

is monotonically increasing for $\nu \in [0, d]$ and $\tilde{\sigma}(0) = 0$. Hence, a similar argument to the one presented in the previous lemma concludes that there is a unique positive root of (7.44).

In addition, the condition (7.43) is necessary for the bifurcation to occur. By assuming that

$$\frac{g}{\gamma_1^2} \leq \nu^2\frac{\cosh(\nu)}{\sinh(\nu)} - \nu\,, \tag{7.45}$$

$q(\tilde{x})$ does not have positive roots and the bifurcation does not occur. To see this, note that (7.45) implies $q(0) > 0$. In addition, $q'(\tilde{x}) > 0$ for all $\tilde{x} > 0$ because

$$q'(\tilde{x}) = 3A\,\tilde{x}^2 + 2B\,\tilde{x} + C\,,$$

where all the coefficients are positive. Note that A is always positive and B is positive for this vorticity function. Finally, $C > 0$ if and only if

$$\frac{1}{\sinh(d)}\left[C + \frac{g}{\gamma_1^2}\sinh(d)\right] > \frac{g}{\gamma_1^2}\,. \tag{7.46}$$

However,

$$\frac{1}{\sinh(d)}\left[C + \frac{g}{\gamma_1^2}\sinh(d)\right] > \nu^2\frac{\cosh(\nu)}{\sinh(\nu)} - \nu\,,$$

which from (7.45) shows that (7.46) holds. Finally, this last inequality holds as long as

$$\nu^2 - 2\nu\sinh(\nu)\cosh(\nu) + \sinh^2(\nu) - \frac{\gamma_2}{\gamma_1}\sinh(\nu)[\sinh(\nu) - 2\nu\cosh(\nu)] < 0\,,$$

which is true for $\gamma_1 < 0$ and $\gamma_2 > 0$. □

The final case, when both layers possess negative vorticity, is analysed the following Lemma.

Lemma 7.3.3. *Assume that* $\gamma_1 < \gamma_2 < 0$. *Then, if* (7.43) *holds, local bifurcation occurs if and only if*

$$\frac{\gamma_2 - \gamma_1}{\gamma_2(d-\nu)}\, H(\nu)\, \sinh(d-\nu) < H(d)\,, \tag{7.47}$$

where

$$H(y) = \frac{g - \gamma_1 x_c}{x_c^2}\sinh(y) - \cosh(y)$$

and

$$x_c = -\gamma_2(d-\nu) - \gamma_1\nu\,.$$

Proof. Let us consider the monic polynomial

$$\begin{aligned} p(x) =& x^3 + \frac{1}{\cosh(d)}\Big\{\nu\gamma_1\cosh(d) + (\gamma_2-\gamma_1)\sinh(d-\nu)\cosh(\nu) + \gamma_1\sinh(d)\Big\}\, x^2 \\ &+ \frac{1}{\cosh(d)}\Big\{\nu\gamma_1^2\sinh(d) + \gamma_1(\gamma_2-\gamma_1)\sinh(d-\nu)\sinh(\nu) - g\sinh(d)\Big\}\, x \\ &+ \frac{g}{\cosh(d)}\Big\{ -\nu\gamma_1\sinh(d) - (\gamma_2-\gamma_1)\sinh(d-\nu)\sinh(\nu)\Big\}\,, \end{aligned} \tag{7.48}$$

which has the same roots as (7.42). We claim that under the condition (7.43), $p(x)$ has three real roots as described in Figure 7.2. The value of the polynomial at the origin is given by

$$\begin{aligned} p(0) &= \frac{g}{\cosh(d)}\Big[-\gamma_1\nu\sinh(d) + \gamma_1\sinh(d-\nu)\sinh(\nu) - \gamma_2\sinh(d-\nu)\sinh(\nu)\Big] \\ &> \frac{g}{\cosh(d)}\Big[-\gamma_1\nu\sinh(d) + \gamma_1\sinh(d-\nu)\sinh(\nu)\Big] \\ &= -\gamma_1\frac{g}{\cosh(d)}\Big[\nu\sinh(d) - \sinh(d-\nu)\sinh(\nu)\Big]. \end{aligned} \tag{7.49}$$

Note that the function

$$\nu \to \sigma(\nu) = \sinh(d)\nu - \sinh(d-\nu)\sinh(\nu)\,, \quad \text{for} \quad \nu > 0$$

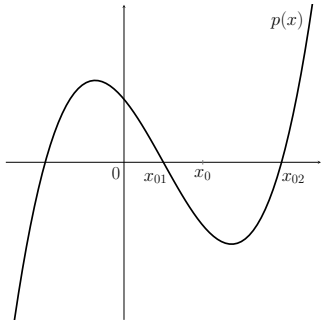

Figure 7.2: Sketch of the graph of the polynomial providing the dispersion relation for two negative vorticities under the condition (7.43). The root x_{01} does not satisfy the non-stagnation condition while the root x_{02} verifies it if and only if (7.47) is assumed.

satisfies $\sigma(0) = 0$ and that σ is a strictly increasing function for $\nu > 0$. Thus, $\sigma(\nu) > 0$ for any positive ν. Therefore, taking into account the negative value of γ_1, (7.49) is strictly positive. It follows from Viète's formula (A.3.1) that the polynomial p has either one or three negative roots. Let us consider now the point $x_0 = -\nu\gamma_1$, for which the polynomial takes the value

$$p(x_0) = \frac{\gamma_1^2(\gamma_1 - \gamma_2)}{\cosh(d)} \left[-\nu^2 \cosh(\nu) + \nu \sinh(\nu) + \frac{g}{\gamma_1^2} \sinh(\nu) \right] \sinh(d - \nu)$$

Since $\gamma_1 - \gamma_2 < 0$, then $p(x_0) < 0$ if and only if

$$-\nu^2 \cosh(\nu) + \nu \sinh(\nu) + \frac{g}{\gamma_1^2} \sinh(\nu) > 0\,,$$

which is equivalent to the condition (7.43). Hence, provided (7.43) holds, the polynomial has at least one positive root because there exists $x_0 > 0$ such that $p(x_0) < 0$. Furthermore, it is clear that

$$p(x) \longrightarrow \pm\infty \quad \text{as } x \to \pm\infty\,.$$

In this situation, p has two positive roots and one negative root, as showed in Figure 7.2.

Let $x_{01} < x_{02}$ be the two positive roots of p. We claim that the first positive root does not satisfy the non-stagnation condition (7.3). In order to see this, note that the first positive root x_{01} is such that $x_{01} < x_0$. On the other hand, the function

given in (7.19) is increasing in $[-d, 0]$ for γ_1 and γ_2 negative. This means that the non-stagnation condition is satisfied for all y in $[-d, 0]$ if and only if $c - u(-d) > 0$, i.e. if and only if

$$-\frac{p_0\sqrt{\lambda}}{d} + (\gamma_1 - \gamma_2)\nu + \gamma_2 d > 0\,.$$

Therefore, from (7.41), any root $x_\lambda = -\frac{p_0\sqrt{\lambda}}{d}$ of p must satisfy

$$x_\lambda > (\gamma_2 - \gamma_1)\nu - \gamma_2 d =: x_c\,. \tag{7.50}$$

However, $x_{01} < x_0$ and $x_0 \leq x_c$ for $\gamma_2 < 0$. Thus, the only admissible positive root agreeing with the non-stagnation condition is x_{02}. Thus, once (7.43) holds, bifurcation occurs if and only if the root x_{02} satisfies (7.50), which is now equivalent to

$$p(x_c) < 0\,. \tag{7.51}$$

Indeed, by the properties of the polynomial p sketched in Figure 7.2, $x_{02} > x_c$ if and only if

$$0 = p(x_{02}) > p(x_c)\,.$$

Evaluating the polynomial at x_c, it follows after some algebraic manipulations that

$$\begin{aligned} p(x_c) = &-\gamma_2(d-\nu)\,x_c^2 + (\gamma_2 - \gamma_1)\,x_c^2\,\frac{\sinh(d-\nu)\cosh(\nu)}{\cosh(d)} + \\ &+ \gamma_2(d-\nu)\big[g - \gamma_1 x_c\big]\tanh(d) - (\gamma_2 - \gamma_1)\,\Big[g - \gamma_1 x_c\Big]\frac{\sinh(d-\nu)\sinh(\nu)}{\cosh(d)}. \end{aligned}$$

Furthermore,

$$-\frac{\cosh(d)}{\gamma_2(d-\nu)x_c^2} > 0$$

and (7.51) is now equivalent to

$$\begin{aligned} \cosh(d) - \frac{\gamma_2 - \gamma_1}{\gamma_2(d-\nu)}\,\sinh(d-\nu)\cosh(\nu) - \frac{g - \gamma_1 x_c}{x_c^2}\sinh(d) + \\ + \frac{\gamma_2 - \gamma_1}{\gamma_2(d-\nu)x_c^2}\,\Big[g - \gamma_1 x_c\Big]\sinh(d-\nu)\sinh(\nu) < 0\,, \end{aligned}$$

which, by rearranging the terms, is equivalent to condition (7.47). □

Remark 7.3.1. *The solutions of* (7.42) *can be obtained by Cardano's formula. However, it can be more instructive to give an estimate of those solutions. This can be done similarly to* [99].

7.4 Stability of the laminar solutions

The study of these small-amplitude solutions is completed here with the analysis of the stability of laminar flow solutions satisfying (7.14) for which the mean depth is fixed. This follows the approach presented in [30, 99], where the fixed quantity was the mass flux instead of the mean depth.

Let us start by considering the following functional

$$\begin{aligned}\mathscr{F}(\psi) = \frac{1}{2dp_0^2}\iint_D \Big[\big|\nabla\psi(x,y)\big|^2 + Q + \frac{p_0^2}{d^2}\,\Gamma\Big(\frac{\psi(x,y)}{p_0}\Big)\Big]\,dxdy \\ - \iint_D \frac{gd}{p_0^2}\big[1+h(x,y)\big]h_y\,dxdy\,.\end{aligned} \tag{7.52}$$

The change of variables (7.8), which transforms the free-surface dependent domain D_η into R, yields the following functional

$$\mathscr{L}(h) = \iint_R \Big[\frac{1+d^2h_q^2}{2d^2(1+h_p)^2} + \frac{Q}{2p_0^2} + \frac{\Gamma(p)}{2d^2}\Big](1+h_p)\,dqdp - \iint_R \frac{gd}{p_0^2}\big[1+h\big]h_p\,dqdp\,. \tag{7.53}$$

The jump in vorticity (7.16) induces a loss in regularity of the solutions $\mathbb{h}$ of (7.10) along the line $p = p_1$. Similarly to [98], it can be shown that given $\alpha \in (0,1)$, there exists a real-analytic curve in $C^{1,\alpha}(\overline{R})$ consisting of solutions

$$\mathbb{h}(q,p) = \begin{cases} H(q,p)\,, & (q,p) \in [0,L]\times[p_1,0]\,, \\ \\ h(q,p) & (q,p) \in [0,L]\times[-1,p_1]\,, \end{cases} \tag{7.54}$$

to the problem (7.11) such that

$$\begin{aligned} H &\in C^{2,\alpha}([0,L]\times[p_1,0]) \cap C^\infty([0,L]\times(p_1,0))\,, \\ h &\in C^{2,\alpha}([0,L]\times[-1,p_1]) \cap C^\infty([0,L]\times(-1,p_1))\,, \end{aligned} \tag{7.55}$$

where $\mathbb{h}$ is continuously differentiable with respect to p along $[0,L]\times p_1$. In order to characterise the critical points of the functional (7.53), the first variation of $\mathscr{L}$ is computed. Let $\mathbb{t}$ be the L-periodic and even-in-q functions given by

$$\mathbb{t}(q,p) = \begin{cases} T(q,p)\,, & (q,p) \in [0,L]\times[p_1,0] \\ \\ t(q,p)\,, & (q,p) \in [0,L]\times[-1,p_1]\,, \end{cases} \tag{7.56}$$

which are continuously differentiable with respect to p along $[0,L]\times p_1$. Moreover, $T\in C^{2,\alpha}([0,L]\times[p_1,0])$ and $t\in C^{2,\alpha}([0,L]\times[-1,p_1])$, satisfying

$$\begin{aligned}\int_0^L T(q,0)\,dq=0\,,\\ T(q,-1)=0\,.\end{aligned}\tag{7.57}$$

Taking $\mathbb{t}$ as test functions, the first variation of $\mathscr{L}$ at $\mathbb{h}$ is given by

$$\begin{aligned}
&\langle\delta\mathscr{L}(\mathbb{h}),\mathbb{t}\rangle:=\lim_{\epsilon\to0}\frac{\mathscr{L}(\mathbb{h}+\epsilon\,\mathbb{t})-\mathscr{L}(\mathbb{h})}{\epsilon}\\
&=\lim_{\epsilon\to0}\frac{1}{\epsilon}\iint_R\left[\frac{1+d^2(\mathbb{h}_q+\epsilon\,\mathbb{t}_q)^2}{2d^2(1+\mathbb{h}_p+\epsilon\,\mathbb{t}_p)^2}-\frac{1+d^2\mathbb{h}_q^2}{2d^2(1+\mathbb{h}_p)^2}\right]\mathbb{t}_p\,dq\,dp\\
&\quad+\iint_R\left[\frac{Q}{2p_0^2}+\frac{\Gamma(p)}{2d^2}\right]\mathbb{t}_p\,dq\,dp-\lim_{\epsilon\to0}\frac{gd}{p_0^2}\iint_R\Big[(1+\mathbb{h})\mathbb{t}_p+\mathbb{t}\mathbb{h}+\epsilon\,\mathbb{t}\mathbb{t}_p\Big]\,dq\,dp\\
&=\lim_{\epsilon\to0}\frac{1}{\epsilon}\iint_R\left[\frac{\epsilon(1+d^2\mathbb{h}_q^2)\mathbb{t}_p-\epsilon\,2d^2\mathbb{h}_q\mathbb{t}_q(1+\mathbb{h}_p)-\epsilon^2d^2\,\mathbb{t}_q(1+\mathbb{h}_p)}{2d^2(1+\mathbb{h}_p+\epsilon\,\mathbb{t}_p)(1+\mathbb{h}_p)}\right]\mathbb{t}_p\,dq\,dp\\
&\quad+\iint_R\left[\frac{Q}{2p_0^2}+\frac{\Gamma(p)}{2d^2}\right]\mathbb{t}_p\,dq\,dp-\frac{gd}{p_0^2}\iint_R\Big[(1+\mathbb{h})\mathbb{t}_p+\mathbb{h}\mathbb{t}\Big]\,dqdp\\
&=\iint_R\left[\frac{(1+d^2\mathbb{h}_q^2)\mathbb{t}_p-2d^2\,\mathbb{h}_q\mathbb{t}_q(1+\mathbb{h}_p)}{2d^2(1+\mathbb{h}_p)^2}\right]\mathbb{t}_p\,dqdp+\iint_R\left[\frac{Q}{2p_0^2}+\frac{\Gamma(p)}{2d^2}\right]\mathbb{t}_p\,dq\,dp\\
&\quad-\frac{gd}{p_0^2}\iint_R\Big[(1+\mathbb{h})\mathbb{t}_p+\mathbb{h}\mathbb{t}\Big]\,dq\,dp
\end{aligned}$$

Based on the properties of the test functions $\mathbb{t}$, integration by parts yields

$$\begin{aligned}
\langle\delta\mathscr{L}(\mathbb{h}),\mathbb{t}\rangle=&-\int_0^L\left[\frac{(1+d^2H_q^2)}{2d^2(1+H_p)^2}+\frac{gd(H+1)}{p_0^2}-\frac{Q}{2p_0^2}\right]T\Big|_{p=0}\,dq\\
&-\iint_R\left[(\frac{1}{d^2}+\mathbb{h}_q^2)\mathbb{h}_{pp}-2\mathbb{h}_q\mathbb{h}_{pq}(1+\mathbb{h}_p)+\mathbb{h}_{qq}(1+\mathbb{h}_p)^2+\frac{\gamma(p)}{p_0}(1+\mathbb{h}_p)^3\right](1+\mathbb{h}_p)^{-3}\mathbb{t}\,dq\,dp\,.
\end{aligned}$$

Hence, the first variation of the functional (7.53) is given by

$$\langle\delta\mathscr{L}(\mathbb{h}),\mathbb{t}\rangle=-\frac{1}{2}\int_0^L\mathscr{G}_0(H)(1+H_p)^{-2}T\Big|_{p=0}\,dq-\iint_R\mathscr{G}(\mathbb{h})(1+\mathbb{h}_p)^{-3}\mathbb{t}\,dq\,dp\,,\tag{7.58}$$

where

$$\mathscr{G}_0(H)=\frac{1}{d^2}+H_q^2+\frac{(1+H_p)^2}{p_0^2}[2gd(H+1)-Q]\tag{7.59}$$

and

$$\mathscr{G}(\mathbb{h}) = \begin{cases} (\dfrac{1}{d^2} + H_q^2)H_{pp} - 2H_qH_{pq}(1+H_p) + H_{qq}(1+H_p)^2 + \dfrac{\gamma(p)}{p_0}(1+H_p)^3 \\ \qquad \text{for} \quad (q,p) \in [0,L] \times [p_1, 0]\,, \\ \\ (\dfrac{1}{d^2} + h_q^2)h_{pp} - 2h_qh_{pq}(1+h_p) + h_{qq}(1+h_p)^2 + \dfrac{\gamma(p)}{p_0}(1+h_p)^3 \\ \qquad \text{for} \quad (q,p) \in [0,L] \times [-1, p_1]\,. \end{cases} \tag{7.60}$$

Therefore, any critical point of the functional $\mathscr{L}$ satisfies

$$\mathscr{G}(\mathbb{h}) = 0 \quad \text{in} \quad R \tag{7.61}$$

$$\mathscr{G}_0(H) = 0 \quad \text{on} \quad p = 0\,, \tag{7.62}$$

i.e. critical points of $\mathscr{L}$ satisfy the height function formulation (7.10).

The notion of stability is formalised by the following definitions. Then, the stability of laminar flow solutions is addressed. First, the second variation of $\mathscr{L}$ at $\mathbb{h}$ in the direction of $\mathbb{t}$ and $\mathbb{f}$ is defined by

$$\langle \delta^2 \mathscr{L}(\mathbb{h})\mathbb{f}, \mathbb{t}\rangle = \lim_{\epsilon \to 0} \frac{\langle \delta \mathscr{L}(\mathbb{h} + \epsilon\, \mathbb{t}), \mathbb{f}\rangle - \langle \delta \mathscr{L}(\mathbb{h}), \mathbb{f}\rangle}{\epsilon}\,.$$

Definition 7.4.1. *The function* $\mathbb{h}$ *is said to be formally stable if* $\langle \delta^2 \mathscr{L}(\mathbb{h})\mathbb{t}, \mathbb{t}\rangle \geq 0$ *for all the functions* $\mathbb{t}$ *given in* (7.56).

Let $\mathbb{h}$ be a critical point of $\mathscr{L}$. Then, it follows from (7.58) and (7.61) that

$$\langle \delta^2 \mathscr{L}(\mathbb{h})\mathbb{f}, \mathbb{t}\rangle = -\frac{1}{2}\int_0^L \mathscr{G}_{0_H}(H)[F](1+H_p)^{-2}T\Big|_{p=0}\, dq - \iint_R \mathscr{G}_{\mathbb{h}}(\mathbb{h})[\mathbb{f}](1+\mathbb{h}_p)^{-3}\mathbb{t}\, dq\, dp\,, \tag{7.63}$$

where

$$\mathscr{G}_{0_H}(H)[F] = \lim_{\epsilon \to 0} \frac{\mathscr{G}_0(H + \epsilon\, F) - \mathscr{G}_0(H)}{\epsilon} \quad \text{and} \quad \mathscr{G}_{\mathbb{h}}(\mathbb{h})[\mathbb{f}] = \lim_{\epsilon \to 0} \frac{\mathscr{G}(\mathbb{h} + \epsilon\, \mathbb{f}) - \mathscr{G}(\mathbb{h})}{\epsilon}$$

are the derivatives of the corresponding functionals (7.59) and (7.60). In particular, we are interested in the stability of laminar solutions

$$\overline{\mathbb{h}}(p) = \begin{cases} \overline{H}(p)\,, & p \in [p_1, 0], \\ \\ \overline{h}(p)\,, & p \in [-1, p_1]. \end{cases}$$

Let λ^* be the critical value for which the bifurcation from the laminar solutions occurs and which is related to the velocity on the surface by (7.14). Then, the following result is shown.

Theorem 7.4.1. *A laminar solution $\overline{\mathbb{h}}(\cdot,\lambda)$ is formally stable if and only if $\lambda \geq \lambda^*$.*

Proof. In order to obtain the second variation of $\mathscr{L}$ at $\overline{\mathbb{h}}$ the test functions $\mathbb{t}$ and $\mathbb{f}$ are taking of the form (7.56). The independence of $\overline{\mathbb{h}}$ on q, yields

$$\mathscr{G}_{0_H}(\overline{H})[F] = \frac{2gd}{p_0^2}(1+\overline{H}_p)^2 F + \frac{2}{p_0^2}(1+\overline{H}_p)[2gd(\overline{H}+1)-Q]F_p$$

and

$$\mathscr{G}_{\mathbb{h}}(\overline{\mathbb{h}})[\mathbb{f}] = \frac{1}{d^2}\mathbb{f}_{pp} + (1+\overline{\mathbb{h}}_p)^2\mathbb{f}_{qq} + 3\frac{\gamma(p)}{p_0}(1+\overline{\mathbb{h}}_p)^2\mathbb{f}_p\,.$$

Thus, from (7.63)

$$\begin{aligned}\langle \delta^2\mathscr{L}(\overline{\mathbb{h}})\mathbb{t},\mathbb{t}\rangle = &-\frac{1}{2}\int_0^L \left[\frac{2gd}{p_0^2}T^2 + \frac{2}{p_0^2(1+\overline{H}_p)}[2gd(\overline{H}+1)-Q]T\,T_p\right]\Big|_{p=0} dq \\ &- \iint_R \left[\frac{1}{d^2(1+\overline{\mathbb{h}}_p)^3}\mathbb{t}\,\mathbb{t}_{pp} + \frac{1}{1+\overline{\mathbb{h}}_p}\mathbb{t}\,\mathbb{t}_{qq} + \frac{3\gamma(p)}{p_0(1+\overline{\mathbb{h}}_p)}\mathbb{t}\,\mathbb{t}_p\right] dq\,dp\,.\end{aligned}$$

Taking into account the regularity of the test functions $\mathbb{t}$ and $\overline{H}$ along $p=p_1$ as well as the assumption $T(q,-1)=0$

$$\begin{aligned}\int_{-1}^0 \frac{1}{d^2(1+\overline{\mathbb{h}}_p)^3}\mathbb{t}\,\mathbb{t}_{pp}\,dp = &\frac{T\,T_p}{d^2(1+\overline{\mathbb{h}}_p)^3}\Big|_{p=0} - \int_{-1}^0 \frac{1}{d^2(1+\overline{\mathbb{h}}_p)^3}\,\mathbb{t}_p^2\,dp \\ &+ \int_{-1}^0 \frac{3\overline{\mathbb{h}}_{pp}}{d^2(1+\overline{\mathbb{h}}_p)^3}\,\frac{\mathbb{t}\,\mathbb{t}_p}{(1+\overline{\mathbb{h}}_p)}\,dp\,. \qquad (7.64)\end{aligned}$$

Using the fact that laminar solutions satisfy the relation

$$\frac{\overline{\mathbb{h}}_{pp}}{(1+\overline{\mathbb{h}}_p)^3} = -\frac{d^2\gamma(p)}{p_0},$$

integrating with respect to q in (7.64) yields

$$\begin{aligned}\iint_R \frac{1}{d^2(1+\overline{\mathbb{h}}_p)^3}\mathbb{t}\,\mathbb{t}_{pp}\,dqdp = &\int_0^L \frac{T\,T_p}{d^2(1+\overline{\mathbb{h}}_p)^3}\Big|_{p=0} dq - \iint_R \frac{1}{d^2(1+\overline{\mathbb{h}}_p)^3}\,\mathbb{t}_p^2\,dqdp \\ &- \iint_R \frac{3\gamma(p)}{p_0(1+\overline{\mathbb{h}}_p)}\,\mathbb{t}\,\mathbb{t}_p\,dqdp\,. \qquad (7.65)\end{aligned}$$

In addition, by (7.13) and (7.14)

$$2gd(\overline{H}(0)+1)-Q=-\frac{p_0^2}{d^2(1+\overline{H}_p(0))^2}\,. \tag{7.66}$$

Then, by (7.65) and (7.66)

$$\langle\delta^2\mathscr{L}(\overline{\mathbb{h}})\mathbb{t},\mathbb{t}\rangle=-\int_0^L\frac{gd}{p_0^2}T^2\Big|_{p=0}dq-\iint_R\left[\frac{\mathbb{t}\,\mathbb{t}_{qq}}{(1+\overline{\mathbb{h}}_p)}-\frac{\mathbb{t}_p^2}{d^2(1+\overline{\mathbb{h}}_p)^3}\right]dqdp\,. \tag{7.67}$$

Due to the requirements of the water wave problem, the test functions have been taken as continuously differentiable L-periodic and even-in-q. Therefore, it is possible to expand $\mathbb{t}$ in Fourier series

$$\mathbb{t}(q,p)=\sum_{n=0}^{\infty}\mathbb{t}_n(p)\cos\Big(\frac{2\pi nq}{L}\Big)\,, \tag{7.68}$$

where

$$\mathbb{t}_0(p)=\begin{cases}T_0(p)=\dfrac{1}{L}\displaystyle\int_0^L T(q,p)\,dq\,, & p\in[p_1,0]\\[2ex] t_0(p)=\dfrac{1}{L}\displaystyle\int_0^L t(q,p)\,dq\,, & p\in[-1,p_1]\end{cases}$$

and

$$\mathbb{t}_n(p)=\begin{cases}T_n(p)=\dfrac{2}{L}\displaystyle\int_0^L T(q,p)\cos\Big(\frac{2\pi nq}{L}\Big)\,dq\,, & p\in[p_1,0]\\[2ex] & \text{for}\quad n\geq 1\\[2ex] t_n(p)=\dfrac{2}{L}\displaystyle\int_0^L t(q,p)\cos\Big(\frac{2\pi nq}{L}\Big)\,dq\,, & p\in[-1,p_1]\end{cases}$$

are both continuously differentiable along $p=p_1$, such that $\mathbb{t}_0(0)=T_0(0)=0$. Now (7.67) takes the form

$$\begin{aligned}\langle\delta^2\mathscr{L}(\overline{\mathbb{h}})\mathbb{t},\mathbb{t}\rangle=&L\left[-\frac{gd}{p_0^2}\mathbb{t}_0^2(0)+\int_{-1}^0\frac{(\mathbb{t}_0'(p))^2}{d^2(1+\overline{\mathbb{h}}_p)^3}\,dp\right]\\&+\frac{L}{2}\sum_{n=1}^{\infty}\left\{-\frac{gd}{p_0^2}\mathbb{t}_n^2(0)+\int_{-1}^0\Big[\frac{(\mathbb{t}_n'(p))^2}{d^2(1+\overline{\mathbb{h}}_p)^3}+\Big(\frac{2\pi n}{L}\Big)^2\frac{\mathbb{t}_n^2(p)}{(1+\overline{\mathbb{h}}_p)}\Big]\,dp\right\}\\&=\frac{L}{2}\sum_{n=0}^{\infty}\left\{-\frac{gd}{p_0^2}\mathbb{t}_n^2(0)+\int_{-1}^0\Big[\frac{(\mathbb{t}_n'(p))^2}{d^2(1+\overline{\mathbb{h}}_p)^3}+\Big(\frac{2\pi n}{L}\Big)^2\frac{\mathbb{t}_n^2(p)}{(1+\overline{\mathbb{h}}_p)}\Big]\,dp\right\}.\end{aligned} \tag{7.69}$$

It was shown in section 3 of [71] that if $\hat{k} = \frac{2\pi n}{L}$ in (7.68), then

$$\inf_{\mathbb{t}} \frac{-\dfrac{gd\mathbb{t}^2(0)}{p_0^2} + \displaystyle\int_{-1}^{0} \frac{(\mathbb{t}')^2}{d^2(1+\overline{\mathbb{h}}_p)^3}\, dp}{\displaystyle\int_{-1}^{0} \frac{\mathbb{t}^2(p)}{(1+\overline{\mathbb{h}}_p)}\, dp} \geq -(\hat{k})^2 \qquad \text{if and only if} \quad \lambda \geq \lambda^* .$$

Therefore, by the last inequality and (7.69), it follows that $\langle \delta^2 \mathscr{L}(\overline{\mathbb{h}})\mathbb{t}, \mathbb{t} \rangle \geq 0$ if and only if $\lambda \geq \lambda^*$.

□

Conclusions

This thesis has provided a mathematically rigorous approach for analysing exact and explicit solutions to the nonlinear geophysical governing equations. The mathematical validity of the Lagrangian description of the solutions has been discussed as well as their hydrodynamic stability. This, together with the examination of some of their flow properties, offers a comprehensive study of these waves.

Throughout this thesis, use has been made of the nonlinear geophysical governing equations which account for the rotation of the Earth. Its derivation from Euler equations and the consideration of a rotating framework was included in Chapter 1. Subsequently, the β and f-plane approximations have been presented and justified. These approximations are still nonlinear in terms of the fluid velocity and therefore an exact solution is normally not expected. However, it has been shown how by means of the Lagrangian description of the fluid motion and within the Gerstner wave framework, it was possible to derive exact and explicit solutions for the nonlinear geophysical governing equations.

A solution describing internal water waves propagating above a thermocline along the Equator was obtained in Chapter 3. This solution incorporates currents in both, the meridional and zonal direction, allowing for more realistic scenarios than previous models available in the literature. The procedure carried out for its derivation exemplifies the use of Lagrangian descriptions for geophysical waves. The main task is the determination of a pressure compatible with the velocity satisfying the corresponding governing equations and boundary conditions. Another interesting observation is that a combination of both, the Eulerian and the Lagrangian descriptions have been used even if an explicit inverse from the labelling to the fluid domain is not available.

Precisely, the study of Lagrangian flow maps is another focal point of this thesis. The conditions required to provide a meaningful description of flows given by this specification are summarised by the concept of dynamically possible flow, defined in Chapter 1. By the utilisation of this concept a mathematically rigorous framework has been provided for the equatorially-trapped internal water waves, described in Chapter 2 and the generalisation of Pollard's wave solution, given in Chapter 6. Furthermore, the mathematical justification of these solutions resulted in conditions on the Lagrangian variables and other parameters that have a physical meaning attached to them. Although remarkable, the generation in real-life experiments of the exact and explicit solutions presented in this thesis is still uncertain. The rotation seems to be a key aspect to transition from Stokes-like waves to Gerstner-like waves and it should be further investigated. Another interesting possibility is to consider perturbations of these solutions that help to alleviate the rigidity of the exact descriptions. Subsequently, the stability of the solutions in terms of the perturbations becomes important. The stability analysis in Chapter 5 established a useful criterion for instability in terms of the wave steepness.

The behaviour of the wave solution given in Chapter 3 was further studied by providing relevant mean flow properties. This was done in Chapter 4 and it offered a way to compare some of the measurements available in the Lagrangian framework with the corresponding Eulerian quantities. It is worth mentioning that the analysis was performed for waves that incorporate current terms and display vorticity.

Gravity waves with discontinuous vorticity constituted the main focus of Chapter 7. In particular, small-amplitude two-dimensional steady water waves were considered. The investigation showed that a discontinuous piecewise constant vorticity function was possible. The problem was formulated in terms of a dispersion relation and a full characterisation in terms of the sign of the vorticity was given for the case of a fixed depth formulation.

Future work

Some of the most interesting avenues of future research are now outlined. The existence of the solution constructed in Chapter 3 depends upon the derivation of a valid pressure. This, in turn, requires solving a nonlinear equation. A numerical solution to this problem, with adequate physical quantities, would provide a more complete description. On the other hand, the behaviour near the thermocline demands more attention. The approach taken assumes a set of interfaces where boundary conditions for inviscid flow are prescribed, which can be unrealistic. Also, the solution derived in Chapter 3 relies on the application of the f-plane approximation of the governing equations. The investigation of better approximations should be pursued.

It is important to expand the discussion of the flow properties given in Chapter 4, establishing a comparison with the results available in the Eulerian framework and the observable phenomena studied in the fluid dynamics literature. Similarly, the instability criteria provided in Chapter 5 would benefit from a better understanding of the breaking down process of the basic flow in terms of the steepness of the wave.

The mathematical analysis carried out in Chapter 6 has produced new constraints on the physical parameters describing Pollard-like solutions. This stresses the importance of our mathematical examination. However, it is essential to further investigate the physical meaning of these constraints. In addition to the discussion of the physically aspects of this model, computer-generated solutions for different arrays of these parameters could bring some new insight.

The study of the vorticity distribution in Chapter 7 led to the analysis of the roots of a cubic polynomial. The coefficients of this polynomial are intricate. However, it would be possible to numerically obtain the expression for its roots by means of Cardano's formula. Finally, our results for the bilinear profile should be further explored in physical terms and in relation to s more realistic vorticity profiles.

Appendix A

Complementary Results

A.1 Mean-value Inequality

The mean value theorem fails to hold for functions of several variables. However, in this scenario, Theorem A.1.1 is valid and in most cases, it is as useful as the mean value theorem for real functions of a single variable. Before discussing this theorem, some definitions are introduced.

Definition A.1.1. *The norm 2 or Euclidean norm of a vector* $\mathbf{x} = (x_1, \ldots, x_n)$ *is given by*

$$|\mathbf{x}|_2 = \sqrt{\sum_{k=1}^{n} |x_k|^2}\,. \tag{A.1}$$

Definition A.1.2. *The matrix norm induced by the previous norm is defined as*

$$\|M\| = \sup\{|M\mathbf{x}|_2 : \mathbf{x} \in \mathbb{R}^n \text{ such that } |\mathbf{x}|_2 = 1\} \tag{A.2}$$

for an arbitrary $n \times n$ *matrix* M*.*

The following result has been generalised to locally convex topological vector spaces by the use of the Gâteaux differential [1]. However, this is beyond the scope of this work so we include a simpler proof similar to the one included in [116].

Theorem A.1.1. *Let* $f : O \subset \mathbb{R}^n \longrightarrow \mathbb{R}^m$ *be a differentiable vector-valued function on a convex open domain* O*. Then*

$$|f(\mathbf{y}) - f(\mathbf{x})|_2 \leq \sup_{\mathbf{z} \in \{\mathbf{x},\mathbf{y}\}} \|Df_{\mathbf{z}}\| \cdot |\mathbf{y} - \mathbf{x}|_2\,, \tag{A.3}$$

where $Df_{\mathbf{z}}$ *represents the Jacobian matrix of* f *at* $\mathbf{z}$ *and* $\{\mathbf{x}, \mathbf{y}\}$ *is the segment joining* $\mathbf{x}$ *and* $\mathbf{y}$*.*

Proof. Let us define the function $\varphi : [0,1] \longrightarrow \mathbb{R}$

$$\varphi(t) = \langle\, f(\mathbf{y}) - f(\mathbf{x}), f(\mathbf{x} + t(\mathbf{y} - \mathbf{x}))\,\rangle\,, \tag{A.4}$$

which is well-defined for all $\mathbf{x}$ and $\mathbf{y}$ because O is a convex domain. In particular,

$$\varphi(1) = \langle\, f(\mathbf{y}) - f(\mathbf{x}), f(\mathbf{y})\,\rangle$$

and

$$\varphi(0) = \langle\, f(\mathbf{y}) - f(\mathbf{x}), f(\mathbf{x})\,\rangle\,.$$

Due to the regularity of the inner product $\langle\,\cdot,\cdot\,\rangle$ and the function f, it is possible to apply the Mean Value Theorem to φ. Thus, there exists $\tau \in (0,1)$ such that

$$\varphi(1) - \varphi(0) = \varphi'(\tau)\,. \tag{A.5}$$

As $\mathbb{R}^m$ is a Hilbert space with the norm 2 given in (A.1),

$$\begin{aligned}
\varphi(1) - \varphi(0) &= \langle\, f(\mathbf{y}) - f(\mathbf{x}), f(\mathbf{y})\,\rangle - \langle\, f(\mathbf{y}) - f(\mathbf{x}), f(\mathbf{x})\,\rangle \\
&= \langle\, f(\mathbf{y}) - f(\mathbf{x}), f(\mathbf{y}) - f(\mathbf{x})\,\rangle \\
&= \big|f(\mathbf{y}) - f(\mathbf{x})\big|_2^2\,.
\end{aligned}$$

The matrix norm (A.2) satisfies that $|M\mathbf{x}| \leq \|M\|\,|\mathbf{x}|$, hence

$$\begin{aligned}
\varphi'(\tau) &= \langle\, f(\mathbf{y}) - f(\mathbf{x}), Df_{\mathbf{x}+\tau(\mathbf{y}-\mathbf{x})}\,[\mathbf{y} - \mathbf{x}]\,\rangle \\
&\leq \big|f(\mathbf{y}) - f(\mathbf{x})\big|_2 \big|Df_{\mathbf{x}+\tau(\mathbf{y}-\mathbf{x})}\,[\mathbf{y} - \mathbf{x}]\big|_2 \\
&\leq \big|f(\mathbf{y}) - f(\mathbf{x})\big|_2 \Big(\big\|Df_{\mathbf{x}+\tau(\mathbf{y}-\mathbf{x})}\big\|\,\big|\mathbf{y} - \mathbf{x}\big|_2\Big) \\
&\leq \big|f(\mathbf{y}) - f(\mathbf{x})\big|_2 \Big(\sup_{t\in(0,1)} \big\|Df_{\mathbf{x}+t(\mathbf{y}-\mathbf{x})}\big\|\,\big|\mathbf{y} - \mathbf{x}\big|_2\Big) \\
&= \big|f(\mathbf{y}) - f(\mathbf{x})\big|_2 \Big(\sup_{\mathbf{z}\in\{x,y\}} \big\|Df_{\mathbf{z}}\big\|\,\big|\mathbf{y} - \mathbf{x}\big|_2\Big)\,,
\end{aligned}$$

where $\mathbf{z} = \mathbf{x} + t(\mathbf{y} - \mathbf{x})$ represents any point on the segment $\{\mathbf{x}, \mathbf{y}\}$. Therefore, from (A.5),

$$\big|f(\mathbf{y}) - f(\mathbf{x})\big|_2^2 \leq \big|f(\mathbf{y}) - f(\mathbf{x})\big|_2 \Big(\sup_{\mathbf{z}\in\{x,y\}} \big\|Df_{\mathbf{z}}\big\|\,\big|\mathbf{y} - \mathbf{x}\big|_2\Big)\,. \tag{A.6}$$

Finally, if $f(\mathbf{x}) = f(\mathbf{y})$, then (A.3) follows trivially. If $f(\mathbf{x}) \neq f(\mathbf{y})$ then it is possible to divide (A.6) by $\big|f(\mathbf{y}) - f(\mathbf{x})\big|_2$ which yields the desired result (A.3). □

A.2 Invariance of Domain theorem

The Invariance of Domain theorem has been of great importance in showing some of the main results contained in this work. Its proof, as it was given in [90] with some adjustments, is included. For a proof based on degree-theoretical arguments, we refer to [115]. Before its proof, the following theorem, which is a generalisation of the intermediate value theorem and which is equivalent to Brower fixed-point theorem, is assumed.

Theorem A.2.1 (Poincaré-Miranda)**.** *Let $\mathbf{I}^n = [-\varepsilon, \varepsilon]^n$ be an n-dimensional cube and let*

$$\mathbf{I}_i^- = \{\mathbf{x} \in \mathbf{I}^n \, : x_i = -\varepsilon\} \quad \textit{and} \quad \mathbf{I}_i^+ = \{\mathbf{x} \in \mathbf{I}^n \, : x_i = \varepsilon\}$$

be its i-th opposite faces. If $f : \mathbf{I}^n \to \mathbb{R}^n$ is a continuous map such that

$$f_i(\mathbf{I}_i^-) \subset (-\infty, 0] \quad \textit{and} \quad f_i(\mathbf{I}_i^+) \subset [0, \infty) \quad \textit{for each} \quad i \leq n\,,$$

then there exists a point $\mathbf{c} \in \mathbf{I}^n$ such that $f(\mathbf{c}) = \mathbf{0} \in \mathbb{R}^n$.

Theorem A.2.2 (Invariance of Domain Theorem)**.** *If $U \subset \mathbb{R}^n$ is an open set and $F : U \to \mathbb{R}^n$ is a continuous one-to-one mapping, then $F(U)$ is an open subset of $\mathbb{R}^n$.*

Proof. Let $\mathbf{u} \in U$. By the translation invariance of the Euclidean space, it is assumed that $\mathbf{u} = \mathbf{0}$ without any lost of generality and the n-dimensional cube containing $\mathbf{u}$ such that $\mathbf{I}^n \subset U$ is considered (it would be possible to work with any other compact set like a closed ball around $\mathbf{u}$). The main result is proven if

$$\mathbf{b} := F(\mathbf{0}) \in \mathrm{Int}[F(\mathbf{I}^n)]\,. \tag{A.7}$$

holds. To see this, note that $\mathrm{Int}[F(\mathbf{I}^n)] \subset \mathrm{Int}[F(U)]$ and so if (A.7) holds for any given $\mathbf{u} \in U$, then $F(U) = \mathrm{Int}[F(U)]$.
Since $\mathbf{I}^n$ is compact and the Euclidean space $\mathbb{R}^n$ is Hausdorff,

$$F : \mathbf{I}^n \to F(\mathbf{I}^n)$$

is a homeomorphism. Thus, it follows that for any $\mathbf{v} \in F(\mathbf{I}^n)$, and in particular for $\mathbf{b}$, there exists $\delta > 0$ such that

$$F^{-1}(B(\mathbf{b}, 2\delta) \cap F(\mathbf{I}^n)) \subset \mathrm{Int}(\mathbf{I}^n)\,.$$

Now, let us assume that $\mathbf{b} \in \partial F(\mathbf{I}^n)$. It will follow that in this case it is possible to find a function that contradicts the Poincaré-Miranda theorem A.2.1. Since $\mathbf{b} \in \partial F(\mathbf{I}^n)$, we are able to choose $\mathbf{c} \in B(\mathbf{b}, \delta) \backslash F(\mathbf{I}^n)$. Then, $\mathbf{b} \in B(\mathbf{c}, \delta) \subset B(\mathbf{b}, 2\delta)$ and so

$$F^{-1}(B(\mathbf{c}, \delta) \cap F(\mathbf{I}^n)) \subset \mathrm{Int}(\mathbf{I}^n)\,.$$

Let us define $X := F(\mathbf{I}^n) \backslash B(\mathbf{c}, \delta)$, $Y := \partial B(\mathbf{c}, \delta)$ and the continuous map

$$L\colon F(\mathbf{I}^n) \cup B(\mathbf{c}, \delta) \backslash \{c\} \longrightarrow X \cup Y$$

$$\mathbf{x} \longmapsto L(\mathbf{x}) := \begin{cases} \mathbf{x}\,, & \mathbf{x} \in X, \\ \\ \mathbf{c} + \dfrac{\mathbf{x} - \mathbf{c}}{\|\mathbf{x} - \mathbf{c}\|}\delta\,, & \mathbf{x} \in B(\mathbf{c}, \delta) \backslash \{c\}. \end{cases}$$

On the other hand, there exists a polynomial map $G\colon \mathbb{R}^n \to \mathbb{R}^n$ such that for each $\mathbf{x} \in X$

$$\|G(\mathbf{x}) - F^{-1}(\mathbf{x})\| < \varepsilon\,, \tag{A.8}$$

where ε defines the cube $\mathbf{I}^n$ as in Theorem A.2.1, such that $\mathbf{0} \notin G(X \cup Y)$. Indeed, let us choose η such that $0 < 2\eta < \varepsilon$ so

$$F^{-1}(X) \cap B(\mathbf{0}, 2\eta) = \emptyset\,. \tag{A.9}$$

By the Weierstrass approximation theorem, there exists a polynomial $P\colon \mathbb{R}^n \to \mathbb{R}^n$ such that for all $x \in X$

$$\|P(\mathbf{x}) - F^{-1}(\mathbf{x})\| < \eta\,.$$

In addition, since any differentiable function maps sets of measure zero to sets of measure zero (see Lemma 7.25 in [117]) and Y is a compact set of measure zero in $\mathbb{R}^n$, it follows that $P(Y)$ is a set of measure zero. Thus, there exists a point $\mathbf{d} \in B(\mathbf{0}, \eta) \backslash P(Y)$. This allows to define the desired map

$$G\colon X \cup Y \longrightarrow \mathbb{R}^n$$

$$\mathbf{z} \longmapsto G(\mathbf{z}) := P(\mathbf{z}) - \mathbf{d}\,,$$

which is trivially a polynomial map and it is such that

$$\|G(\mathbf{x}) - F^{-1}(\mathbf{x})\| = \|P(\mathbf{x}) - \mathbf{d} - F^{-1}(\mathbf{x})\| \leq \|P(\mathbf{x}) - F^{-1}(\mathbf{x})\| + \|\mathbf{d}\| \leq 2\eta < \varepsilon\,.$$

Furthermore, $\mathbf{0} \notin G(Y)$. This follows from the fact that

$$G(\mathbf{y}) = 0 \iff P(\mathbf{y}) = \mathbf{d} \quad \text{and} \quad \mathbf{d} \notin P(Y)\,.$$

In addition, $\mathbf{0} \notin G(X)$. Otherwise, if $G(\mathbf{x}) = \mathbf{0}$ for some $\mathbf{x} \in X$, it would follow from the properties of G that $F^{-1}(\mathbf{x}) \in B(\mathbf{0}, 2\eta)$, contradicting (A.9). Therefore, $\mathbf{0} \notin G(X \cup Y)$. Finally, the composite function defined by

$$f := G \circ L \circ F \colon \mathbf{I}^n \to F(\mathbf{I}^n) \cup B(\mathbf{c}, \delta) \backslash \{\mathbf{c}\} \to X \cup Y \to \mathbb{R}^n \backslash \{0\} \tag{A.10}$$

does not take the value $\mathbf{0} \in \mathbb{R}^n$. However, it satisfies the assumptions of the Poincaré-Miranda theorem A.2.1. To see this, first note that the map f is such that for any $\mathbf{t} \in \mathbf{I}_i^-$, $f_i(\mathbf{t}) < 0$. We have that $F(\mathbf{t}) \in X$. Otherwise, if

$$F(\mathbf{t}) \in B(\mathbf{c}, \delta) \subset B(\mathbf{b}, 2\delta)\,,$$

the continuity of F^{-1} implies that $\|\mathbf{t}\| < \varepsilon$. However, for any $\mathbf{t} \in \mathbf{I}_i^-$,

$$\|\mathbf{t}\| > \varepsilon\,.$$

Then,

$$\|f(\mathbf{t}) - \mathbf{t}\| = \|G[L(f(\mathbf{t}))] - F^{-1}(F(\mathbf{t}))\| = \|G[F(\mathbf{t})] - F^{-1}(F(\mathbf{t}))\| < \varepsilon\,.$$

Therefore,

$$|f_i(\mathbf{t}) - (-\varepsilon)| = |f_i(\mathbf{t}) - t_i| \leq \|f(\mathbf{t}) - \mathbf{t}\| < \varepsilon\,,$$

which implies that $f_i(\mathbf{t}) < 0$. Similarly, it is possible to show that $f(\mathbf{t}) > 0$ for all $\mathbf{t} \in \mathbf{I}_i^+$. Thus, f must take the value $\mathbf{0}$ and is a continuous function. This is a contradiction arising from the assumption that $\mathbf{b} \in \partial F(\mathbf{I}^n)$. □

A.3 Viète's formulae

The following formulae, used throughout Chapter 7, relating the coefficients of a polynomial to sums and products of its roots, are given without proof.

Lemma A.3.1 (Viète's formulae for third-order polynomials)**.** *Let x_1, x_2, x_3 denote the roots of the polynomial*

$$P(x) = Ax^3 + Bx^2 + Bx + D.$$

It holds that

$$x_1\, x_2\, x_3 = -\frac{D}{A}\,, \tag{A.11a}$$

$$x_1 + x_2 + x_3 = -\frac{B}{A}\,. \tag{A.11b}$$

References

[1] Ambrosetti, A. & Prodi, G., *A Primer of Nonlinear Analysis*, Cambridge University Press, 1995.

[2] Batchelor, G., *An Introduction to Fluid Dynamics*, Cambridge University Press, 1967.

[3] Bayly, B. J., *Three-dimensional Instabilities in Quasi-two Dimensional Inviscid Flows*, *American Society of Mechanical Engineers, Applied Mechanics Division, AMD*, **87**, ASME, pp. 71–77, 1987.

[4] Bennett, A., *Lagrangian Fluid Dynamics*, Cambridge University Press, 2006.

[5] Boyd, J. P., *Dynamics of the Equatorial Ocean*, Springer, 2018.

[6] Constantin, A., Edge waves along a sloping beach, *Journal of Physics A: Mathematical and General* **34**, no. 45, 9723–9731, 2001.

[7] Constantin, A., On the deep water wave motion, *Journal of Physics A: Mathematical and General* **34**, no. 7, 1405–1417, 2001.

[8] Constantin, A., The trajectories of particles in Stokes waves, *Inventiones Mathematicae* **166**, no. 3, 523–535, 2006.

[9] Constantin, A., *Nonlinear Water Waves with Applications to Wave-current Interactions and Tsunamis*, CBMS-NSF Regional Conference Series in Applied Mathematics, SIAM, Philadelphia, PA, 2011.

[10] Constantin, A., Dispersion relations for periodic traveling water waves in flows with discontinuous vorticity, *Communications on Pure & Applied Analysis* **11**, no. 4, 1397–1406, 2012.

[11] Constantin, A., An exact solution for equatorially trapped waves, *Journal of Geophysical Research: Oceans* **117**, no. C05029, 2012.

[12] Constantin, A., On the modelling of equatorial waves, *Geophysical Research Letters* **39**, no. 5, L05602, 2012.

[13] Constantin, A., Some three-dimensional nonlinear equatorial flows, *Journal of Physical Oceanography* **43**, no. 1, 165–175, 2013.

[14] Constantin, A., Some nonlinear, equatorially trapped, nonhydrostatic internal geophysical waves, *Journal of Physical Oceanography* **44**, no. 2, 781–789, 2014.

[15] Constantin, A., The flow beneath a periodic travelling surface water wave, *Journal of Physics A: Mathematical and Theoretical* **48**, no. 14, 143001,25pp, 2015.

[16] Constantin, A., Ehrnström, M. & Wahlén, E., Symmetry of steady periodic gravity water waves with vorticity, *Duke Mathematical Journal* **140**, no. 3, 591–603, 2007.

[17] Constantin, A. & Escher, J., Symmetry of steady deep-water waves with vorticity, *European Journal of Applied Mathematics* **15**, no. 6, 755–768, 2004.

[18] Constantin, A. & Escher, J., Symmetry of steady periodic surface water waves with vorticity, *Journal of Fluid Mechanics* **498**, 171–181, 2004.

[19] Constantin, A. & Escher, J., Analyticity of periodic traveling free surface water waves with vorticity, *Annals of Mathematics* **173**, 559–568, 2011.

[20] Constantin, A. & Germain, P., Instability of some equatorially trapped waves, *Journal of Geophysical Research: Oceans* **118**, no. 6, 2802–2810, 2013.

[21] Constantin, A., Ivanov, R. I. & Martin, C. I., Hamiltonian formulation for wave-current interactions in stratified rotational flow, *Archive for rational mechanics and analysis* **221**, no. 3, 1417–1447, 2016.

[22] Constantin, A., Ivanov, R. I. & Prodanov, E., Nearly-hamiltonian structure for water waves with constant vorticity, *Journal of Mathematical Fluid Mechanics* **10**, no. 2, 224–237, 2008.

[23] Constantin, A., Ivanov, R. I. & Prodanov, E., A hamiltonian approach to wave-current interactions in two-layer fluids, *Physics of Fluids* **27**, 086603, 2015.

[24] Constantin, A. & Johnson, R. S., The dynamics of waves interacting with the Equatorial Undercurrent, *Geophysical & Astrophysical Fluid Dynamics* **109**, no. 4, 311–358, 2015.

[25] Constantin, A. & Johnson, R., An exact, steady, purely azimuthal equatorial flow with a free surface, *Journal of Physical Oceanography* **46**, no. 6, 1935–1945, 2016.

[26] Constantin, A. & Monismith, S., Gerstner waves in the presence of mean currents and rotation, *Journal of Fluid Mechanics* **820**, 511–528, 2017.

[27] Constantin, A. & Strauss, W., Exact steady periodic water waves with vorticity, *Communications on Pure and Applied Mathematics* **57**, no. 4, 481–527, 2004.

[28] Constantin, A. & Strauss, W., Pressure beneath a stokes wave, *Communications on Pure and Applied Mathematics: A Journal Issued by the Courant Institute of Mathematical Sciences* **63**, no. 4, 533–557, 2010.

[29] Constantin, A. & Strauss, W., Periodic traveling gravity water waves with discontinuous vorticity, *Archive for rational mechanics and analysis* **202**, no. 1, 133–175, 2011.

[30] Constantin, A. & Strauss, W. A., Stability properties of steady water waves with vorticity, *Communications on Pure and Applied Mathematics: A Journal*

Issued by the Courant Institute of Mathematical Sciences **60**, no. 6, 911–950, 2007.

[31] Constantin, A. & Varvaruca, E., Steady periodic water waves with constant vorticity: regularity and local bifurcation, *Archive for rational mechanics and analysis* **199**, no. 1, 33–67, 2011.

[32] Constantin, A., Strauss, W. & Vărvărucă, E., Global bifurcation of steady gravity water waves with critical layers, *Acta Mathematica* **217**, no. 2, 195–262, 2016.

[33] Cushman-Roisin, B. & Beckers, J.-M., *Chapter 21 - Equatorial Dynamics*, International Geophysics, Academic Press, 2011.

[34] Drazin, P. G. & Reid, W. H., *Hydrodynamic Stability*, Cambridge University Press, 1981.

[35] Dubreil-Jacotin, M., Sur les ondes de type permanent dans les liquides hétérogenes, *Atti della Accademia Nazionale dei Lincei* **6**, 814–819, 1932.

[36] Dugundji, J., *Topology*, Boston: Allyn and Bacon, Inc., 1966.

[37] Ehrnström, M., Escher, J. & Wahlén, E., Steady water waves with multiple critical layers, *SIAM Journal on Mathematical Analysis* **43**, no. 3, 1436–1456, 2011.

[38] Escher, J., Regularity of rotational travelling water waves, *Philosophical Transactions of the Royal Society A* **370**, no. 1964, 1602–1615, 2012.

[39] Escher, J., Matioc, A.-V. & Matioc, B.-V., On stratified steady periodic water waves with linear density distribution and stagnation points, *Journal of Differential Equations* **251**, no. 10, 2932–2949, 2011.

[40] Escher, J. & Matioc, B.-V., On the analyticity of periodic gravity water waves with integrable vorticity function, *Differential Integral Equations* **27**, no. 3-4, 217–232, 2014.

[41] Fedorov, A. & Brown, J., Equatorial waves, *In Encyclopedia of Ocean Sciences (ed. J. Steele)*, 3679–3695, 2009.

[42] Friedlander, S. & Vishik, M. M., Instability criteria for the flow of an inviscid incompressible fluid, *Physical review letters* **66**, no. 17, 2204, 1991.

[43] Friedlander, S. & Vishik, M. M., Instability criteria for steady flows of a perfect fluid, *Chaos: An Interdisciplinary Journal of Nonlinear Science* **2**, no. 3, 455–460, 1992.

[44] Friedlander, S. & Yudovich, V., Instabilities in fluid motion, *Notices of the AMS* **46**, no. 11, 1358–1367, 1999.

[45] Froude, W., On the rolling of ships., *Trans INA* **2**, 180–227, 1861.

[46] Genoud, F. & Henry, D., Instability of equatorial water waves with an underlying current, *Journal of Mathematical Fluid Mechanics* **16**, no. 4, 661–667, 2014.

[47] Gerstner, F., Theorie der wellen samt einer daraus abgeleiteten Theorie der Deichprofile, *Annals of Physics* **2**, 412–445, 1809.

[48] Gilbarg, D. & Trudinger, N. S., *Elliptic Partial Differential Equations of Second Order*, Springer-Verlag, Berlin, 2001.

[49] Henry, D., The trajectories of particles in deep-water stokes waves, *International Mathematics Research Notices*, 1–13, 2006.

[50] Henry, D., On Gerstner's water wave, *Journal of Nonlinear Mathematical Physics* **15**, no. sup2, 87–95, 2008.

[51] Henry, D., On the deep-water Stokes wave flow, *International Mathematics Research Notices* **2008**, 7 pp, 2008.

[52] Henry, D., Analyticity of the streamlines for periodic travelling free surface capillary-gravity water waves with vorticity, *SIAM Journal on Mathematical Analysis* **42**, no. 6, 3103–3111, 2010.

[53] Henry, D., Dispersion relations for steady periodic water waves of fixed mean-depth with an isolated bottom vorticity layer, *Journal of Nonlinear Mathematical Physics* **19**, no. suppl. 1, 58–71, 2012.

[54] Henry, D., Dispersion relations for steady periodic water waves of fixed mean-depth with an isolated layer of vorticity at the surface, *Nonlinear Analysis: Real World Applications* **14**, no. 2, 1034–1043, 2013.

[55] Henry, D., An exact solution for equatorial geophysical water waves with an underlying current, *European Journal of Mechanics-B/Fluids* **38**, 18–21, 2013.

[56] Henry, D., Large amplitude steady periodic waves for fixed-depth rotational flows, *Communications in Partial Differential Equations* **38**, no. 6, 1015–1037, 2013.

[57] Henry, D., Steady periodic waves bifurcating for fixed-depth rotational flows, *Quarterly of Applied Mathematics* **71**, 455–487, 2013.

[58] Henry, D., Internal equatorial water waves in the f- plane, *Journal of Nonlinear Mathematical Physics* **22**, no. 4, 499–506, 2015.

[59] Henry, D., Equatorially trapped nonlinear water waves in a beta-plane approximation with centripetal forces, *Journal of Fluid Mechanics* **804**, R1, 2016.

[60] Henry, D., Exact equatorial water waves in the f-plane, *Nonlinear Analysis: Real World Applications* **28**, 284–289, 2016.

[61] Henry, D., A modified equatorial β-plane approximation modelling nonlinear wave-current interactions, *Journal of Differential Equations* **263**, no. 5, 2554–2566, 2017.

[62] Henry, D., On three-dimensional Gerstner-like equatorial water waves, *Philosophical Transactions of the Royal Society A: Mathematical, Physical and Engineering Sciences* **376**, no. 2111, 20170088, 2017.

[63] Henry, D. & Hsu, H.-C., Instability of equatorial water waves in the $f-$ plane, *Discrete & Continuous Dynamical Systems-A* **35**, no. 3, 909–916, 2015.

[64] Henry, D. & Hsu, H.-C., Instability of internal equatorial water waves, *Journal of Differential Equations* **258**, no. 4, 1015–1024, 2015.

[65] Henry, D., Martin, C.-I. & Sastre-Gómez, S., *Large amplitude steady periodic water waves for fixed-depth flows with discontinuous vorticity*, Manuscript submitted for publication.

[66] Henry, D. & Matioc, A.-V., Global bifurcation of capillary–gravity-stratified water waves, *Proceedings of the Royal Society of Edinburgh Section A: Mathematics* **144**, no. 4, 775–786, 2014.

[67] Henry, D. & Matioc, A.-V., On the symmetry of steady equatorial wind waves, *Nonlinear Analysis: Real World Applications* **18**, 50–56, 2014.

[68] Henry, D. & Matioc, B.-V., On the regularity of steady periodic stratified water waves., *Communications on Pure & Applied Analysis* **11**, no. 4, 1453–1464, 2012.

[69] Henry, D. & Matioc, B.-V., Aspects of the mathematical analysis of nonlinear stratified water waves, *Elliptic and Parabolic Equations. Springer* **119**, 159–177, 2015.

[70] Henry, D. & Sastre-Gomez, S., Mean flow velocities and mass transport for equatorially-trapped water waves with an underlying current, *Journal of Mathematical Fluid Mechanics* **18**, no. 4, 795–804, 2016.

[71] Henry, D. & Sastre-Gomez, S., Steady periodic water waves bifurcating for fixed-depth rotational flows with discontinuous vorticity, *Differential and Integral Equations* **31**, no. 1/2, 1–26, 2018.

[72] Henry, D., Regularity for steady periodic capillary water waves with vorticity, *Philosophical Transactions of the Royal Society A* **370**, no. 1964, 1616–1628, 2012.

[73] Henry, D. & Martin, C.-I., Exact, purely azimuthal stratified equatorial flows in cylindrical coordinates, *Dynamics of Partial Differential Equations* **15**, no. 4, 337–349, 2018.

[74] Henry, D. & Martin, C.-I., Free-surface, purely azimuthal equatorial flows in spherical coordinates with stratification, *Journal of Differential Equations*, 2018.

[75] Horn, R. A. & Johnson, C. R., *Matrix Analysis*, Cambridge University Press, 1990.

[76] Hsu, H.-C., An exact solution for nonlinear internal equatorial waves in the f-plane approximation, *Journal of Mathematical Fluid Mechanics* **16**, no. 3, 463–471, 2014.

[77] Hsu, H.-C., Some nonlinear internal equatorial flows, *Nonlinear Analysis: Real World Applications* **18**, 69–74, 2014.

[78] Ionescu-Kruse, D., An exact solution for geophysical edge waves in the f-plane approximation, *Nonlinear Analysis: Real World Applications* **24**, 190–195, 2015.

[79] Ionescu-Kruse, D., Short-wavelength instabilities of edge waves in stratified water, *Discrete & Continuous Dynamical Systems* **35**, 2053–2066, 2015.

[80] Ionescu-Kruse, D., Instability of equatorially trapped waves in stratified water, *Annali di Matematica Pura ed Applicata (1923-)* **195**, no. 2, 585–599, 2016.

[81] Ionescu-Kruse, D., Instability of Pollard's exact solution for geophysical ocean flows, *Physics of Fluids* **28**, no. 8, 086601, 2016.

[82] Ionescu-Kruse, D., On the short-wavelength stabilities of some geophysical flows, *Philosophical Transactions of the Royal Society A: Mathematical, Physical and Engineering Sciences* **376**, no. 2111, 20170090, 2017.

[83] Ionescu-Kruse, D. & Martin, C. I., Periodic equatorial water flows from a hamiltonian perspective, *Journal of Differential Equations* **262**, no. 8, 4451–4474, 2017.

[84] Ionescu-Kruse, D. & Martin, C. I., Local stability for an exact steady purely azimuthal equatorial flow, *Journal of Mathematical Fluid Mechanics* **20**, no. 1, 27–34, 2018.

[85] Johnson, R. S., *A Modern Introduction to the Mathematical Theory of Water Waves*, Cambridge University Press, 1997.

[86] Kluczek, M., Exact and explicit internal equatorial water waves with underlying currents, *Journal of Mathematical Fluid Mechanics* **19**, no. 2, 305–314, 2017.

[87] Kluczek, M., Equatorial water waves with underlying currents in the f-plane approximation, *Applicable Analysis* **97**, no. 11, 1867–1880, 2018.

[88] Ko, J. & Strauss, W., Effect of vorticity on steady water waves, *Journal of Differential Equations* **608**, 197–215, 2008.

[89] Ko, J. & Strauss, W., Large-amplitude steady rotational water waves, *European Journal of Mechanics - B/Fluids* **27**, no. 2, 96–109, 2008.

[90] Kulpa, W., Poincaré and domain invariance theorem, *Acta Universitatis Carolinae. Mathematica et Physica* **39**, no. 1, 127–136, 1998.

[91] Leblanc, S., Local stability of Gerstner's waves, *Journal of Fluid Mechanics* **506**, 245–254, 2004.

[92] Lifschitz, A. & Hameiri, E., Local stability conditions in fluid dynamics, *Physics of Fluids A: Fluid Dynamics* **3**, no. 11, 2644–2651, 1991.

[93] Longuet-Higgins, M. S., *On the transport of mass by time-varying ocean currents*, *Deep Sea Research and Oceanographic Abstracts*, pp. 431–447, 1969.

[94] Longuet-Higgins, M. S., Mass transport in water waves, *Philosophical Transactions of the Royal Society A* **245**, no. 903, 535–581, 1953.

[95] Martin, C. I., Dispersion relations for periodic water waves with surface tension and discontinuous vorticity, *Discrete & Continuous Dynamical Systems - A* **34**, 3109–3123, 2013.

[96] Martin, C. I., Dispersion relations for rotational gravity water flows having two jumps in the vorticity distribution, *Journal of Mathematical Analysis and Applications* **418**, no. 2, 595–611, 2014.

[97] Martin, C. I. & Matioc, B.-V., Gravity water flows with discontinuous vorticity and stagnation points, *Communications in Mathematical Sciences*, no. 2, 415–441, 2016.

[98] Martin, C.-I. & Matioc, B.-V., Existence of capillary-gravity water waves with piecewise constant vorticity, *Journal of Differential Equations* **256**, no. 8, 3086–3114, 2014.

[99] Martin, C. I., Dispersion relations for gravity water flows with two rotational layers, *European Journal of Mechanics-B/Fluids* **50**, 9–18, 2015.

[100] Matioc, A.-V., Exact geophysical waves in stratified fluids, *Applicable Analysis* **92**, no. 11, 2254–2261, 2013.

[101] Matioc, A.-V. & Matioc, B.-V., Capillary-gravity water waves with discontinuous vorticity: existence and regularity results, *Communications in Mathematical Physics* **330**, 3086–3114, 2013.

[102] Matioc, A.-V. & Matioc, B.-V., On the symmetry of periodic gravity water waves with vorticity, *Differential and Integral Equations* **26**, no. 1/2, 129–140, 2013.

[103] Nachbin, A. & Ribeiro-Junior, R., Capturing the flow beneath water waves, *Philosophical Transactions of the Royal Society A: Mathematical, Physical and Engineering Sciences* **376**, no. 2111, 20170098,17pp, 2017.

[104] Okuda, K., Internal flow structure of short wind waves, *Journal of the Oceanographical Society of Japan* **38**, no. 1, 28–42, 1982.

[105] Peregrine, D., Interaction of water waves and currents, *Advances in Applied Mechanics* **16**, 9–117, 1976.

[106] Phillips, O. & Banner, M., Wave breaking in the presence of wind drift and swell, *Journal of Fluid Mechanics* **66**, no. 4, 625–640, 1974.

[107] Pollard, R. T., Surface waves with rotation: An exact solution, *Journal of Geophysical Research* **75**, no. 30, 5895–5898, 1970.

[108] Rankine, W. J. M., On the exact form of waves near the surface of deep water, *Philosophical Transactions of the Royal Society of London* **153**, 127–138, 1863.

[109] Reech, F., Sur la théorie des ondes liquides périodiques, *Comptes Rendus Mathematique Academie des Sciences Paris* **68**, 1099–1101, 1869.

[110] Rodríguez-Sanjurjo, A., Global diffeomorphism of the lagrangian flow-map for equatorially-trapped internal water waves, *Nonlinear Analysis: Theory, Methods & Applications* **149**, 156–164, 2017.

[111] Rodríguez-Sanjurjo, A., Global diffeomorphism of the lagrangian flow-map for pollard-like solutions, *Annali di Matematica Pura ed Applicata (1923-)* **197**, 1787–1797, 2018.

[112] Rodríguez-Sanjurjo, A., Internal equatorial water waves and wave–current interactions in the f-plane, *Monatshefte für Mathematik* **186**, no. 4, 685–701, 2018.

[113] Rodríguez-Sanjurjo, A., Instability of equatorially-trapped nonhydrostatic internal geophysical water waves, *Wave Motion* **88**, 144–152, 2019.

[114] Rodríguez-Sanjurjo, A. & Mateusz, K., Mean flow properties for equatorially trapped internal water wave–current interactions, *Applicable Analysis* **96**, no. 13, 2333–2345, 2017.

[115] Rothe, E. H., *Introduction to Various Aspects of Degree Theory in Banach Spaces*, no. 23, American Mathematical Soc., 1986.

[116] Rudin, W., *Principles of Mathematical Analysis*, McGraw-Hill New York, 1976.

[117] Rudin, W., *Real and Complex Analysis*, McGraw-Hill New York, 1987.

[118] Sastre-Gomez, S., Global diffeomorphism of the lagrangian flow-map defining equatorially trapped water waves, *Nonlinear Analysis* **125**, 725–731, 2015.

[119] Stokes, G. G., On the theory of oscillatory waves, *Transactions of the Cambridge Philosophical Society* **8**, 441, 1847.

[120] Stuhlmeier, R., Internal Gerstner waves: applications to dead water, *Applicable Analysis* **93**, no. 7, 1451–1457, 2014.

[121] Thomas, G. & Klopman, G., Wave-current interactions in the near shore region, *International series on advances in fluid mechanics* **10**, 255–319, 1997.

[122] Ursell, F., On the theoretical form of ocean swell on a rotating earth, *Monthly Notices of the Royal Astronomical Society - Geophys. Suppl.* **6**, no. 1, 1–8, 1950.

[123] Vallis, G. K., *Atmospheric and Oceanic Fluid Dynamics*, Cambridge University Press, 2017.

[124] Wahlén, E., Steady water waves with a critical layer, *Journal of Differential Equations* **246**, no. 6, 2468–2483, 2009.

[125] Walsh, S., Stratified steady periodic water waves, *SIAM Journal on Mathematical Analysis* **41**, no. 3, 1054–1105, 2009.

[126] Walsh, S., Steady stratified periodic gravity waves with surface tension I: Local bifurcation, *Discrete & Continuous Dynamical Systems-A* **34**, no. 8, 3241–3285, 2014.